Liquid flow through obstructed passages; with special reference to the influence of the approach on the discharge through orifices and nozzles.

Thesis for the degree of
Doctor of Philosophy
of the
University of London
by

Flight Lieutenant R. A. Collacott, R.A.F.V.R.,
B.Sc.(ENG.), A.M.I.Mar.E.

January, 1944.

Book 1. — Dissertation.

A **critical** study of the existing information published on the flow of fluids through obstructed passages.

Foreword.

The following notes have been prepared in order that the reader may approach the subject contained in this thesis from the same angle as the author.

Firstly, it was decided to treat the subject from a purely practical aspect such as that adopted by many engineers. For this reason, a physical interpretation of the phenomena associated with this subject has been attempted. Despite the many objections to the use of coefficients, the author has based his conjectures very largely upon these factors since the practical engineer tends to use coefficients more frequently and with greater confidence than he does pure mathematics. For this, and personal reasons, the author has strictly avoided the use of advanced mathematical deductions and has concentrated instead on the application of well accepted definitions or principles despite, in certain circumstances stated herein, the limitations which apply to these more elementary mathematical calculations.

In addition, an attempt has been made to coordinate the whole subject in such a manner that further developments may spring from this work. The existing reports on this subject have been thoroughly analysed and suitably coordinated with Part I of this thesis. The author's own experimental work in Part II has been compared with these former reports and comparison made. Keeping in mind the possibility of future development work the author has produced a report of the outstanding problems and suggested, wherever possible, means for their solution.

Despite these optimistic anticipations of the future the author has experienced considerable personal difficulties in its completion. This work was first contemplated and elementary work started in the early part of 1939. By the middle of the year apparatus had been collected for the experimental part and a mass of notes prepared for the dissertation. After the declaration of war the author was able to complete some experiments before joining the services. From thereon the experimental work has only been completed during those short periods of leave from duty which the author was fortunate enough to receive. The compilation of this manuscript was only completed at odd off duty hours under conditions not always conducive to serious study. For these reasons the author begs the reader's tolerance should any minor mistakes inadvertently arise in the text.

In view of his Service committments the author has been unable to consult many people whose opinions he would have respected regarding several of the points raised by this thesis. This represents therefore the author's sole opinion on the many aspects

/

raised. It is hoped therefore, that whatever may be lacking from this thesis in technical accuracy will be offset by the demonstration of individual powers of investigation.

The author's impending departure for service overseas has prevented the completion of a third section which had been contemplated and in which it was hoped to relate the characteristics of these orifices to the performance of engineering equipment.* It is nevertheless hoped that this work will provide the reader with inspiration and will make some contribution to this subject.

R. A. Collacott.

Rochester.

November, 1943.

---

* Should the author be able to collect this information, it is proposed to publish it later in the proceedings of the professional institutions.

Field for future research.

The introductory chapter of this dissertation shows that there has not been a really serious effort to determine the relationship of the C_c and C_v of an orifice to any of the other controlling factors. There is need for a systematic investigation, both quantitative and physical, of the whole phenomena associated with the flow of fluids through obstructed passages.

2. Scattered references have been assembled describing the variations of C_c with orifice ratio. Most of the experiments referred to have been conducted on free jet, not on submerged orifices. Experiments to determine the contraction of the jet should be made in order to ascertain the variations of Cc, not only with 'm', but also with the other variables associated with orifice flow.

3. At the same time it would be valuable to evaluate Cv. This could be carried out most suitably by determining the velocity distribution in the vicinity of the orifice. No such determination has yet been carried out and if C_D were obtained at the same time by measuring the flow, a check on the values of Cc and Cv deduced from the velocity-distribution curves would be obtained. In addition, such an investigation would assist in determining the contours of the lines of flow through the orifice.

4. A similar study of re-entrant nozzles should also be made, for in view of their favourable discharge characteristics the author believes these nozzles may be applied more extensively than is at present realised. No work has been published, so far as can be ascertained, on the effects of champfer on the C_D of the nozzles.

5. The effects of viscosity appear to have received a considerable amount of attention, yet, as the author indicates in the following dissertation, this has all been concentrated on the flow through sharp-edged thin plate orifices. Very little information has been published concerning the viscous flow of fluids through nozzles and champfered orifices. It would also be interesting to study in greater detail the limiting Re for viscous flow discussed from the results described in section 5.

6. The effects of vapours flowing through pipes, of vapour locks and their effect on CD require to be investigated more completely than has been possible in this dissertation. It would also be interesting to study the flow of a freezing mixture when passing through an aperture.

7. The results relating C_D to the total head still require clarification, the results quoted by the author require greater amplification.

8. Much remains to be studied of the effect of edge length upon the C_D of an orifice or nozzle. The review which has already been made of this aspect indicates that besides a lack of information regarding the flow through long nozzles a considerable amount remains to be known of the effect of the edge-length of thin plate orifice. With submerged nozzles, the shape and general proportions of the nozzle will have an interesting influence upon the rate at which the flow recovers. With plate orifices the actual deflection of a thin plate would be an interesting study.

9. The author has endeavoured to show that a relationship exists between the tangent to the jet where it breaks away from the edge and the angle of champfer of the orifice. It is felt that the actual angle of breakaway of the jet should be studied - probably by coloured filaments in a glass pipe - in order to obtain the fundamental causes for CD acquiring such high values when fluid passes through a champfered orifice.

10. A more detailed study of the pressure rise upstream of the orifice. A more complete description of the upstream vortex is also required.

11. Of the characteristics of orifices used to produce sprays, much remains to be studied. There is very little positive information relating the atomisation and penetration of these sprays to the characteristics of the orifices producing them. Even in the formation of single droplets the effects of orifice size have not been studied.

12. It has been suggested to the author that the roughness of the bore of an orifice produced by reamering has very little influence upon the CD. No published information is available to confirm these remarks and for that reason it would be useful to determine the CD of a series of an orifice with a known roughness factor. Similarly, microphotographs of the edges of fine bore orifices would give useful information for production of jets for injection pumps. In addition, the susceptibility of the edge of a jet to corrosion and cavitation erosion influence should be studied.

The foregoing review covers only those aspects of orifice flow involving the fundamental principals either of the design or operation of orifices under normal conditions of operation. This information is required to improve the manufacture of many types of apparatus. With the development of exhaust ejectors, internal combustion turbines and other new equipment, the characteristics of orifices both under high temperatures and with fluids at supersonic velocities will have to be studied.

LIST OF SYMBOLS.

The following represent the symbols used for the general purposes enumerated; when these symbols are used for other purposes, references are given to these special applications in the text.

Suffixes, prefixes, etc., refer to special conditions involving the same generalised applications.

Q	=	discharge, cu. ft./sec.
a	=	area (sectional) of orifice, sq. ins.
A	=	" " " approach, sq. ins.
v	=	velocity through orifice, ft./sec.
V	=	" " approach, ft./sec.
p	=	pressure in orifice, lb./sq. ins.
P	=	" " approach, lb./sq. ins.
d	=	orifice diameter, ins.
D	=	pipe " ins.
m	=	orifice area ratio $\frac{a}{A} = (\frac{d}{D})^2$
b	=	orifice thickness.
u, U	=	velocities across the section of a jet or pipe.
α (alpha)	=	angle of bevel of orifice, measured between the bevel and orifice face.
ψ (psi)	=	included angle of bevel = 180 – 2 α
e	=	size of roughness in approach.
ν (upsilon)	=	kinematic viscosity $= \frac{\mu}{w}$, sq. ft./sec.
μ (mu)	=	coefficient of viscosity, lb./ft./sec.
w (omega) or ρ (rho)	=	density, lb./cu. ft.
σ (sigma)	=	surface tension lb./ft.
γ (gamma)	=	ratio of specific heats, (gases.)
Re	=	Reynolds' Number $= \frac{V.d.w}{\mu} = \frac{V.d}{\nu}$
Mach. No.	=	$\frac{\text{Velocity}}{\text{Velocity of Sound}}$
Ny	=	Capillarity Number $= \frac{d.w.V^2}{Re}$
H	=	discharge head.
g	=	acceleration due to gravity (32.2 ft./sec./sec.
λ (lamma)	=	friction coefficient (also used as wavelength of stationary oscillations of a jet.)

τ (tou)	=	turbulence.
ϕ (phi)	=	angle of jet, measured between the tangent to the jet and approach face
i	=	included angle of tangent of the jet.
f	=	frequency of vortex formation.
t	=	time of drop formation.

I N D E X.

Page

Chapter 1.
Introduction.

Chapter 2.
The Effect of the Fluid and Flow Properties on the Discharge.

Chapter 3.
The Effect of Orifice Design on the Discharge.

CHAPTER I.

Introduction.

1. Object of the investigations.

An earlier paper by the author* aroused his interest in the operation of the reduction valve used in refrigerating apparatus. It was desirable to know the influence of the refrigerant flow upon the pressure difference across the valve and its effects upon the coefficient of performance of the refrigerator. Other examples of fixed obstructions in fluid systems such as valves, filters, etc., also occurred to the author as involving some relationship between the pressure drop, head-loss and flow. Such data is of use in the design of hydraulic systems and is of great importance in the construction of automatic control apparatus, it also has other wide applications. The author therefore determined to investigate the flow of fluids through obstructed passages.

To reduce these investigations into reasonably general terms applicable to a number of different obstructions it was decided to study in detail the flow through orifices and nozzles together with the influence of obstructions on their discharge characteristics. These throttling devices have been used in a variety of apparatus and have a simpler function than other types of apparatus.

Before commencing any experimental research the existing data on this subject was carefully examined. Many publications exist giving the influence of various factors on the discharge characteristics of orifices, particularly with regards to their use as flow-meters. Other contributions with a bearing on this subject have been found in reports on injection nozzles, carburettors, steam nozzles, etc. This data does not yet exist in one whole collected work and has been assembled into the critical dissertation, part 1 of this thesis, a feat involving some considerable amount of pioneer research into a mass of published literature on this subject.

The experimental work falls into two parts, (1) fundamental calibration of certain orifices and nozzles (2) determinations of the influence of obstructions on the discharge characteristics of these pre calibrated orifices and nozzles. The results obtained from the first series of investigations were used to compare with the statements of other experiments described in the dissertation and were applied as a basis of comparison for the second series.

---

*R. A. COLLACOTT. Control Apparatus in Marine Refrigerating Plant. Trans. I Mar. E. March, 1940.

This work has been conducted only for liquid flow. By this means the study has been simplified by eliminating the compressibility factor associated with gaseous flow and the apparatus has not been so sensitive to such physical changes as the temperature, viscosity and density.

From these investigations it has been possible to place the effect of the approach on a rational basis. Further experimental and analytical work remains to be carried upon the vortex formation in a contracting stream and other extensive subjects which are far beyond the scope of this thesis. The author has however considered it advisable as a guide to those who may follow in his path and seek to develop this subject, to append a short review of the work which in the light of his experience, remains to be pursued.

2. Flow Coefficients.

When a liquid flows through a pipe and is then constricted to pass through an orifice, the mean velocity is increased in order to maintain continuity of flow. The pressure energy is therefore reduced in order to compensate for the gain in kinetic energy, thus, referring to fig. (2.1.) for continuity of flow the rate of discharge Q = a.v. = A.V., i.e. $v = \frac{A}{a}V$ $V = \frac{1}{m}V$

Assuming no energy is lost in the contraction, then, by Bernoullis' equation

$$\frac{P}{w}+\frac{V^2}{2g} = \frac{p}{w}+\frac{v^2}{2g}$$

$$\frac{v^2 - V^2}{2g} = \frac{P - p}{w}$$

$$\text{i.e.} \quad \underset{\sim}{v} = \sqrt{\frac{2g.\ \frac{(P-p)}{w}}{(1-m^2)}} \quad \ldots\ldots\ldots\ldots\ldots\ldots\ldots\ldots 2.1.$$

This expression is based entirely upon the assumption that there is no loss of energy by fluid friction, eddy formation, etc. In practice these losses do occur so that the true mean velocity is less than the theoretical. In order to facilitate design and the study of fluid flow it has been necessary to introduce a factor to compensate for this velocity variation, thus the

$$\text{Coefficient of Velocity, } C_v = \frac{\text{True mean velocity.}}{\text{Theoretical mean velocity.}}$$

In a similar way, the true cross section of the flow varies from the theoretical section obtained by measurement of the aperture. This results from the inability of the stream lines to conform to the contours of the aperture owing to the high centrifugal pressure created at high rates of flow. A factor has therefore been introduced to compensate for this variation, so that the

$$\text{Coefficient of Contraction, } C_c = \frac{\text{True sectional area of flow.}}{\text{Theoretical area.}}$$

As both the mean velocity and the sectional area vary from the theoretical, the actual rate of discharge will vary from the theoretical value. For this also, a factor has been introduced given by

$$\text{Coefficient of Discharge, } C_D = \frac{\text{Actual rate of discharge.}}{\text{Theoretical rate of discharge.}}$$

Each of these flow coefficients is subject to variations according to the conditions of flow, thus with viscous flow the contraction is unity but the velocity coefficient is low. Under turbulent flow the coefficient of velocity is nearly unity while the coefficient of contraction is low. These coefficients are also influenced by the orifice - pipe diameter ratio, the inlet champfer on the orifice, its length and a variety of other conditions. Generally the effect of these conditions on the individual coefficients have not been ascertained, it still remaining a matter of speculation as to their relative influence, as the cumulative effect on the discharge coefficient is most usually obtained in practical tests.

The difficulties involved in separating these coefficients are very great. This is because they do not remain independent constant quantities but are inter-related with each other. An elementary determination of this relationship has been given by Ower (1). If the pressure tappings for P are taken in the undisturbed part of the approach to the orifice and for p at the position of least section of the jet, i.e. the vena-contracta, it can be shewn that the theoretical discharge with contraction but without loss of velocity is

$$Q_t = C_c.\ a.\sqrt{\frac{2g\ (P-p)}{w\ (1 - C_c^2\ m^2)}} \quad \ldots\ldots\ldots\ldots\ldots\ldots\ 2.2.$$

If C_v is taken into account however, then the true discharge will be given by

$$Q = C_v.\ C_c.\ a\sqrt{\frac{2g\ (p-p)}{w\ (1-C_c^2\ m^2)}} \quad \ldots\ldots\ldots\ldots\ldots\ldots\ 2.3.$$

If the discharge coefficient C_D is obtained from that derived from the theoretical velocity in equation (1) and the sectional area of the orifice "A", then the true discharge is

$$Q = C_D.\ A.\sqrt{\frac{2g\ (P-p)}{w\ (1-m^2)}} \quad \ldots\ldots\ldots\ldots\ldots\ldots\ 2.4.$$

so that from equations (3) and (4)

$$C_D = C_v.\ C_c.\sqrt{\frac{1-m^2}{1-C_c^2\ m^2}} \quad \ldots\ldots\ldots\ldots\ldots\ldots\ 2.5.$$

This formula is frequently simplified when m is small, to the expression $C_D = C_v.\ C_c.$ The head lost by the fluid may be divided into two parts (1) viscous (2) eddy losses. Under viscous flow the viscous loss is high and C_v very small but under turbulent flow the viscous loss is small and the eddy loss - which is proportionately greater than the viscous loss under turbulent flow - is also low.

It may therefore be taken that for turbulent flow $C_V \rightarrow 1{\cdot}0$. Hence, expanding equation (5)

$$C_c = \frac{C_D}{\sqrt{1-m^2(1-C_c^2)}} \text{ approximately} \quad \ldots\ldots\ldots\ldots\ldots\ldots \quad 2.6.$$

Care must be taken in applying this equation to obtain the correct value of C_c since the pressure drop used to calculate C_D must be taken between the undisturbed upstream and the vena-contracta. This complicates really accurate determination of the relationship between C_c and C_D as the position of the vena-contracta varies with the rate of flow; it is in fact becoming customary with flow-metering technique to take pressure tappings from each face of the orifice and so avoid difficulties arising with the vena-contracta tappings.

Experiments by Witte (2) quoted by Ower yield the values for C_c with various values of "m", given in Table I.

TABLE 2.1.

m	0·1	0·2	0·3	0·4	0·5	0·6	0·7
C_c	0·601	0·610	0·623	0·639	0·658	0·678	0·702

The conditions of the experiments from which these results were produced have not been ascertained by the author. It is important to verify that vena-contracta tappings were taken but, even without such assurances, the results given lie within the generally accepted range of values.

2a. The Coefficient of Contraction.

The values of C_c given in Table I have been plotted against "m" in fig. 2.2. which emphasises the manner in which the coefficient of contraction decreases with the ratio "m". The pictorial representations of the flow in fig. 2.3. (a) (b) and (c) indicate that this variation is probably the result of an almost constant depression (x) at the vena contracta. The area of the jet at the vena contracta is $\pi(d-2x)^2 = \pi d^2(1-\frac{2x}{d})^2$ so that the

$$\text{Coefficient of Contraction } C_c = (1-\frac{2x}{d})^2$$

$$\therefore \qquad \frac{x}{d} = \tfrac{1}{2}(1-\sqrt{C_c}) \quad \ldots\ldots\ldots\ldots \quad 2\ (7)$$

TABLE 2.2.

m	0·1	0·2	0·3	0·4	0·5	0·6	0·7
$\sqrt{C_c}$	0·775	0·781	0·789	0·800	0·811	0·823	0·838

TABLE 2.2. (Contd.)

$1-\sqrt{C_c}$	0·225	0·219	0·211	0·200	0·189	0·177	0·162
$\frac{1}{2}(1-\sqrt{C_c})$	0·113	0·109	0·106	0·100	0·094	0·089	0·081 $= \frac{x}{d}$
$\frac{x}{D} = \frac{x}{d}m$	0·036	0·049	0·058	0·063	0·067	0·069	0·068

It will be seen from Fig. 2.2. that x varies with the diameter-ratio, but that the actual value of $\frac{x}{D}$ is really small. It can be seen that $\frac{x}{D}$ rises to a maximum at m = 0·60 and then decreases slowly as m increases to unity. Actually, the depression x depends upon the curvature of the stream-lines at the edge of the orifice which is itself controlled by the centrifugal pressures acting on the fluid as it converges through the constriction. It would seem that a mathematical analysis of these forces should yield a solution to the contraction.

An attempt at this problem was made by Villamil (4) based on the same assumptions as those quoted by Prandtl (3) who attributed the variations in contraction for various diameter-ratios to different degrees of curvature of the stream lines in their attempt to follow radial paths. The transverse component of the radial velocity being zero at the vena-contracta. Villamil assumed that a hemisphere could be drawn around the orifice, the velocity being the same at each point on its surface and directed radially to the centre of the orifice. The hemisphere of diameter equal to that of the orifice was assumed to possess the same velocity as the discharging jet so that the volume of liquid contained by this surface, i.e. $\frac{\pi}{3} d^3$ must resolve itself into a jet of length equal to the orifice radius. Hence, if A_1 = area of cross section of the equivalent cylinder.

$$\text{Volume of liquid discharged} = \frac{\pi}{3} d^3 = A_1 \frac{d}{2}$$

$$\therefore \quad A_1 = \frac{2}{3} \pi d^2 = \frac{2}{3} \text{ Orifice Area,}$$

$$\text{i.e. Coefficient of Discharge } C_c = \frac{2}{3} \quad \ldots\ldots\ldots\ldots \quad 2.8.$$

This solution has many faults and requires several refinements, the answer is so close to that given by experiment however, that the idea seems worthy of further development.

This development has actually been made to some extent by Howland and Richetta (5) basing their analysis on the previous work by Professor Hooper (6). They assumed that the pressure reduction at a point was $\frac{w v^2}{2 g}$ where v was the velocity at that point and which they further assumed to be on an equi-velocity hemisphere so that the velocity $v = \frac{\text{Discharge}}{\text{Area of surface of hemisphere}} = \frac{Q}{2 \pi r^2}$ where r = radius of the hemisphere. By equating all the forces and applying the elementary momentum theory they were able to deduce the ratio of area of the jet to that of the orifice and by solving the quadratic equation

$$1 - 2C_c + \frac{Cc^2}{4} = 0 \quad \dots\dots\dots\dots\dots\dots\dots\dots\dots\dots\dots\dots \quad 2.9.$$

obtained $C_c = \frac{2 - \sqrt{3}}{\frac{1}{2}} = 0{\cdot}536$ instead of the value $0{\cdot}590$ computed by Professor Hooper. This same result they claim has been deduced in a slightly different manner by Wittenbauer (7). The author has not verified this claim.

That the coefficient of contraction must certainly be greater than 0·5 was demonstrated by Rayleigh (8) in 1876, for the velocity acquired in the absence of friction is , $v^2 = 2p$ and if the area at the vena-contracta is σ' the true discharge is v and momentum/unit time is $(\sigma' v) v = \sigma' v^2$, which requires that force to keep the vessel still, namely $p\sigma$ where σ is the area of the orifice. A relief pressure must however exist around the orifice corresponding to the velocity at that region, i.e. $p\delta\sigma$* Hence, by equating the forces

$$p(\sigma + \delta\sigma) = \sigma' v^2 = \sigma' 2p.$$

$$\text{i.e. } C_c = \frac{\sigma'}{\sigma} = \frac{1}{2}\left[1 + \frac{\delta\sigma}{\sigma}\right] \quad \dots\dots\dots\dots\dots\dots\dots \quad 2.10$$

This shews that as $\delta\sigma \to 0$, $C_c \to 0{\cdot}50$. By this reasoning the reaction force produced by a change of momentum around the jet extends for an area $\delta\sigma = (2C_c - 1)\sigma$ so from Table 2.2. we get

TABLE 2.3.

m	0·1	0·2	0·3	0·4	0·5	0·6	0·7
$\frac{\delta\sigma}{\sigma}$	0·202	0·220	0·246	0·278	0·316	0·356	0·404

*This suggests an experimental method of flow calibration which does not appear to have been published before

$$\text{Force } F = \text{Momentum/sec.} = \frac{w.Q.v.}{g} = \frac{w}{g}.Q.Cv.\ 2gH$$

$$\therefore C_v = \frac{F}{\frac{w}{g} Q.\ \ 2gH}$$

This application is not strictly correct as Rayleigh's theory applies to an orifice in an infinite wall which certainly is not comparable with an orifice in a pipe. The additional area was originally thought by the author to result from an equi-velocity spherical surface shewn in fig. 2.4., this being the basis of previous assumptions for C_c.

$$\text{Area of surface} = \pi d\,(r - x) = \delta\sigma + \sigma = \frac{\pi}{4} d^2 + \delta\sigma$$

$$\therefore\ \frac{\delta\sigma}{\sigma} = \frac{\pi d\,(r - x)}{\frac{\pi}{4} d^2} - 1 = \frac{4\,(r - x)}{d} - 1 \quad \ldots\ 2.11.$$

Thus, from table 2.3.

TABLE 2.4.

m	0·1	0·2	0·3	0·4	0·5	0·6	0·7
$\frac{r-x}{d}$	0·300	0·305	0·315	0·319	0·329	0·339	0·351
$\frac{x}{d}$	·267	·253	·238	·230	·215	·198	·180

which shews that the radial flow theory does not entirely hold for the values used, the position of the focal point varying considerably with the orifice diameter.

A classical deduction of the coefficient of contraction for a perfect fluid issuing through a slit in the wall of a large vessel, was given by Lamb (9) but which he attributes to Kirchoff (10) and is based on the theory of free stream lines. By the application of mathematics he deduced the form of the boundaries of the jet to be given by

$$x = \frac{4b}{\pi}\sin^2\frac{\theta}{2} \qquad \text{and } y = \frac{2b}{\pi}\left\{\log.\tan\left(\frac{\pi}{2} + \frac{\theta}{2}\right) - \sin\theta\right. \quad \ldots\ 2.12.$$

where 2b is the asymptotic width to which the jet contracts, and is a mathematical parameter. From this, the width of the slit is given by $\frac{2b}{\pi}(\pi + 2)$ so that the ratio of areas is

$$\frac{\pi}{\pi + 2} = 0{\cdot}610 \quad \ldots\ 2.13.$$

Footnote continued from page 7.

All the quantities Q, w, H may be determined and if the apparatus is mounted on guides on ball bearings or other frictionless supports, one end of the experimental tube may be connected by rubber tubing to the supply and the other discharge through the orifice into space. If the axial stiffness is pre-calibrated, deflection during flow may be obtained with a clock gauge or travelling microscope and hence the reaction force may be deduced.

This figure is very frequently quoted as the true theoretical value Co. It is only calculated however for the flow through a slit and the effect of three dimensional flow will probably modify this value; it is interesting to record however that the opinions generally do not anticipate any considerable modification to Cv from this source. An approximate solution by Jacob (II) gives a value of 0.618 for the theoretical coefficient which is in reasonable agreement with the value obtained by Lamb.

An attempt to deduce by more direct methods a value of the coefficient of contraction in terms of the flow was proposed by Swift (12.) By a mathematical treatment of the equation to motion and from a study of its application to the curvature of the boundaries it was possible to deduce the area at the vena contracta. This method, which is presented in detail later, gives a solution of the form

$$Cc = 1 - a.\ Re. \qquad \text{.......... } 2.14.$$

where a is a constant. This indicates a linear reduction from unity as the Reynolds Number increases, a result which in practice, is only applicable to viscous flow, experiments indicating that a constant value of 0.610 applies to the turbulent zone.

Smith & Walker (13) investigated the free discharge of jets through holes of varying size and under different heads. Measurements of the contraction of this jet, as taken by a ring-gauge were used to deduce the coefficient. This method does not appear to offer results of sufficiently high accuracy for precise determinations, but nevertheless enabled the authors to conclude that the coefficient never becomes less than 0.61 and for the region of turbulent flow, could be related to the head and orifice diameter by the expression

$$Cc = 1 - \frac{a}{e^x} \qquad \text{.......... } 2.15.$$

where $x = f\,(h,\ d) = \frac{0.15}{d^2\ h^{0.125}}$ and since $Cc \to 1$ when h & d are small

and Cc 0.610 when they are large, it is possible to deduce a = 0.39. It is difficult to substitute a function of Reynolds Number for x which complicates comparison between equations 15 and 14. When Smith & Walker's equation is expanded,

$$Cc = (1-0.39) + 0.39x - \frac{0.39x^2}{\lfloor 2} + \text{ .... etc.}$$

$$= 0.610 + 0.39x - 0.195x^2 + \text{ .... etc. } \qquad \text{.......... } 2.16.$$

or, substituting for x, $Cc = 0.610 + \frac{0.0586}{d^2\ h^{0.125}}$ .... 2.17.

neglecting the second and higher powers of x because for turbulent flow both d and h are sufficiently large for the product to make high powers of x negligible.

Working on the principles of his previous paper, Howland (14) shewed that in the transition and turbulent zone

$$Cc = \frac{2 - \sqrt{4 - \frac{2.104}{Cv^2}}}{1.052} \quad \text{.................................} \quad 2.18.$$

which reduced to $Cc = \frac{0.500}{Cv^2}$ if $Cv > 0.723$. At the same time, Howland related Cv to Reynolds Number by the expression

$$Cv = \frac{1}{\sqrt{\frac{M}{R} + 1}} \quad \text{.................................} \quad 2.19.$$

which can be simplified by reducing it to

$$Cv = 1 - \frac{M}{2\sqrt{R}} \quad \text{.................................} \quad 2.20.$$

provided $R > M^2$. Substituting equation 2.20 in the reduced version of equation 2.18. ....

$$Cc = 0.500 \left[1 - \frac{M}{2\sqrt{R}}\right]^{-2}$$

$$= 0.500 \left(1 + \frac{M}{\sqrt{R}}\right) \quad \text{..........................} \quad 2.21.$$

$$= 0.500 + \frac{M}{2\sqrt{R}} \quad \text{..........................} \quad 2.22.$$

This equation does not agree with the observations made by Smith and Walker that as $R \to \infty$ $Cc \to 0.61$. It is therefore suggested that a more suitable expression would be

$$Cc = 0.610 + \frac{\alpha}{\sqrt{R}} \quad \text{..........................} \quad 2.23.$$

In view of the favourable indications shown in Table IV of the radial-flow theory, it appears to afford the most convenient approach to construe a physical solution to the problems of contraction; it may provide an answer to the problems of the position of the vena-contracta and the velocity coefficient.

<u>2 (b). The Coefficient of Velocity.</u> The original definition of coefficient of velocity was given as the ratio between the actual and theoretical velocities of flow and a definite note was made after equation 6 to indicate certain precautions to be taken in selecting tapping points. It is essential that a correct knowledge be acquired of the variations in pressure across the constriction in order that the theoretical mean velocity may be correctly ascertained.

When a liquid flows through an orifice there is a slight gradient due to frictional losses followed by a comparatively steep increase in pressure close to the plate as shewn in fig. 2.5. This rise of pressure is generally attributed to the impact of filaments on the plate, and is therefore called the "impact pressure." This reference to impact is not quite happily made, but it will be shewn in a following section (Section 15) that this increase arises from the transverse velocity component of the contracting stream.

To apply Bernoullis' theorum it is necessary for the filaments of the fluid stream to be parallel. Although not strictly correct, (such conditions only apply to the steady flow part upstream and the vena-contracta,) under these conditions the equation is

$$\frac{p1}{w} + \frac{V^2}{2g} = \frac{p2}{w} + \frac{v2}{2g} \quad \text{and } V = m\,v \text{ for continuity}$$

$$\text{i.e.} \quad v = \sqrt{\frac{29}{w}\,\frac{(p1 - p2)}{(1 - m2)}} \quad \text{.. assuming the Cc term is neglected} \quad \ldots\ldots\ldots\ldots\ldots \; 2.24.$$

This represents what is the only true theoretical velocity in accordance with the general requirements of Bernoullis' theorum.

The distance in which contraction takes place is so small that ordinary "pipe" friction for the distance between the measuring points is negligible, momentum losses are also small in the contracting portion. It is therefore highly probable that equation 2.24 represents the actual or true mean velocity. If then, the discharge is calculated on p1 p3 and p2 (where p3 is the "impact pressure" derived from the increase of head at the plate)

$$\text{i.e.} \quad V = \sqrt{\frac{2g}{w}\,\frac{(p1 + p3 - p2)}{(1 - m2)}} \quad \ldots\ldots\ldots\ldots\ldots\ldots\ldots\ldots \; 2.25.$$

as the theoretical velocity, then calculated against v from equation (24) as the true velocity

$$Cv = \sqrt{\frac{p1 - p2}{p1 + p3 - p2}} = 1 - \frac{1}{2}\,\frac{p3}{p1 - p2} \text{ approx.} \quad \ldots\ldots\ldots\ldots\ldots \; 2.26.$$

The author is of the impression that considerations of friction loss between tapping points as made by some writers are not very practical and that the true determination of the velocity coefficient centres around the evaluation of p3.

Working on the lost head hypothesis, if we let px = head lost in the contraction of the jet (note, this is not the same as the head lost in the expansion of the jet which is much greater) then, from Bernoullis' equation:

$$\frac{P}{w} + \frac{V^2}{2g} = \frac{p+px}{w} \quad \frac{v_1^2}{2g} \quad \ldots\ldots\ldots\ldots\ldots\ldots\ldots\ldots \quad 2.27.$$

Again the mis-use of Bernoulli should be observed, for it is not correct to use this energy equation for conditions involving a loss of head.

Equation 2.27 combined with the continuity expression $V = m\,v_1$ gives

$$v_1 = \sqrt{\frac{2g.(P - p_x - p)}{w(1 - C_c^2 . m^2)}} \quad \text{- - - - - - - -} \quad 2.28.$$

Under ideal conditions with no loss of head the theoretical velocity is

$$v_1 = \sqrt{\frac{2g\,(P-p)}{w(1-m^2)}} \quad \text{- - - - - - - -} \quad 2.29.$$

hence,

$$\text{Coefficient of Velocity, } Cv = \frac{v_1}{v} = \sqrt{\frac{P - p_x - p}{P - p}}$$

$$= \sqrt{1 - \left(\frac{px}{P - p}\right)} \quad \ldots\ldots\ldots\ldots\ldots\ldots\ldots \quad 2.30.$$

From this it can be easily shown that if $\frac{px}{P-p}$ is small then $Cv = 1 - \frac{px}{2\,(P-p)}$.

With viscous flow the whole "loss of pressure" px is very nearly equal to the pressure drop and therefore $Cv \rightarrow 0$ as $Re \rightarrow 0$; but with turbulent flow the viscous losses are very small, i.e. p_x is negligible. Various text-books quote $Cv = 0.98$ so that $\frac{px}{P-p} = 0.04$.

Howland's attempts to predict a theoretical velocity coefficient for the turbulent zone have been described. The equation $Cv = 1 - \frac{M}{2\sqrt{Re}}$ does not seem open to serious objection and certainly lies in the correct range for turbulent flow. If then, we equate this to equation 30 and $\frac{px}{P - p}$ is assumed small,

$$Cv = 1 - \frac{px}{2\,(P-p)} = 1 - \frac{M}{2\sqrt{Re}}$$

$$\text{i.e.} \quad \frac{px}{P - p} = \frac{M}{\sqrt{Re}} \quad \ldots\ldots\ldots\ldots\ldots\ldots\ldots\ldots \quad 2.31.$$

This represents but one particular condition for it is most probable that the value M is a complex function representing the form of the approach and the orifice. It is open to the objection that it was derived on the assumption that the loss of head varies as $V^{1.5}$ whereas in practice this is true only of a limited portion of the turbulent zone.

It should be noted that if $p_x = A.\ V^{1.5}$, $\frac{P - p}{w} = \frac{1}{m^2}\ \frac{V^2}{2g}$ and $Re = \frac{V.d}{\nu}$, then

$$\left(\frac{A.V^{1.5}}{\frac{w}{m^2}\ \frac{V^2}{2g}}\right) = \frac{M}{\sqrt{\frac{V.d}{\nu}}}$$

$$\therefore\quad M = \frac{2g.m^2\ A}{w}\sqrt{\frac{d}{\nu}} \qquad \ldots\ldots\ldots\ldots\ldots\ldots\ldots\ldots\ 2.32$$

and therefore varies according to a number of physical conditions of the flow.

Swift (12) proved, by equating the head loss to V, that

$$H_x = \frac{V^2}{2g}.\alpha.\frac{1}{Re} \quad \ldots\ldots\ldots\ldots\ldots\ldots \text{where } \alpha \text{ is a constant}$$

so that $Cv = (1+\frac{\alpha}{Re})^{-\frac{1}{2}}$

$$= 1 - \frac{\alpha}{2\ Re} \quad \text{approx.} \qquad \ldots\ldots\ldots\ldots\ldots\ldots\ldots\ldots\ 2.33.$$

Hence $\frac{px}{P-p} = \frac{\alpha}{Re}$. Assuming that Cv = 0.98 when Re = 2000, then

$\alpha = 80.$ i.e. $\frac{px}{P-p} = \frac{80}{Re}$ $\ldots\ldots\ldots\ldots\ldots\ldots\ldots\ldots\ 2.34.$

To generalise the whole position in regard to the determination of Cv, let N = index of approach velocity representative of the head loss.

$$\left.\begin{array}{l} \text{i.e. } H_x = \frac{V^N}{2g} = M\frac{V^2}{2g}\ (Re.\ C_v)^{N-2} \\ \text{But } Hx = \frac{V^2}{2g}\left[\frac{1}{C_v^2} - 1\right] \end{array}\right\} \frac{1}{C_v^2} - 1 = M.C_v^{\ N-2}Re^{N-2} = K.\frac{Cv^N}{Cv^2}$$

where $K = M.Re^{N-2}$ and $2 > N > 1$

hence $1 - K\ Cv^N = Cv^2$

$$KC_v^N + C_v^2 - 1 = 0 \ \ldots\ldots\ldots\ldots\ldots\ldots\ldots\ldots\ldots\ 2.35.$$

This expression is too complicated to give a simple relationship between Cv and N,K. Even if this were an easy mathematical equation, its direct usefulness is in doubt, for the head-loss index N varies as Re and therefore as K.

Mellanby and Kerr (15) have suggested a method to determine Cv from the velocity profile. Thus, assuming that for turbulent flow the velocity distribution, such as in fig. 2.6. follows the law

$$v = v_{\phi} - b.\, x^{2m} \quad \ldots\ldots\ldots\ldots \quad 2.36.$$

and noting that v = o for x = c.

$$v = v_{\phi} \left(1 - \left(\frac{x}{c}\right)^{2m}\right) \quad \ldots\ldots\ldots\ldots \quad 2.37.$$

so that the area under the curve is

$$v_{\phi} \int_{-c}^{c} \left[1 - \left(\frac{x}{c}\right)^{2m}\right] dx = 2\, v_{\phi}\, c\, \frac{2m}{2m+1}$$

If the theoretical velocity is v_t then the area under the curve is $2 v_t.c.$

$$\text{i.e. } Cv = \frac{v_{\phi}}{v_t} \quad \frac{2m}{2m+1}$$

or if $v_{\phi} = v_t$

$$Cv = \frac{2m}{2m+1} \quad \ldots\ldots\ldots\ldots \quad 2.38.$$

This has a fundamental defect however, as the ratio of areas is no criterion. The rate of discharge is a deciding factor if the mouthpiece is full.

$$dQ = 2\pi\, x.dx.u$$

$$Q = \int_{0}^{c} u_{\phi} \left[1 - \left(\frac{x}{c}\right)^{2m}\right] 2\pi\, x.dx = \frac{c^2}{2}\, 2\pi\, u_{\phi} \left(\frac{m}{m+1}\right)$$

If u_t = theoretical uniform velocity

$$Q_t = \pi c^2 u_t.$$

$$\text{Hence,} \quad Cv = \frac{Q1}{Qt} = \frac{u1}{ut} \quad \left(\frac{m}{m+1}\right)$$

assuming $u_t = u_1$

$$= \frac{m}{m+1} \quad \ldots\ldots\ldots\ldots \quad 2.39.$$

which gives a lower value for C_v than does equation 38.

The value of the index m depends upon a variety of factors including the rate of flow, Reynolds number, wall roughness or pipe loss and other variables which it is not possible to determine briefly.

Work on the velocity profile of liquids through pipes has taken a considerable time to develop and the present stage of research indicates that the fundamental law assumed by Mellanby & Kerr is not satisfactory.

A solution derived along the lines indicated by these authorities cannot be complete unless a good knowledge of the velocity distribution before the constriction is available. Once more the author considers that a simplified assumption such as that of "radial flow" will provide a certain amount of fundamental data to form the basis of coefficient and other calculations.

3. The Principles of Flow Similarity.

In the pre-calibration of hydraulic apparatus it is necessary to obtain both geometrical and dynamic similarity in the apparatus and flow pattern. When two systems are similar, the flow coefficients should be equal and other hydraulic phenomena are likewise similar. If the principles of flow similarity are maintained it is possible to compare the performance of two systems.

With orifice flow, similarity is difficult to obtain because of the large number of variables introduced with restricted flow. For this reason it is difficult to compare test results by a number of different investigators without vitiating the precise conditions of similarity. It is therefore convenient to divide the conditions into a number of parts each representative of some controlling factor.

(a) Geometrical Similarity.

To compare one orifice system with another it is necessary for all the dimensions to be in the same ratio as each other. This principle of similarity is shewn in fig. (3.1a); it is necessary for every essential detail of the hydraulic system to be scaled in an accurate ratio. This involves geometrical similarity in the approach and discharge lengths, in the diameters and orifice thickness.

In some cases the orifice is radiused or champfered as in fig. 3.1b. To obtain similarity in these cases it is necessary for the dimensions to be arranged in the same manner. With champfered edges it is considered that geometrical similarity of the linear dimensions should be maintained. Hence,

$$\text{Angle subtended by large orifice} = 2.\ \tan^{-1}\left(\frac{d_1 - d}{2.\ l.}\right) \quad \ldots\ldots\ 3.1.$$

$$\text{" \quad " \quad " smaller "} = 2.\ \tan^{-1}\frac{k(d_1 - d)}{2\ k\ l}$$

$$= 2.\ \tan^{-1}\left(\frac{d_1 - d}{2\ l}\right) \quad \ldots\ldots\ldots\ 3.2.$$

from which it will be seen that to preserve geometrical similarity the angle of champfer must remain constant.

It is of utmost importance that the approach and discharge sections should be in correct proportion. There are limits of straight pipe which have been set, beyond which it is not necessary that similarity should be maintained. Up to these limits it is essential that the system shall be geometrically similar in order that the flow shall suffer the same conditions in each case. This is important with regards to such details as wall roughness. Experiments have shewn that the wall roughness influences the boundary layer thickness and the velocity profile across the stream, both of which have an effect on the orifice discharge characteristics.

(b) Dynamical Similarity.

The conditions necessary for flow similarity require the production of similar dynamic patterns, generally covered by the expression "scale effect." Vortices of proportionate strength, pitch and spacing are often classified as examples of dynamic patterns. With orifice flow the deductions made by Reynolds are fairly satisfactory as a basis for flow calibration.

Reynolds Number must not be regarded as a completely satisfactory basis of correlation for obstructed flow. This question was discussed by Tuve and Sprenkle (16) who raised the following points.

(1) The flow must be steady, non-pulsating and non-helical. In practice, undamped pulsations in the approach violate these conditions and restrict the application of Reynolds' number in this section of the system; vortex formation in the discharge section is constrained by the pipe walls and therefore pulsations are transmitted through the fluid and Reynolds' number again fails as a basis of correlation.

(2) The approach velocity = mx orifice velocity so that corrections for the approach flow are not independent of the geometrical similarity of the system.

(3) The discharge vortex system is not wholly dependent upon Reynolds' Number.

(4) Reynolds number does not account for all the properties of the fluid.

By applying Lord Rayleigh's theory of dimensional similarity to geometrically similar orifices, Mawson (17) has demonstrated that it is possible to apply these principles and shewed that

$$C_D = A + B \, f\left(\frac{\nu}{4\sqrt{2\,g\,H}}\right) \qquad \text{......} \; 3.3.$$

while Swift has shewn that for viscous flow

$$C_D = A_1 + B_1 \left(\frac{\nu}{L.\sqrt{2\,g\,H}}\right) \qquad \text{......} \; 3.4.$$

Cornish (18) on the other hand, regards the "capillarity-number" expressed by $\frac{d.w.Q^2}{6\ A^2}$ to give a better basis for comparison with free discharge through small orifices under low heads.

In view of the considerable conflict of views in this matter it seems that a method suggested by Swift is the easiest method of obtaining a comparison when a large number of factors are involved. This method, which was derived from the mathematical theorems of Riabouchinsky (19) gives:

$C_D = C_o +$ arithmetical summation of functions of the modifying factors.

$$\text{i.e. } C_D = C_o + f'(V) + f''(H) + f'''(d) \quad \text{..... etc......} \quad 3.5.$$

for which it is necessary to obtain the functions in order to effect comparison. The author considers that this method affords excellent scope for development.

4. The Re-entrant Nozzle.

Borda shewed from theoretical reasonings based upon the momentum theorem, that the theoretical contraction coefficient for a re-entrant nozzle was 0.500, which corresponds to the minimum possible value for a non-entrant orifice as deduced by Rayleigh. In his classical researches Borda (20) obtained a value of 0.5149 for the contraction coefficient. Other experimenters have also attempted to obtain the minimum coefficient of contraction yet Bidone (21) only reached 0.5547 and Weisback (22) 0.534. These discrepancies appear to arise from a number of factors due to instability at the approach to the nozzle. This causes the curvature of the stream lines to increase the jet at the vena-contracta and so increase the coefficient of contraction.

A point of practical significance was brought out by Unwin (23) when he stated that it was possible for a re-entrant pipe to run full if there was the slightest disturbance in the approach. This confirms that the issuing jet is far from stable and any source of disturbance, no matter how slight, which may arise from experimental imperfections, must inevitably tend to increase the contraction coefficient. In order to obtain the minimum coefficient then, it is necessary to mount the apparatus entirely free from vibration and to ensure that the approaching stream is not disturbed. In practice, these conditions can rarely be obtained, it is most probable that a re-entrant nozzle will run full.

Experiments on the flow of various liquids (including mercury) through glass tubes shew that it is possible to obtain a low coefficient of contraction by waxing the sides of the tube. This removes any possibility of the jet-surface adhering to the tube so that contraction is completed.

Investigations by Binnie (24) on the use of a vertical pipe as the overflow for a large tank and in particular its application to large reservoirs, shew that the discharge is greatly affected by the type of flow existing at the entrance to the pipe. In general, three types of flow are distinguishable, (1) full flow in which the stream expands to the full diameter of the pipe after the vena-contracta, (2) Borda flow in which the stream contracts to a minimum diameter which is maintained after the vena-contracta and (3) an intermediate flow in the transition stage from (1) to (2). It can be seen from figs. 4. 1a. that at very low heads the water adheres to the pipe while surrounding an undisturbed core of air (water appears black in the photograph and air is white.) Fig. 4. 1b. shows various stages of pulsation in the flow which produce a gulping noise after the head has increased to about 0.90 ins. As the head increases so the frequency of the noise decreases until in fig. 4. 1f. a fluttering, transient ripples are produced which grow until at fig. 4. 1h. the base of a high head vortex becomes visible. The critical head at which noise ceased (indicating the cessation of air entrainment) was determined by Binnie for several arrangements, these are given together with the flow rates in table I below.

TABLE 4.1.

Arrangement.	Critical Head (ins.)	Flow (cu. ins/sec.)
a. Flat end, 1" dia. pipe 2 ft. long	0.95	75
b. Sharp end " " " " " "	0.92	68
c. " " " " " 5 ft. long	1.02	93
d. 1" dia. pipe 5" trumpet 5 ft. long overall	0.60	116

Calculations based on the assumption of full-flow show that the discharge coefficients under the above circumstances are as given in Table II.

TABLE 4.2.

	Head (ins.)	Velocity (Ins./sec)	Theoretical Discharge (cu. ins/sec.)	C_D
a.	24.95	99.80	78.40	0.957
b.	24.92	99.75	78.30	0.867
c.	61.02	153.00	120.10	0.774
d.	60.60	152.60	111.90	0.968

The high values revealed by this analysis are such as may be expected with full-flow.

In general, the literature for re-entrant mouthpieces is extremely scant, possibly due to the assumption that a low C_D must always exist. This erroneous impression has probably arisen from the widespread publication of Borda's theoretical coefficient without reference to practical results. That this flow is unstable and full-flow with high coefficients more probable should be more fully appreciated and the applications of this mouthpiece better recognised.

CHAPTER 2.

The Effect of the Fluid and Flow Properties on the Discharge.

5. Viscosity.

The straight isothermal flow of a fluid through a long straight pipe was shewn by the classical experiments of Osborne Reynolds to take place by means of one of several mechanisms. At low Reynolds Numbers the individual particles of a fluid flow in straight lines parallel to the axis of the pipe, they have no appreciable radial component of velocity. This is known as laminar, streamline or viscous flow which persists for Reynolds Numbers between 0 and about 2000. A transition zone exists between 2000 and 3100 in which the flow is partly laminar and partly turbulent. With turbulent flow at high Reynolds Numbers the individual particles move in irregular paths with velocity components in all directions. Sound waves originate at very high Reynolds Numbers* in the region of supersonic velocities, shock waves being produced by the propagation of pressure through the flowing fluid. This briefly explains the types of flow which may be distinguished when a fluid flows isothermally through a straight pipe; in practice the flow is mainly turbulent but in some cases the flow through the orifice is viscous. More frequently (and this is a point which is not always appreciated) the approach flow may be viscous while flow in the orifice region to the vena-contracta and further downstream until stable conditions are resumed, the flow may be turbulent. Thus, if

$$Re_{approach} = \text{approach Reynolds Number}$$

$$= \frac{V.D}{\nu} \quad \ldots\ldots\ldots\ldots\ldots\ldots\ldots\ldots\ldots\ldots \quad 5.1.$$

$$\text{Rate of flow, } Q = V.\frac{\pi D^2}{4} = v\,\frac{\pi}{4}d^2$$

$$\text{i.e. } V.D = v.d.\left(\frac{d}{D}\right) = \sqrt{m} \quad v.d. \quad \ldots\ldots\ldots\ldots\ldots \quad 5.2.$$

Substituting in 5.1.

$$Re_{approach} = \sqrt{m}.\ \frac{v.d}{\nu} = \sqrt{m}.\ Re.\ orifice$$

Thus it is possible for the approach flow to be viscous over a large range of orifice Reynolds Numbers even though the orifice flow is definitely turbulent. When such a state exists - and the authors experiments have included this condition - the flow in the approach

---

* Or, under the aeronautical system of supersonic definitions, at MACH NUMBERS greater than 1.0

will commence as viscous, some way before the orifice it will ~~entire~~ enter the transition zone and finally pass turbulently through the orifice. The following will show that when viscous forces predominate the discharge coefficients are low, rising to a constant value when turbulence prevails in both the approach and through the orifice. It is therefore to be anticipated that under conditions of viscous approach and turbulent discharge the coefficient will be lower than for complete turbulence.

At low Reynolds Numbers the flow is completely viscous and considerable influence on the flow is exercised by the shear forces between adjacent particles and layers of fluid. It is possible by an elementary mathematical manipulation* to shew that the velocity distribution across a pipe under purely viscous flow is

$$v = V_{max.} \left(1 - \frac{y^2}{R^2}\right) \qquad \ldots\ldots\ldots\ldots\ldots\ldots\ldots\ldots \quad 5.3.$$

where y = variable radius, R = radius of the pipe.

Integration of 5.3. shews that the mean velocity of flow, $V_{mean} = \frac{1}{2}.\ V_{max.}$

$$\text{hence,} \quad v = 2.\ V_{mean} \left(1 - \frac{y^2}{R^2}\right) \qquad \ldots\ldots\ldots\ldots\ldots\ldots\ldots \quad 5.4.$$

This variation of velocity is interesting, studied in conjunction with the velocity distribution in the region of the orifice it shews that while some of the stream lines will be retarded, others will be accelerated. The effect of these forces are negligible for purely viscous flow but in the viscous-turbulent systems previously described they must influence the discharge.

5a. Viscous flow through orifices.

When liquid flows through an orifice at very low Reynolds Numbers the streamlines converge and diverge symmetrically around the edge as in fig. 5.1. Johansen (25) shewed in a series of photographs of the flow pattern that as the rate of flow, i.e. Reynolds Number increased, the divergence of the stream lines in the jet behind the orifice was not so rapid. At very low Reynolds Numbers there is little or no contraction of the jet, i.e. there is no perceivable vena-contracta so that the coefficient of contraction is very nearly unity.

---

* Consider an elemental cylinder radii y and $y + dy$, length l pressure difference p.

Viscous forces = Area x Viscous Stress = $2\pi\, y\, l\, \mu \frac{dV}{dy}$

Pressure force = Area x Pressure Difference = $p.\ \pi\, y^2$

Equating $\quad dV = \frac{p}{2\mu l}\ .\ y\, dy$

Integrating $\quad V = \int_y^R \frac{p}{2\mu l}\, y\,dy = \frac{p}{4\mu l}(R^2 - y^2) = V_{max.} \left(1 - \frac{y^2}{R^2}\right)$

Many investigators have conducted experiments to determine the effect of viscosity on the discharge coefficient. The most complete series of results have been published by Johansen (26) in R. & M. 1252 for the flow through sharp-edged orifices at very low heads. Five orifices of diameter ratios $(\frac{d}{D})$ 0.090, 0.209, 0.400, 0.595 and 0.793 were used and in each case, geometrical similarity with regards to diaphragm thickness was maintained. The results of these experiments shewn in figs. 5.2. indicate

(i) at very low Reynolds Numbers the discharge coefficient varies directly as $\sqrt{Re}$.

(ii) considerable variations in the discharge coefficient occur in the transition zone according to the variations in the diameter ratio.

All Reynolds Numbers plotted in these curves refer to the orifice, this is a common practice but the author believes that they should be made with reference to the pipe as this would offer a better ready basis for comparison with the friction loss and similar data.

It can be shown from fig. 5.2(a) that conclusion (i) above holds for each orifice. Let this be expressed by

$$C_D = N. \sqrt{Re} \qquad \text{5.5.}$$

The variations of N with the orifice diameter are shewn in table 1. together with the range of flow over which this linear law holds.

TABLE 5.1.

$\frac{d}{D}$ =	0.090	0.209	0.400	0.595	0.794
$\frac{1}{\sqrt{\frac{m}{N}}}$	0.1561	0.1539	0.1481	0.1389	0.1273
Re at which change occurs	$3.1^2 = 9.68$	$2.6^2 = 6.80$	$2.9^2 = 8.45$	$3.0^2 = 9.00$	$3.2^2 = 10.30$

In order to reduce discrepancies in viscosity due to variations in the rate of shear. Bond (27) used mixtures of glycerine and water to obtain variations in the kinematic viscosity of from 0.001 to 7.00. With such mixtures flowing through a sharp-edged orifice 0.1469 c.m. diameter 0.0075 c.m. thick in a glass tube 2.85 c.m. diameter, Bond obtained a curve similar to fig. 5.2(a). Measurements were made from the published graph (with some difficulty as the graph was small and no values were tabulated) the following values were obtained.

TABLE 5.2.

$\frac{d}{D}$	0.0515
N	0.180
R_e	$1.8^2 = 3.26$ (very approximately)

Bond shewed on his curve that previous experiments by Davidson (28) obtained with thick engine oil flowing through a rounded orifice, differed very considerably according to the viscosity. He attributed this to variations in the rate of shear owing to the engine oil. The effects of rate of shear were neglected by Tuve & Sprenkle (16) who used a considerable number of different liquids with a wide variation in viscosities; the results which they obtained were consistent with those of other investigators.

In all experiments other than those by Davidson the variation in R_e of each liquid was derived by varying the velocity. Davidson varied R_e by heating the oil. It would seem therefore that the discrepancies in the latter's results arose from two sources (i) the use of rounded orifices (ii) variations in temperature across the jet. Rounded or bevelled orifices, as will be shewn later, influence the discharge coefficient considerably so that it is difficult to compare them with the results of sharp-edged orifices. When the fluid is heated the temperature across the jet depends upon the rate of heat transferrence, i.e. upon the rate of convection and conduction which are themselves proportional to the fluid velocity. With viscous flow it has been shewn in equations 5.3 and 5.4 that the velocity distribution is parabolic. A pioneer investigation by Pannell (29) in 1916 shewed that the temperature distribution resembled the velocity distribution for liquids in turbulent flow. A similar resemblance with laminar flow was indicated by McAdams (30) who stated that the application of heat to a liquid in laminar flow gave the particles a transverse velocity which distorts the form of the velocity-profile curve; the effect was small however and the temperature varied systematically across the section.

The effect of thermal flow cannot be easily resolved for a basis of flow similarity. Viscosity will vary over the section so that some correction may be necessary when using the mean value given by the ordinary methods of viscosity measurement. These variations are therefore more likely to be more important than rate of change of shear due to variations in velocity. This conclusion appears to be supported by the results of Griffiths (31) for the viscosity of water at low rates of shear in which no experimental evidence could be found that at low rates of shear the viscosity of air-free water differed from that at normal rates of shear. This would confirm the impression that rate of shear is not critical for the viscous flow through orifices.

Tuve and Sprenkle obtained their curves from a great number of readings, the results of numerous experiments. Their results shew that with very viscous liquids the discharge coefficient is independent of the diameter ratio. The following results were taken from their published graph.

TABLE 5.3.

$\frac{d}{D}$	Not known.
N.	0.16
Re.	4.50

Emmons (32) showed from theoretical considerations derived by applying the Navier-Stokes equations that $C_D \propto R_e^{\frac{1}{2}}$ and indicated that the curves of Smith & Steele (33) gave $C_D \propto R_e^{0.48}$ and that those by Edward S. Smith (34) follow the law $C_D \propto R_e^{0.51}$. It would seem that the power of R_e given by experiment is not always consistent and that the theoretical index of 0.50 satisfies most conditions. The following values have been compiled from the curves published by Emmons.

TABLE 5.4.

Author.	Smith & Steele.	Hodgson.	A.S.M.E.
$\frac{d}{D}$	0.10 (Nozzle)	0.842	0.50
N	0.074	0.097	0.06
* B	0.003	0.0137	0

* This is a constant term introduced in the equation $C_D = N.R_e^{\frac{1}{2}} + B$.

Experiments by Hodgson quoted by Johansen gave the results of Table 5.5 taken from "smoothed" curves.

TABLE 5.5.

$\frac{d}{D}$	0.00	0.2	0.4	0.6	0.8
N	0.1565	0.1505	0.1376	0.1209	0.1005

These were obtained with sharp-edged orifices and not square-edged orifices of constant thickness/orifice diameter ratio as used by Johansen himself.

5b. Co-ordination.

When the results of these experimenters are co-ordinated as in fig. 5.3. it will be seen that considerable variations exist in the values of the slope "N." The results obtained a consistent and uniform method presenting various values of N and $\frac{d}{D}$ such as those of Johansen and Hodgson follow regular laws of variation. The maximum value of N is obtained with $\frac{d}{D} = 0$ and agrees in both series of results, the maximum value obtained by Tuve and Sprenkle is only slightly higher than that given by the others.

By plotting $\frac{1}{N}$ against $(\frac{d}{D})^2$ Johansen obtained the empirical formula

$$\frac{1}{N} = 6.38 + 2.333\,(\frac{d}{D})^2 \quad \text{.......................... 5.6.}$$

which applies to all values of $(\frac{d}{D})$ up to 0.8, which may be expanded into

$$N = 0.1568 - 0.0573\,(\frac{d}{D})^2 \quad \text{...................... 5.7.}$$

The values obtained by Hodgson plotted in fig. 5.3. gives

$$\frac{1}{N} = 6.40 + 5.140\,(\frac{d}{D})^2 \quad \text{.......................... 5.8.}$$

In order to explain the disparity between the slopes of these graphs, Johansen considers the effect of the parallel portion of the square-edged orifice to cause an additional resistance in the velocity of the flow and therefore to cause a reduction in Cv. To confirm this it seems that further data relating the effect of orifice length on the discharge characteristics at low rates of flow, is required.

The comparisons serve to show some variations in the viscous region at various different diameter ratios. The results presented by Bond, Smith & Steele, and the A.S.M.E. Summary appear to lie outside the range of systematic variation, but this may be due to experimental errors and to variations in geometrical similarity. This latter factor was rigidly maintained by Johansen, which probably accounts for the uniformity of his results. An interesting substitution by this author was to determine the equivalent length of pipe with the same diameter as the orifice which would produce the same resistance to flow as the orifice. Hence, on the basis of Poisevilles equation for laminar flow he produced

$$\frac{b}{d} = \frac{1 - (\frac{d}{D})^4}{64.N^2} \quad \text{.............................. 5.9.}$$

No systematic variation in the Reynolds Number at which the flow departs from the square-root law is to be found, it is probable that completely viscous flow exists only in the region of R_e less than 10. Some indication of the behaviour at low Reynolds Numbers is to be found in the work of Davies & White (35) for the flow of fluids through rectangular and square pipes. These investigations shewed that a complete state of laminar flow existed up to an R_e of 140 in which vortex formation was not possible, Johansen also determined a region of laminar stability up to an R_e of 141. The closeness of these two results serves to indicate the existance of a laminar state up to 140-141 and a sub-laminar flow in the higher range.

5c. <u>Theoretical Conjectures on the Laminar Flow of Fluids through Orifices.</u>

Visual observations of the flow through orifices confirm that at very low Reynolds Numbers the coefficient of contraction approaches unity so that the low coefficients of discharge arises from the very small coefficient of velocity. Under viscous flow the loss of pressure is due to the energy loss by shear between adjacent concentric tubes of fluid.

In equations 5.3 and 5.4 the pressure drop along a pipe was shown to vary directly as the mean velocity and pipe length

$$\text{thus,}\quad p = 2.V_{mean} \times \frac{4\mu.l}{R^2} \quad \ldots\ldots\ldots\ldots\ldots\ldots \quad 5.10.$$

Johansen shewed from his results that the pressure loss through an orifice could be expressed in terms of an "equivalent pipe," equation 5.9. The physical significance of this deduction has not yet been made clear, but from general laws of viscous flow it seems that the pressure drop through an orifice is due to

(i) the theoretical Bernoulli - pressure-drop due to interchange of kinetic energy,

(ii) viscous losses which depend upon

(a) the velocity (b) length of "equivalent pipe"
(c) reciprocal of the coefficient of viscosity.
This viscous loss represents the pressure loss.

Now, adopting the loss of head method used by both Swift and Howland it will be seen that the loss of head, $h_x = (\frac{1}{C_v}2-1)\frac{v^2}{2g} = \frac{p}{w}$, and

using the value given in equation 5.10 for the values of an "equivalent pipe," with viscous flow,

$$(\frac{1}{C_v}2 - 1)\frac{v^2}{2g} = (\frac{8 v \mu L}{r^2})/w$$

$$= \text{Constant} \times \frac{v^2}{2g} \quad \frac{1}{Re} \quad \ldots\ldots\ldots\ldots\ldots\ldots \quad 5.11.$$

where v = mean velocity through the orifice

L = "equivalent pipe length" of orifice bore

R_e = Reynolds Number for the orifice.

and therefore the <u>Constant K</u> = $8.g. \frac{L}{r}$

Equation 5.11 gives a value for C_V of

$$C_V = \left(1+\frac{K}{Re}\right)^{-\frac{1}{2}} \quad \text{..................................5.12.}$$

and assuming $K > R_e$ we get

$$C_V = \left(\frac{Re}{K}\right)^{\frac{1}{2}} - \frac{1}{2}\left(\frac{Re}{K}\right)^{3/2} \quad \text{..................................5.13.}$$

When Re is small, the second term of this equation may be neglected so that

$$C_V = \left(\frac{1}{K}\right) \sqrt{R_e} \quad \text{..................................5.14.}$$

Assuming C_c = 1.0 at very low Reynolds Numbers over the range in which equation 5.14 applies,

$$C_D = \left(\frac{1}{K}\right) \sqrt{R_e} \quad \text{..................................5.15.}$$

Comparing this with equation 5.5 we see that the constant

$$N = \frac{1}{\sqrt{K}} = \sqrt{\frac{r}{8g.L}} \quad \text{..................................5.16.}$$

The factor L in this equation is empirical,

$$\therefore \frac{L}{d} = \frac{1}{16g.N^2} \quad \text{..................................5.17.}$$

Although devised in a different manner to 5.9 this equation is of the same form although it indicates a very short "equivalent-length" of pipe.

It is interesting to note that if the value of $N = \frac{1}{K}$ given by Johansen in 5.6. is substituted in 5.13 and C_c taken as 1.00, i.e. $C_D = C_V$, it will be seen that

$$\frac{d(C_D)}{d\,R_e} = \frac{1}{2} K^{\frac{1}{2}}(R_e)^{-\frac{1}{2}} - \frac{1}{2}K^{3/2}\ 3/2(R_e)^{\frac{1}{2}} \text{.................5.18.}$$

and that when C_D is maximum, i.e. 5.18 is zero, we have

$$R_e = 3/2\ K$$
$$= 61.4 + 44.6\ m^2 + 8.20\ m^4 \quad \text{.........................5.19.}$$

This will be seen to vary from $R_e = 61.4$ at $m = o$ to $R_e = 114.2$ at $m = 1.0$, both of which are much lower than those obtained in experiments and recorded by Engel & French (36) in fig. 5.4. From an analysis of this graph it would appear that at $R_e = 140$ corresponding to $m = o$ there is a limit to a type of flow in which no eddies can develop, i.e. it is entirely viscous. Furthermore, the value $R_e = 4{,}500$ corresponding approximately to $m = 1.0$, i.e. a smooth pipe, although high, is somewhere in the region of the known transition point which is usually taken to be about 2,300 although laminar flow has been recorded up to values of 20,000 or more. For these reasons it is quite possible that this curve gives the correct relationship between Re and m while equation 5.19 gives values which are far too low. No physical explanation appears to be available to explain this discrepancy.

6. Capillarity or Surface Tension.

The effect of this property on the discharge of a liquid through an orifice is very small. The "skin-tension" property opposes contraction of the jet so that liquids of high surface tension have larger coefficients of contraction than those of lower surface tension. Surface tension does, however, reduce the velocity and causes a lowering of the coefficient of velocity; although this effect is very small and takes place in the short column of liquid between the orifice plate and vena contracta it has a greater relative value than on C_c with the result that the coefficient of discharge is in effect very slightly reduced by surface tension.

Cornish (37) considers however, that capillarity has a far greater influence on the discharge through orifices at very low rates of flow than has viscosity. In support of this view, Cornish quoted experiments which he made on different liquids passing through very fine bores under low heads. Under these conditions it was stated that Reynolds Number (which is based on the laws of similarity for viscous flow) did not yield satisfactory results, but that by using a "capillarity number" (N_y) where

$$N_y = \frac{d.w.Q.^2}{\sigma\ a^2} \quad \ldots\ldots\ldots\ldots\ldots\ldots \quad 6.1.$$

and d = Core of the pipe,

w = density of the fluid,

σ = surface - tension coefficient,

Q = discharge rate,

a = area at vena-contracta.

it was possible to obtain a satisfactory comparison of the various results.

Swift has also reviewed the influence of capillarity and pointed out that while it is almost negligible it has a slightly measurable effect on the free discharge of a fluid under the previous conditions. Capillarity causes a pressure-drop across the jet which may be readily calculated at the vena-contracta, thus from the definition of the surface-tension coefficient

$$2\sigma = \delta p.d = hs.\ w.\ d. \quad \ldots\ldots\ldots\ldots\ldots\ldots \quad 6.2.$$

The back pressure given by this equation will be set up inside the jet so as to reduce the effective head by an amount

$$h_s = \frac{2.\sigma}{w.d.} \quad \ldots\ldots\ldots\ldots\ldots\ldots \quad 6.3.$$

using the constants for water, this equation may be written,

$$h_s = \frac{0.022}{d} \text{ ins.} \quad \ldots\ldots\ldots\ldots\ldots\ldots \quad 6.4.$$

where d is measured in inches at the vena-contracta. It is clear that under favourable capillary conditions, i.e. small orifice diameters and low heads, the effect of capillarity on the discharge may be quite large. By substituting for h_s in the energy equation for discharge it can be shewn that

$$C_c = C_o + \frac{h_s}{2H-h_s}\left(C_o - \lambda\sqrt{2C_o - 1.}\right) \quad \ldots\ldots\ldots\ldots \quad 6.5.$$

and since $C_o = 0.610 > \frac{1}{2}$ this indicates a slight increase in area at the vena-contracta for all positive values of h_s. The constant λ is introduced to allow for variations in the velocity-distribution across the jet between the orifice face and the vena-contracta.

If h_s is the only resistance to flow that is encountered, then we may assume

$$C_V = 1 - \frac{h_s}{2H} \quad \ldots\ldots\ldots\ldots\ldots\ldots \quad 6.6.$$

so that by multiplication of equations 6.5. and 6.6. we obtain

$$C_D = C_o + \frac{h_s}{2H-h_s}\left(C_o - \lambda\sqrt{2C_o - 1}\right) - C_o\frac{h_s}{2H} - \frac{h_s^2}{2H(2H-h_s)}\left(C_o - \lambda\sqrt{2C_o - 1.}\right) \quad \ldots\ldots\ldots\ldots \quad 6.7.$$

which, for capillary flow, with h_s very small, may be written approximately as

$$C_D = C_o - \frac{\lambda h_s}{H}\left(C_o - \tfrac{1}{2}\right) \quad \ldots\ldots\ldots\ldots\ldots\ldots \quad 6.8.$$

which as $h_s \propto 6$, equation 6.3. makes it possible to introduce f (6) as a modifying factor. The value of λ must be $> 0 < 1$, Swift considers that it is probably equal to C_o. But in the extreme case of $\lambda = 1$ the correction for capillary will be $\frac{2\,6}{Hwd}\left(C_o - \frac{1}{2}\right)$ which has a value of about $\frac{.002}{dH}$ for water at normal temperature where d and H are measured in inches.

Expanding equation 6.8.,

$$C_D = C_o - \frac{2\lambda}{\left(\frac{d.w.H}{6}\right)}\left(C_o - \tfrac{1}{2}\right) \quad \ldots\ldots\ldots\ldots\ldots\ldots \quad 6.9.$$

and by definition, $v = \frac{Q}{a} = C_V . \sqrt{2\,g\,H}$

i.e. $\frac{Q^2}{a^2} = (C_V^2 . 2g)H$

$$\text{i.e. } H = \frac{Q^2}{C_v^2 a^2 \, 2g} \quad \ldots\ldots \quad 6.10$$

and substituting in 6.9.

$$C_D = C_o - \frac{2.\lambda C_v^2.2g}{\left(\frac{d\,w.Q^2}{6.a^2}\right)} \left(C_o - \tfrac{1}{2}\right)$$

$$= C_o - \frac{K}{N_y} \quad \ldots\ldots \quad 6.11$$

where N_y = capillarity number, used as a modifying factor

K = constant used in conjunction with function N_y = $2\lambda C_v.^2 2g(C_o - \tfrac{1}{2})$

Equation 6.11. based on the calculations of Swift substantiates the conclusion reached by Cornish that N_y is a good basis of correlation for that type of flow in which capillary predominates.

7. Density.

Broadly speaking, fluid density plays a very small part in orifice flow phenomena. This is perhaps due to the fact that most fluids have densities of about the same order; except for mercury, the density range is very restricted. Density has two main influences, (1) on Reynolds number, (2) on the pressure-variation of gases.

Considering the basic formula for orifice flow given in equation 2.1. namely

$$V = \sqrt{\frac{2g}{w} \left(\frac{P - p}{1 - m^2}\right)} \quad \ldots\ldots\ldots\ldots\ldots\ldots\ldots\ldots\ldots\ldots\ldots\ 7.1.$$

it is seen that the theoretical velocity of discharge varies inversely as the square-root of the density. Again, Reynolds Number varies as the ratio of velocity and density, so that using the theoretical velocity,

$$R_e \propto \frac{V}{w}$$

$$\propto \frac{1}{w^{3/2}} \quad \ldots\ldots\ldots\ldots\ldots\ldots\ldots\ldots\ldots\ldots\ldots\ldots\ 7.2.$$

The laws of discharge for viscous liquids show that in the very viscous range, $C_D \propto R_e^{\frac{1}{2}}$

$$\text{hence,} \quad C_D \propto \frac{1}{w^{\frac{3}{4}}} \quad \ldots\ldots\ldots\ldots\ldots\ldots\ldots\ldots\ldots\ldots\ 7.3.$$

It will therefore be seen that in the region for which density has the greatest of its effects the result upon C_D is not very great. The original statement that fluid density does not play a very large part in orifice flow phenomena is borne out by the first superficial examination. In practice the field of application of these conditions is very restricted and even with chemical engineering installations the range of viscosity is greater than that of density. Some very special fields of application in connection with molten metals may some day require an investigation of the density effect, but even this seems a remote, unpractical possibility.

7a. Compressibility.

Although an attempt has been made to limit this dissertation to the flow of liquids, the effect of density is most pronounced on the effect of pressure variation on the density of gases as they flow through nozzles and orifices. But this aspect is partly applicable to the flow of hot liquids through in an aperture when vapour passes off at the low pressures at the vena-contracta. This problem is more complex than gaseous flow even and is best approached from an initial study of the compressibility effect and density variation of contracted gas flow.

The criterion which represents the effect of compressibility may be written in the form $\chi = \frac{r}{\gamma}$ where

r = ratio of pressure difference to initial pressure = $\frac{p1 - p2}{p1}$

γ = ratio of the specific heats of the gas.

This is applied to orifice flow through the introduction of an "attenuation factor C_A" which is used to account for the variation between the actual weight of gas which is discharged as compared with that which is calculated from the equation based on St. Venants formula (38) which is based on the initial density

i.e. C_A = Actual weight discharged ÷ Weight based on the initial density

$$= \frac{1}{r} \cdot \frac{\gamma}{\gamma - 1} \cdot R^{2/\gamma} \quad 1 - R^{\frac{\gamma - 1}{\gamma}} \quad \frac{m^2 - 1}{m - R^{2/\gamma}} \quad \ldots\ldots\ldots\ldots\ldots\ldots \quad 7.4.$$

where $R = \frac{p2}{p1} = 1 - r$. It should be noted that for an inviscid liquid, C_A corresponds to C_D. In most metering apparatus, r is very nearly equal to 1, so that

$$C_A = (1 - \tfrac{3}{4} \cdot \tfrac{r}{\gamma}) \sqrt{\frac{m^2 - 1}{m - R^{2/\gamma}}} \quad \text{approximately}$$

and when m is small, it further approximates to

$$C_A = 1 - \tfrac{3}{4} \cdot \frac{r}{\gamma} \quad \ldots\ldots\ldots\ldots\ldots\ldots\ldots\ldots\ldots\ldots\ldots\ldots \quad 7.5.$$

These calculations assume $C_c = 1.00$ although experiments by Hodgson (39) for the flow of gases through a sharp-edged orifice shewed that it was possible to express the coefficient of contraction in the form

$$C_c = C_o \; (1 \quad 0.585 \, \frac{r}{\gamma}) \quad \ldots\ldots\ldots\ldots\ldots\ldots\ldots\ldots\ldots\ldots \quad 7.6.$$

so that

$$C_D = C_o \; (1 - \tfrac{1}{6} \cdot \frac{r}{\gamma}) \quad \ldots\ldots\ldots\ldots\ldots\ldots\ldots\ldots\ldots\ldots \quad 7.7.$$

7b. Vapours.

Some common installations such as carburettors involve fluid metering under evaporating conditions, volatile fuel approaching the orifice in the liquid state and passing off as a vapour when the pressure falls so that the vapour is liberated. In the case of the carburettor this feature is coupled with excessive evaporation and mechanical disintegration. Vapourisation introduces complications (1) in that the true densities and viscosities cannot be easily determined (2) the pressure conditions are influenced by the expansion of the vapour. Except for a few casual references in scattered publications this does not appear to have been studied very seriously yet.

8. Total Head.

The velocity of flow varies directly as the square-root of the pressure-head for turbulent flow; and directly as the pressure-head for viscous flow. It is known that the total head influences the discharge coefficient and experiments have shewn that although the effect is small, it is easily measureable.

The precise effect of variations of head cannot be traced to any marked influence upon either the coefficients of velocity or of contraction since it follows a fairly uniform law over the whole flow range. It may be, however, that the change in flow similarity produces these fairly systematic variations in the discharge coefficient.

Swift has shewn that in order to introduce a modifying factor to compensate for the effects of head it is possible to relate the total head and orifice diameter in the form

$$C_D = f\left(\frac{H}{d}\right) \quad \ldots\ldots \quad 8.1.$$

For an aperture placed in a vertical plane the head of liquid is not the same for each filament, but corrections on a rational basis which have been proposed by Monteil (40) may be expressed in the form

$$C_D = C_o - A\left(\frac{r}{H}\right)^2 \quad \ldots\ldots \quad 8.2.$$

for rectangular and circular orifices, where r is the semi-vertical dimension of the orifice. For values of $H > 4\,r$ the modification is quite small and almost negligible, but with lower heads the position of the orifice influences the discharge.

With an orifice fitted in the horizontal plane, all filaments are placed under the same head and no correction factor between the orifice dimensions and head is required.

The equation

$$C_D = C_o + K.H^{-\frac{1}{2}} \quad \ldots\ldots \quad 8.3.$$

has been supported by experiment as a relationship between C_D and H. Swift quotes Hamilton Smith and Bovey (41) for the relationship

$$C_D = C_o + \frac{0.036}{d\sqrt{H}} \quad \ldots\ldots \quad 8.4.$$

where d and H are measured in inches; it was found that $C_o \rightarrow 0.590$. Mawson (17) found from the values of Hamilton Smith and Balton (42) that the expression

$$C_D = 0.592 + 0.002637\left(\frac{1}{d\sqrt{H}}\right)^{0.736} \quad \ldots\ldots \quad 8.5.$$

could be obtained. It seems however that Mawson has worked to an over-large accuracy in computing this formula and that experimental errors have caused the 0.736 power to be obtained. Unwin (23) quotes Mair (43) for the relationship

$$C_D = 0.6075 + \frac{0.0028}{\sqrt{H}} - 0.0037\, d \quad \ldots\ldots\ldots\ldots\ldots\ldots\ldots \quad 8.6.$$

where H is in feet and d in inches; and if H is in inches equation 8.6. may be written

$$C_D = 0.6075 + \frac{0.0028}{\sqrt{H}} - 0.0037\, d \quad \ldots\ldots\ldots\ldots\ldots\ldots\ldots \quad 8.7.$$

Values quoted by Bazin (44) yield the expression

$$C_D = 0.626 + \frac{0.001}{\sqrt{H}}$$ where H is in metres; which becomes

$$C_D = 0.626 + \frac{0.00016}{\sqrt{H}} \quad \ldots\ldots\ldots\ldots\ldots\ldots\ldots\ldots\ldots \quad 8.8.$$

where H is in inches.

It seems from the foregoing that except for Mawson's equation at 8.5. the discharge coefficient may be expressed as a function of $\sqrt{H}$. Swift gave a value of 0.590 as the possible value for C_0 but the experiments quoted indicate discrepancies between the values obtained for both C_0 and K. If other modifying factors were not present it is possible that the correct value for C_0 should be about 0.610.

9. Approach Conditions.

With flow metering apparatus, every effort is made to instal the orifice in such a manner that the contracting stream lines are not under the influence of preceding disturbances. That means that the approach conditions must not upset the flow.

For this reason, devices are used to "damp out" any unwanted approach disturbances. In general, a length of approach pipe is placed before the orifice, this length must always be greater than a certain prescribed minimum, the value of which does not yet appear to have been completely determined, but which depends upon the disturbances at the entrance to the pipe. Only in metering instruments is the method of installation important; in connection with such apparatus as fuel injection pumps and nozzles, or in carburettors, the approach piping is governed by other requirements and probably conforms to a very tortuous form.

The discharge characteristics of these devices will vary considerably according to the proximity of the metering device to the disturbance. Disturbances may arise from bends, pipe roughness, contractions, valves or other obstructions involving the formation of eddies.

9a. The "inlet-length" for liquid entering a pipe.

When liquid enters a pipe it usually has an almost constant velocity profile as in fig. 9.1. This constant-velocity condition may be quite definitely obtained if a short trumpet-shaped funnel is fitted to the pipe-inlet and no disturbances allowed to effect the inflowing liquid; it is however, a condition which may also be quite easily obtained with a straight, square-entry pipe if swirl, etc., is eliminated from the approach. As the liquid passes along the pipe, fluid near the walls is retarded and the central portion accelerated in order to ensure a constant discharge across each section. The retarded fluid (which eventually forms the boundary layer) gradually grows until the ultimate thickness is reached and a stable velocity distribution is attained. This process is shewn in fig. 9.1.

With viscous flow, the boundary layer ultimately extends to the centre of the pipe. It will be seen that until the boundary layer reaches the centre of the pipe a core of fluid exists which has been practically uninfluenced by viscosity, furthermore it will be seen that as the core accelerates there is a corresponding fall in pressure. For orifice metering it is usual (as has been previously explained) to place the orifice at a place free from disturbance, in this case the distance must be such that the central core has vanished and the boundary layer has fully formed.

The "inlet length" has been calculated from the approximations of. Pohlhausen (45) and Schiller (46) for the transition region of fluid flowing in viscous flow, giving approximately

$$x = 0.075 . r . Re. \qquad 9.1.$$

and that the pressure at this point is given by

$$p_o - p = 1.5 . w . (V_{mean})^2 \qquad 9.2.$$

where p_o = pressure at the entrance

V_{mean} = mean flow velocity.

These values hold only for undisturbed entry. The form of disturbance associated with the transition from laminar flow to turbulent flow in a straight pipe of circular cross-section with various types of entry have been examined experimentally by Schiller (47) and Naumann (48), a coloured indicator being used for visual and photographic inspection. Three types of flow were distinguished in these investigations,

(1) At very low Reynolds Numbers, even if the approach before entering the pipe was disturbed the motion inside the pipe was not interrupted and the coloured thread remained perfectly straight. Naumann considers this condition to be maintained throughout the "viscous range" discussed in section 5(c), but, however, he quoted Re = 280 as a limiting factor. This requires further investigation in view of the value 140 - 141 previously ascribed.

(2) A wave-like form is assumed by the filament at higher Reynolds Numbers which is maintained for roughly the "inlet length" but becomes straight further downstream. The wave is apparently due to a vortex sheet being formed at the edge of the entry pipe which is probably unstable at fairly high speeds. This is maintained up to Re = 1600.

(3) When Re is between 1600 and 1700 the vortex sheet breaks up into a single large stationary single eddy which extends from the pipe entry to a distance downstream. This breaks down into a series of eddies so that damping-out of the initial disturbances cannot be achieved and the flow is wholly turbulent.

The sequence of these operations is shewn in fig. 9.2.

With turbulent flow it has only been possible to calculate the transition or inlet-length by assuming a wholly turbulent flow at inlet. Latzo (49) based his calculations on the momentum equation with an assumption of the 1/7th power law for the velocity distribution in the boundary layer. This calculation gave a value of

$$x = 1.386 . r . (R_e)^{\frac{1}{4}} \quad \text{.......... 9.3.}$$

This value is smaller than that given by experiment, the nearest value being that attributed to Nikuradse with a value of 40 diameters at $R_e = 9 \times 10^5$, when the theoretical value was 21 diameters. Such discrepancies are probably due to the difficulty of obtaining completely turbulent entry conditions such as the calculations assume.

If an orifice is placed anywhere between the pipe entry and the inlet length, the approach velocity will not be stabilised and some of the undisturbed core will contract into the orifice. It would thus be possible for a combined viscous-turbulent flow to exist, which would then control the flow characteristics. Since the individual effects of these types of flow are so distinctly different it is usual for metering apparatus to be installed at considerable distances downstream. Rules have been made quoting the minimum inlet length and a very extensive series of regulations are specified by the American Society of Mechanical Engineers in its publication "Fluid Meters: their Theory and Application," a treatise which stipulates minimum lengths for a variety of inlet conditions including free-entry, valves and pipe-bends.

9b. The effect of bends on the flow of liquid through a pipe.

When fluid flows through curved pipes the pressures due to the centrifugal forces create a secondary rotational motion which, when superimposed on the original translatory motion produces a swirl in the fluid flowing through a pipe.

This secondary motion is more pronounced at low Reynolds Numbers, i.e. for viscous flow, than at higher numbers, owing to the fact that the velocity varies so considerably across the section a liquid under viscous flow that centrifugal forces have more influence in producing flow variations than with turbulent flow. Under favourable circumstances the spiral flow will not be easily damped out, therefore a tangential velocity component will exist for some distance along the pipe. If an orifice is placed in the vicinity of this bend the swirl will not be damped out when the stream contracts. It is therefore possible that the contraction and velocity coefficients will be larger under such conditions.

9c. The flow through rough pipes.

The term "pipe roughness" covers the irregularities left on the bore of pipes by minute, irregular undulations as the result of manufacture. When these irregularities project into the fluid the flow may be disturbed setting up eddies and causing loss of head due to self-created variations in the velocity distribution.

Schiller (50) has devised a unique, simple method of estimating the maximum size (e) of these protuberances which will have no effect on the character of the flow through a pipe under viscous forces. Thus from the law (deduced in section 5)

$$v = 2\, V_{mean} \left[1 - (\tfrac{y}{r})^2\right] \quad \text{.............................. 9.4.}$$

the velocity at the tip of a protuberance will be

$$v_e = 2\, V_{mean} \left[1 - (1 - \tfrac{e}{r})^2\right] \quad \text{.............................. 9.5.}$$

$$= 4\, V_{mean} \tfrac{e}{r}, \text{ approximately when e is small.} \quad \text{...... 9.6.}$$

If, therefore, the roughness has not disturbed the flow, the Reynolds Number at this tip will be

$$R_{(e)} = \frac{e.\ Ve}{v} = 2(\tfrac{e}{r})^2 .\ R \quad \text{.............................. 9.7.}$$

where $R = \frac{2.\ r.\ Vmean}{\nu}$. It is stated in "Modern Developments in Fluid Dynamics" (reference 51) that so long as Re is below a critical value depending on the shape of the protuberance, that no vortices will form in the wake, i.e. the velocity distribution will not be affected by wall roughness. Thus, for a cylinder, a critical Reynolds Number of about 50 may exist; this leads, from equation 9.7. to the condition that provided

$$2\, (\tfrac{e}{r})^2\, R < 50$$

i.e. $$\frac{e}{r} < \frac{5}{\sqrt{R}} \quad \text{.................................. 9.8.}$$

the existance of surface roughness will have no effect on the flow. A flat plate normal to the stream has a critical $R_{(e)} = 30$ so that $\frac{e}{r} < \frac{4}{\sqrt{R}}$ is the condition for sharp-edge roughness.

These conditions, based on purely theoretical grounds give some indication of the possible magnitude of the pipe roughness. Thus, taking as a rough general rule

$$\frac{e}{r} < \frac{4.5}{\sqrt{R}} \quad \text{.................................. 9.9.}$$

for a 2" I.D. pipe with R = 900, the maximum value of e is 0.15 ins. (Viscous flow only).

It will be seen that e diminishes as R increases and increases as R decreases. Again, since e varies directly as r its size increases with large pipes and decreases with small bores.

Under turbulent flow it is necessary to include a factor not only for (e) but for the spacing of the protrusions. Generally speaking, if the irregularities do not project into the laminar sub-layer the arguments used for viscous flow will hold; even when these protuberances extend completely in to the boundary layer it is possible to use this reasoning since under such circumstances both the viscous stresses and Re are of comperable magnitude. Bakmetoff (52) presented a general equation deduced from the works of Prandtt, for the velocity distribution in a pipe, thus

$$\frac{v}{V} = \frac{1}{k} \sqrt{\frac{\lambda}{8}} \left\{ \left(k.\sqrt{\frac{8}{\lambda}} + \frac{3}{2} \right) + \log_e. \left(1 - \frac{d}{D} \right) \right\} \quad \ldots\ldots\ldots\ldots\ldots 9.10.$$

in which λ represents the friction coefficient and is related to the roughness size (e) in the manner given in table 9.1. below, and k is a constant taken as 0.40.

TABLE 9.1.

Friction Coefficient λ	0.02	0.03	0.04	0.05	0.06
Roughness $\frac{r_o}{e}$	500	100	45	25	15

The possibilities afforded by equation 9.10 of giving a means of deducing C_D have been exploited by Engel and Davies (53) which is discussed in section 9 (f). It seems however that the methods originally suggested by Kerr and Mellanby (15) in section 2 (b) may be applied indirectly to this equation for the velocity distribution with pipe friction.

Engel and Davies (53) have surveyed the effect of pipe roughness on orifice flow from the aspect of kinetic energy in conjunction with Bernoullis' equations. They showed that compared with the discharge coefficient C_D, for flow through a pipe where $\lambda = 0.002$ the discharge coefficient C_D is given by

$$C_D = C_m \sqrt{\frac{1 - m^2}{a_2 - a_1 m^2}} \quad \ldots\ldots\ldots\ldots\ldots\ldots\ldots\ldots\ldots 9.20.$$

$$\text{where } a = 2\int_0^1 \left(\frac{u}{U}\right)^3 . \frac{r}{r_o} . \; d\left(\frac{r}{r_o}\right) \quad \ldots\ldots\ldots\ldots\ldots\ldots\ldots\ldots\ldots 9.21.$$

which receives the values a_1, a_2 according to the effect of roughness on the velocity distribution and on $\frac{u}{U}$. From Bakmeteff, equation 9.10, it was shewn that for $\lambda = 0.02$, $a_2 = 1.054$, while the value of a_1 depends upon the roughness selected.

When plotted as in fig. 9.5. it will be seen that roughness increases C_D which is a characteristic common to all conditions of turbulent approach. It would therefore appear that if the fundamental characteristics of the turbulence behind an obstruction can be determined it should be possible to apply the results to orifice flow.

9d. Flow through Honeycombs and Grids.

In flow measuring apparatus the use of a grid as a "flow straightener" is frequently suggested. This device uses the principle that the non-translatory velocity, i.e. radial and tangential, will be suppressed by the grids so that only translatory energy will be retained in the fluid. By removing the swirl velocities the necessary "inlet length" decreases to that required by a straight-entry pipe.

A considerable study has been made of the turbulence introduced into a fluid stream by a mesh. This problem has been popular owing to the application of the momentum theory of turbulence diffusion to the mixing length behind a grid. It is stated (51) that the distance downstream at which the wake due to the bars of a grid will be dissipate depends roughly on the ratio $\frac{D}{M}$ where D = diameter of the grids and M = mesh of the grid, and that when $\frac{D}{M}$ is as large as $\frac{1}{5}$ the length is approximately 20M; it is possible that a law of the form

$$x = K_1 \frac{D}{M} + K_2 \quad \ldots\ldots \quad 9.11.$$

relates the mixture length and $\frac{D}{M}$. Allowances, which will not be discussed, are required to modify 9.11 for the effects of the intensity of pre-grid swirl, of the pipe size and with plate grids, the effect of plate length.

9e. Valves and other obstructions.

As with a mesh, the inclusion of a valve or other obstruction causing a contraction of the lines of flow produces a wake consisting of a regular succession of vortices. At very low Reynolds numbers the wake is not formed, because the necessary surfaces of discontinuity are not sufficiently strong. Instead, the flow parts to flow around the obstacle and then returns to its original distribution in the manner shewn for "potential flow." The critical Reynolds number at which this potential flow gives way to an eddy-forming flow depends upon the shape of the obstacle, its relative proportions and also, to a slight extent upon its surface smoothness. The values of R_e = 50 for a cylinder and R_e = 30 for a flat plate edgewise to a stream are only very approximate and are in practice subject to modification under the influence of a number of factors.

As Reynolds number increases beyond the critical, so the eddies which form the wake proceed to break off at a regular frequency and at well-defined spacings. When complete turbulence sets in these eddies are lost in the confusion of the flow, so that it is only for a limited range of flow that they are distinctly visible. The disturbances introduced by these eddies require some considerable distance before they are removed.

In studying the effect of valves and other obstructions on the flow it is necessary to investigate (i) the critical Reynolds number (ii) the strength of the eddies (iii) the transition length in relation to the dimensions of the obstruction. In connection with orifice flow the effects of valves and obstructions are more involved in view of the contraction of the flow and its effect on the eddies.

9f. The effects of turbulence and suppressed contraction on the discharge coefficient.

No exhaustive study has yet been made of the relationship between the approach and CD; it is the object of this dissertation to fill in some of this gap between the various hydrodynamic phenomena. Swift (54) has dealt with the geometry of approach and the effects of a forced turbulence on the discharge through an orifice otherwise very little has been published on this important aspect of orifice flow.

Referring to the suppressed contraction when an orifice is placed in the side of a pipe, fig. 9.3. and the answer to a question in the Maths. Tripos (ii) examination, 1900, Swift showed that the dimensions of the approach chamber normal to the orifice modifies C_o according to the equation

$$\frac{1}{C_o} = 1+\frac{1}{\pi} \left(k_o + \frac{1}{k_o}\right) \log_e \frac{1+k_o}{1-k_o} \quad \ldots\ldots\ldots\ldots\ldots 9.12.$$

where $k_o = \frac{a}{b_1}$

This equation must be treated with some reserve as it does not hold for the zero or infinite values of k_o but it is valuable to demonstrate that for fairly small values of k_o at least greater then 1.0, any alteration to the normal dimension b, will cause a considerable variation in the coefficient C. Similarly, Mitchell (55) has shewn that restrictions to the lateral approach to an orifice, fig. 9.4. will modify the coefficient C_o according to the equation

$$\frac{1}{c} = 1 + \frac{2}{\pi} \left(\frac{1}{k_1} - k_1\right) \tan^{-1} k_1 \quad \ldots\ldots\ldots\ldots\ldots\ldots\ldots 9.13.$$

where $k_1 = \frac{a}{b_2}$

For small values of k_1, i.e. $a \doteq b_2$ this expression may be written approximately in the form

$$C = C_o + 0.12.\ k_1^2 \quad \ldots\ldots\ldots\ldots\ldots\ldots\ldots\ldots\ldots\ldots \quad 9.14.$$

Turbulent approach has been mathematically (and partly experimentally) investigated by Swift in which he suggests that $\frac{l}{\xi}$ would provide a simple unit for comparison, l being a typical linear dimension of the apparatus and ξ is a representative dimension of the eddy system characteristic of the turbulence. Here it should be noted that in general, the degree of turbulence is in some way dependent upon the statistical size of the eddy-formation. Under such conditions the loss of head due to turbulence may be expressed in the form

$$h_x = \frac{v^2}{2g} \cdot a.\ T \quad \ldots\ldots\ldots\ldots\ldots\ldots\ldots\ldots\ldots\ldots \quad 9.15.$$

so that $C_v = (1 + a.\ T)^{-\frac{1}{2}}$

$$= 1 - \frac{a.T}{2} \quad \ldots\ldots\ldots\ldots\ldots\ldots\ldots\ldots\ldots\ldots \quad 9.16.$$

where $T = f\left(\frac{l}{\xi}\right)$ and 'a' is a constant. The discussion on streamlines given by Swift in 1926 shewed that

$$C_c = C_o + b.\ T(1 - C_o)(2 - C_o) \quad \ldots\ldots\ldots\ldots\ldots\ldots\ldots\ldots \quad 9.17.$$

where b is a constant. It can therefore be shewn from equations 9.16/17 that if $C_D = C_v .\ C_c$. then,

$$C_D = C_o + b\ T(1 - C_o)(2 - C_o) - C_o.\ \frac{a.T}{2} \quad \ldots\ldots\ldots\ldots\ldots\ldots \quad 9.18.$$

These shew that although turbulence tends to increase the area of the jet it also reduces the velocity. The increase of jet size is however the dominant factor so that

$$b\ (1 - C_o)(2 - C_o) > \frac{a\ C_o}{2}$$

i.e. if C = 0.610,

$$b > 0.560 \quad a \quad \ldots\ldots\ldots\ldots\ldots\ldots\ldots\ldots\ldots\ldots \quad 9.19.$$

Experiments were made by Swift, turbulence being induced by stirring and by lowering the head, which confirmed the fact that C_D was increased by turbulence. It was found that when the discharge under a gradually falling head was measured it was found that a mean increase of 0.05% was obtained over the mean value.

From the definition of T it is to be expected that turbulence - and therefore C_D - will increase with the orifice diameter, and that the size of the eddies will decrease with the increase of Re.

10. Accelerating (or Pulsating) Fluid.

The calibration of an orifice under conditions of variable flow has not yielded satisfactory results. It is probable that the coefficient is higher for pulsating than for steady flow owing to turbulence; experiments to verify this have not been published, partly due perhaps to several difficulties which are involved in the production of a controlled flow together with complications in the measurement of the pressure-drop.

Discharge varies according to several features characteristic of the flow, (1) velocity-time variations (2) amplitude of the motion and (3) speed of the impulses. An attempt has been made to control these by using a leather, liquid filled bag which was struck by a hammer operated by a cam, this is an indirect method which must necessarily be employed for practical measurements but which is rather hampered by lack of absolute accuracy. It would seem however that the first step to be taken in an investigation of this nature would be to measure the effect of acceleration on the discharge, which could then be applied in a step-by-step integration of the velocity-time curve.

With most commercial plate meters operating under conditions favourable to pulsating flow every effort is first made to eliminate pulsations in the flow to the orifice and then to obtain a steady measuring head. This involves some damping-out of oscillatory pressures arising out of the pulsating head, so that a steady mean value $\bar{q}$ is shewn. Swift (56) states that in order to compute the mean rate of flow from the observed (damped) pressure-difference it is necessary to use a factor given by $\frac{\bar{q}}{q}$ where

$\bar{q}$ = damped reading of the pressure-difference,

q = root-mean-square pressure difference

In order to compute the correct pressure-difference reading it is obvious that q must be used,

$$\text{i.e. } q = \bar{q} \div \frac{\bar{q}}{q}$$

= Observed Reading (damped) ÷ form Factor.

Elementary mathematics have been used to determine $\frac{\bar{q}}{q}$ for various wave forms, thus with liquids under impulsive forces which vary in the manner of two sinusoidal arcs,

$$\frac{\bar{q}}{q} = \sqrt{\frac{8}{\pi}} = 0.90 \text{ approximately} \qquad \text{.......... 10.1.}$$

For the general case in which the flow pulsations follow the law

$$Q = q_o + q_1, \ \text{Sin w.t.} \qquad \text{.......... 10.2.}$$

it can be shewn that

$$\frac{\bar{q}}{q} = \left[1 + \tfrac{1}{2}.\left(\frac{q_1}{q_o}\right)^2\right]^{\frac{1}{2}} \qquad \text{.......... 10.3.}$$

The effectiveness of these artifices when used on flow meter installations has to some extent removed the urgency for calibrating orifices under pulsating flow. It would help to reduce the complications and expense of an installation due to the embodiment of reservoirs and special "damped" manometers, if the coefficients of an orifice under pulsating flow were found. This would also facilitate the design of carburettor jets, injection nozzles and other power plant equipment where flow metering is periodic. The author agrees that the difficulties of such a task are very great but believes that the problem may be tackled directly by the study of accelerating flow, experiments being made on a rotating arm, radius and rotational speed being variable.

CHAPTER 3.

The Effect of the Orifice Design on the Discharge.

11. Orifice Size. The Area Ratio 'm.'

The influence of the area ratio "m" on the approach velocity with also its effect on the flow coefficients were initially detailed in section 2. The theoretical discharge coefficient decreases with increase of m and vice-versa so that the large orifice gives a smaller rate of flow for the same head and general conditions than the small orifice. For this to be obeyed it is necessary to maintain flow similitude. The variations in orifice dimensions arising from changes in the value of m, alter the conditions for geometrical similarity so that comparisons must be based in terms of the area ratio in the manner suggested by Swift.

11a. The Turbulent Zone.

By taking the pressures from tappings on each side of an orifice Engel (57) obtained a series of readings giving the discharge coefficient of orifices of different area-ratios for a wide range of Reynolds Number. From the "smoothed curve" given by Engel the following values have been tabulated:-

TABLE 11.1.

m	0.0287	0.0477	0.0954	0.143	0.285	0.382	0.477	0.525	0.573	0.620	0.668	0.715	0.763	0.816
$Re = 200.10^3$ C_D	0.602	0.611	0.600	0.603	0.609	0.615	0.603	0.603	0.602	0.597	0.592	0.581	0.568	0.548
$Re = 400.10^3$ C_D	0.602	0.611	0.600	0.603	0.609	0.611	0.600	0.598	0.597	0.589	0.583	0.576	0.561	0.537
$Re = 600.10^3$ C_D	0.602	0.611	0.600	0.603	0.609	0.609	0.599	0.596	0.593	0.588	0.581	0.574	0.556	0.529
$Re = 800.10^3$ C_D	0.602	0.611	0.600	0.603	0.609	0.607	0.598	0.596	0.592	0.588	0.581	0.574	0.555	0.528
$Re = 1000.10^3$ C_D	0.602	0.611	0.600	0.603	0.609	0.605	0.598	0.595	0.591	0.587	0.581	0.574	0.554	0.526

When these values are plotted it can be shewn that for any particular flow the curve relating CD to m (where CD is calculated from plate-taps) varies in the manner shewn in fig. 11.1. The curves are only plotted for Reynolds Numbers of 200.10^3, 400.10^3 and 600.10^3 which appears to shew a maximum value for CD of about 0.608 at m = 0.4 approximately. At higher values of m, C_D decreases very rapidly, so that the curves for various Reynolds Numbers almost run together. It will be seen from table 11.1. that in the turbulent zone, increase of Reynolds number causes the curves to develop a steady contour. Engels experiments therefore lead to the following conclusions:

(1) For large values of m at all Reynolds Numbers the discharge coefficient is greatest for a value of m = 0.4 approximately and decreases rapidly as m increases.

(2) For values of m $>$ 0.35, the discharge coefficient in the turbulent region varies inversely as some function of Re so that as Re increases the discharge coefficient decreases to an almost asymptatic value.

These results only cover a limited range which, although it may be described as the 'useful' or 'practical' range, does not provide a complete picture of the problem. Thus the effect of Reynolds Number at small area ratios in the turbulent and laminar zone must be explained.

11b. <u>The Transition Zone.</u>

The general curve shewing the effect of Reynolds Number, given by Johansen, is shown in fig. 5.2. (b) which shews that the discharge coefficient is maximum when in the transition zone and that considerable discrepancy arises due to variations in $\frac{d}{D}$ in this region. Taking the values of CD for various values of $\frac{d}{D}$ in this region, the related values at the constant Reynolds numbers quoted are given in table II. 2.

TABLE II. 2.

Re	$\frac{d}{D}$	0.794	0.595	0.401	0.209
	$m = (\frac{d}{D})^2$	0.630 ~~0.794~~	0.354 ~~0.595~~	0.161 ~~0.401~~	0.045 ~~0.209~~
3600	C_D	0.750	0.675	0.640	0.620
2500	C_D	0.810	0.690	0.645	0.625
1600	C_D	0.890	0.710	0.650	0.625
900	C_D	0.920	0.730	0.660	0.640
400	C_D	0.890	0.755	0.695	0.660
225	C_D	0.820	0.745	0.710	0.685
100	C_D	0.725	0.720	0.690	0.685

It will be seen from fig. 11.2. that for all values of Re the discharge coefficient varies as the orifice ratio m and so decreases as m is reduced.

11c. Laminar or viscous flow.

From a study of fig. 11.2. it will be seen at each value of "m" the slope of the C_D - m curve increases to a maximum with reduction of Re so that beyond the critical, further reduction of Re causes a rapid decrease in slope.

As the value of Re approaches the viscous range the slope of the curve gradually falls so that at very low values of Re, the value of C_D is almost constant for all values of m. Referring back to section 5 (a) equation 5.5. it was stated that $C_D = N.\sqrt{Re}$ and an empirical value of $N = 0.1568 - 0.0573\ m$ was given by equation 5.7. It is evident therefore from these equations that at very small values of Re

$$\frac{d.(C_D)}{dm} = -0.0573\sqrt{Re} \quad \ldots\ldots\ldots\ldots\ldots\ldots\ldots\ldots \quad 11.1.$$

and so as $Re \rightarrow o$ the value of C_D becomes almost constant for all values of m.

11d. Maximum discharge coefficients.

The maximum discharge coefficients shewn by Johansen in fig. 5. 2 (b) exhibit a regular variation with diameter ratio as regards both magnitude and the value of the Re at which they occur. These features are shewn in fig. 11.3 (a) and (b). Extrapolation of fig. 11.3 (a) to values of $\sqrt{m}$ greater than 0.80 suggests that C_D may exceed unity. This is stated to be confirmed by a maximum C_D of 1.04 obtained by Hodgson at $\sqrt{m} = 0.845$. A part explanation of this apparent anomoly is attributed to the disparity in velocity distribution across the pipe at the approach to the orifice and across the jet which is discharged. On the basis that the true kinetic energy of the fluid is obtained from the integration of the velocity distribution curve, Johansen showed that if ϕ is the true discharge coefficient based on the actual distribution of velocity at the two sections where static pressure is measured, then

$$\left[\frac{C_D}{\phi}\right]^2 = \left[\frac{1-(\frac{d}{D})^4}{1-2(\frac{d}{D})^4}\right] \quad \ldots\ldots\ldots\ldots\ldots\ldots\ldots\ldots \quad 11.2.$$

which gives the following values for ϕ

TABLE III.

$\sqrt{m}$	0.209	0.401	0.595	0.794
$C_{D Max}$	0.685	0.708	0.760	0.925
ϕ	0.684	0.698	0.704	0.542

These values are plotted in fig. 11.3 (a) which shews signs of similarity to fig. 11.1.

It is interesting to note that when the approach Re is plotted as in fig. 11.3 (b) that the difference is greatest at small values of m and also that when m = 1.0, $\sqrt{Re}$ = 48, i.e. Re = 2304. The closeness of this to the accepted transition point is a further example of the accuracy of Johansen's results; m = 1.0 corresponds to a straight pipe.

11e. Empirical Formulae.

A cumbersome series of formulae by Buckingham and Bean, was appended to the paper by Beitler (58). This was not satisfactory and has not been adopted very widely. A simpler form taking into account the effects of orifice diameter and which is due to Barnes (59) accounts for both the orifice ratio and Reynolds Number in the form

$$C_D = \frac{0.620}{\left(\frac{Re}{2025}\right)^N} \quad \text{.......... 11.3.}$$

where the index N is a function of the orifice ratio. This equation may be modified in accordance with the experiments of Johansen and Engel, to be of the form

$$C_D = \frac{0.610}{\left(\frac{Re}{2500}\right)^S} \quad \text{.......... 11.4.}$$

where the index S is a function of the orifice ratio. The equations strongly resemble the well-known equation given by Blasius for the frictional coefficient of a smooth pipe but are only valid over the limited range of orifice ratios greater than 0.35 and Reynolds Numbers between 50,000 and 2,000,000. This restricts the operation of these formulae so that the method of modifying factors proposed by Swift is perhaps a better basis for calculations.

Many empirical formulae based on modifying factors have been proposed by many past experimenters. Mair (60) gives the relationship

$$C_D = 0.6075 + \frac{0.0098}{\sqrt{h}} - 0.0037\, d. \quad \ldots\ldots\ldots\ldots \quad 11.5.$$

where h is in ft. and d in inches as an empirical formula relating factors. It would seem from the power of 'd' as though the factor $m^{\frac{1}{2}}$ would apply and that the modifying equation should be of the form

$$C_D = C_o + K.\, m^{\frac{1}{2}} \quad \ldots\ldots\ldots\ldots \quad 11.6.$$

When the values of C_D given in Table I are plotted against $m^{\frac{1}{2}}$ the result is a parabolic type curve with only the slightest resemblence to linearity in the range of $m^{\frac{1}{2}}$ between 0.60 and 0.80. A very rough value for equation 11.6 when Re = 200.10^3 is given by

$$C_D = 0.684 - 0.11\, m^{\frac{1}{2}} \quad \ldots\ldots\ldots\ldots \quad 11.7.$$

It does not yet seem however that a successful solution has yet been obtained so that in the design of flow-meters it is necessary to use the standard values rather than to apply an empirical formula.

12. The Effect of Orifice Shape.

Variations of shape have little application to most common engineering apparatus; for in the manufacture of instruments with which a precise knowledge of the discharge characteristics is essential it is not economical to manufacture anything but orifices of circular shape. Some comparative tests have been made with square, rectangular and triangular orifices but it is probable that slight inaccuracies of manufacture may have masked the effects of shape.

Smith and Walker stated that for any orifice shape the greater the value of perimeter ÷ area of the orifice, the greater does the value of the coefficient of contraction become, they did not however amplify this statement with any experimental evidence. These authorities also stated that it was probable that adhesion of the surface of the jet to the walls of the orifice played an important part in the effect of orifice shape on the discharge. This indicates that surface tension has a large influence on the effect of shape which takes the discussion back to the paper by Cornish where it was claimed that the capillarity number was a more important factor in orifice flow than was Reynolds number* but this is only likely to be true for very small heads. The experiments by Cornish on apertures of various shapes did not indicate any systematic variation due to differences in the periphery of the apertures. It seems that the effect of shape is negligible and that variations due to manufacture induce errors of greater magnitude than those due to the influences of adhesion or surface tension.

A possible effect of shape may also lie in the suppression of radial velocity. Although the author believes that this has no greater influence than capillary it is probable that it influences the position of the vena-contracta. This is due to variations in the rate of application of these axial forces causing a subsequent decrease in the rate of contraction and therefore placing the vena-contracta farther from the orifice.

---

* It should be noted from the definition of "capillarity number" that

$$N_y = R_e^2 \cdot \frac{\mu^2}{d.w.\rho}.$$

13. Orifice Edge-Length.

A "thin-plate" orifice is usually specified in the design of orifices for use in flow measurement. This means that the axial length of the orifice must be small compared with its diameter. When the orifice diameter is fairly large, e.g. greater than $\frac{1}{8}$ inch, the thickness is sufficient to enable the orifice to be cut out of sheet metal and it is therefore more convenient to produce thin-plate orifices than those of greater length. Thin orifices have low discharge coefficients but this is not greatly influenced by slight variations in edge-length so that when made commercially, thin-plate orifices for flow meters are able to be produced more economically and accurately than are long orifices, generally termed "mouthpieces" or "nozzles."

Unwin (23) states that with a thin orifice discharging freely into the atmosphere the jet is completely contracted so that C_D is about 0.610, but with a long orifice or nozzle the contraction of the jet is suppressed so that it issues "full-bore" and C_c becomes unity so that allowing for C_V, C_D is about 0.98. The transition between thin plate and nozzle flow is stated to occur at an edge length about equal to $\frac{3}{4}$ orifice diameter. Gelalles and Marsh (60) found on testing fuel injection nozzles that the coefficient of discharge was constant for $\frac{L}{D}$ between 1.0 and 4.0 but that for $\frac{L}{D}$ greater than 4.0 friction losses in the nozzle bore cause C_D to decrease, while for $\frac{L}{D}$ less than 1.0 the effects gave irregular results but indicated that C_D decreased with reduction of $\frac{L}{D}$. It is probable that irregularities in the bore of these injection nozzles (they are very fine) together with some slight inadvertent burring and beveling of the bore may have caused the inconsistency of these results. Pye (61) states without referring to any experimental works that the effect of $\frac{L}{D}$ is to cause the C_D to be 0.62 for thin plates and 0.98 with long carburettor jets.

In the tests made by Beitler (58) on submerged orifices it was shewn that the coefficient of discharge was constant up to the ratio edge length ÷ orifice diameter = $\frac{1}{8}$ after which C_D increased with $\frac{L}{D}$. An interesting application made by Beitler was the plotting of the coefficient against the "dam height" as represented by $\frac{D - d}{2}$; this showed that the critical height was approximately 4 x edge-length. By introducing the "dam height" Beitler ingeniously contrived to include the orifice ratio as a controlling factor. The effect of pipe diameter was noted by Buckingham (62) in the study which he made regarding the effect of flange and vena-contracta taps.

The Reynolds Number of the flow is also an important factor controlling the critical edge-length since with laminar flow the fluid follows the contours of the obstruction very closely. Thus the critical edge length is a factor, not only of the orifice size, but also of Reynolds Number. It will be seen from the following that the ratio edge length: orifice diameter supplies a favourable bases for comparison.

The effect of edge-length and Re.

Several investigations have been made to determine the influence of the thin edge-length; but in few cases has the "critical" length (for transition between mouthpiece and thin-plate flow ~~occur~~) been evaluated as a function of Re.

A comprehensive investigation was made by Ruppel (63) for very thin orifices. These experiments led to the conclusion that for all diameter ratios the discharge coefficient of cylindrical-edged orifices of ratio $\frac{l}{d}$ less than 0.20 is independent of the edge length at Reynolds numbers of about 5000 and higher. Zuckrow (64) made a thorough study of the effect of nozzle length and Reynolds number. Thus while Ruppel covered the range of small edge-lengths, Zuckrow covered the longer nozzles. Of the two works it would seem that the experiments by Zuckrow give the most reliable results. Plotting the curve obtained from these experiments, fig. 13.1. it will be seen

(1) the "critical" length occurs at about $\frac{l}{d} = 1.0$ for all values of Re.

(2) for $\frac{l}{d}$ greater than the critical the value of C_D decreases as $\frac{l}{d}$ increases.

(3) for $\frac{l}{d}$ greater than the critical C_D increases with increase of Re in the manner shewn in fig. 13.2. for $\frac{l}{d} = 2.0$ and that the curve tends to acquire an asymptotic value of C_D as Re tends to infinity.

The experiments by Zuckrow are unreliable for the range of $\frac{l}{d}$ less than 1.0 and the author does not find Ruppel's results easy to follow. The extra-polated values of fig. 13.1 appear to indicate that the relationship between C_D and Re for the small length ratios follows very different laws to those dictated in the previous paragraphs. No reliable results are available for this zone, but from the work of Zuckrow and also a curve presented by Fisher (65) it would appear that while CD is greatest at low values of Re, this situation is reversed with long orifices or mouthpieces which acquire their maximum coefficients at very large values of Re.

From these results it appears that the effect of edge-length is dependent upon the type of flow. The author is not satisfied however that sufficient experimental information is available to frame a theory from which to deduce the distinguishing characteristics of each type of flow although a preliminary examination of the whole question appears to show that flow through orifices of varying length is governed partly from considerations of viscosity and partly momentum. The pressure distribution at the vena-contracta during momentum flow is probably the criterion for edge-length.

14. Bevel and Rounding.

It has been found from experience with flow-metering orifices and carburettor jets that the slightest rounding or turning of the bevel on the inlet edge will increase the discharge-coefficient considerably. This increase is due to the sensitivity of the CD - Angle of Bevel (α) Curve in the region of the square-edge condition, the slope of this curve is so great when $\alpha = 0$ that a small increment of $d\alpha$ is accompanied by a large increase of dC_D.

Swift showed that for rounded nozzles, if the tangent to the jet at the leading edge made an angle θ with the diameter of the orifice then it could be shown that the coefficient of contraction may be determined by the equation

$$C_c = \frac{\pi}{\pi + 2\cos\theta} \quad \ldots\ldots\ldots\ldots\ldots\ldots\ldots\ldots \quad 14.1.$$

the plot of which shows that Co varies from 0.61 to 1.00 in the manner of fig. 14.1. This curve, it must be agreed, does not comply with the statements previously made, for when $\theta = 0$ the slope of the curve is very small. In practice however, the jet makes an angle with the plate (refer Chapter 4) so that, while giving a very good result, it does not appear desirable to use equation 14.1. too seriously. It is felt that if the relationship between the angle of jet and the angle of bevel were deduced, some use may be then made of the foregoing equation.

In order to simplify this equation for small angles it is possible to show that

$$Co = Co + \pi \sin^2\theta$$

or to reduce this to an even more general form we may write

$$C_D = Co + A.\sin^2 \quad \ldots\ldots\ldots\ldots\ldots\ldots\ldots\ldots \quad 14.2.$$

where α is the angle of champfer and A is a constant including the value of π and the relationship between θ and α

Factors controlling the effect of bevelling on the orifice flow.

When an orifice is champfered the controlling factors can only be conveniently introduced through the use of modifying factors. In general, the effective factors influencing the flow through a bevelled orifice are

(1) radius of curvature, or the angle of bevel,
(2) length of the arc of curvature, or the depth of the bevel,
(3) orifice size,
(4) Reynolds number.

Downie Smith (66) tested three geometrically similar rounded orifices and found that for two orifices 0.250 and 0.5035 inches diameter the curves relating CD and Re were continuous when Re was varied by using hot oil and hot water, but that in relation to each other the discharge coefficient for the large orifice was about 0.50% higher than for the smaller orifice at the same Reynolds number. It is difficult however to treat these results analytically as the curvature of Downie Smith's orifices was made up from two arcs of different radii and centres of curvature. Watson and Schofield (67) made comparative tests with four orifices ranging from sharp edged to rounded with a radius equal to ½ orifice plate thickness. Their experiments on these orifices indicated (1) an increase in radius of curvature on the orifice-edge caused an increase in CD, (2) an increase in diameter of the orifice with radius of rounding = ½ plate thickness caused a decrease of CD as shown in Table 14.1.

TABLE 14.1.

Diameter of Orifice, ins.	0.50	1.0	2.0
Increased Discharge %. (Compared with sharp-edged) Orifice	4.8 to 5.1	1.80	1.70

Pye (61) found that the degree to which the edge of a carburettor jet was rounded or champfered made little difference once the original sharp edge had been removed. It therefore appears that small orifices are not susceptible to changes in the amount of rounding but that such variations do effect the discharge coefficients of larger orifices.

A valuable contribution to our knowledge of the flow through champfered orifices and nozzles was made by Zuckrow (68) who experimented with several orifices of different angles of champfer using "small" and "deep" champfers. The results of these tests are given in figs. 14.2, 3, 4 and 5 from which it will be seen that the discharge coefficient is a function of the flow criterion Re for constant angles of champfer. Although Zuckrow did not publish any values it is estimated from a "faired" curve of his results that the angles of champfer giving maximum flow were as follows in table 14.2.

TABLE 14.2.

Small Champfer.	w.ϕ.r.	4600	2400	1200
	α	39	40	40
Deep Champfer.	w.ϕ.r.	4600	2400	1200
	α	50	45	55

It will be seen also, that

(i) the angle of maximum flow is, as far as can be ascertained, independent of the Reynolds Number, in the region of viscous flow, and

(ii) occurs at 40° for small champfer and 50° (approximately) for the deeper champfers.

The "depth" of champfer which is analogous to the "arc" of curvature has a very decided effect on the maximum discharge conditions.

Zuckrow's experiments, while advancing in the correct direction, i.e. attempting to make a fundamental study of the effect of champfer, fail to be entirely satisfactory,

(i) because his apparatus involved approach disturbances,

(ii) because his readings were insufficient.

The results given, are however, suitable for a comparison with basic formulae and for the general conclusions which have been given.

Bean, Buckingham and Murphy (69) when discussing the flow of liquids through orifices remarked that centrifugal forces introduced by the curvature of the jet, influenced the coefficient of contraction. The relationship between the curvature of the flow and the bevel of the orifice must be determined before this theory is developed.

To obtain some relationship between the angles α and θ the author has extrapolated between figs. 14.1. and 14.2. Thus the value of i given by theory for a certain CD and the values obtained for the included angle ψ by experiment are assumed to be related. Although such a condition as this is possibly incorrect from a detailed point of view, it is considered to be sufficiently satisfactory to give a general relationship between i & ψ. Values are therefore given in the following tables for an orifice with depth of champfer 0.008 ins, $\frac{L}{D}$ 3.55.

TABLE 14.3.

w.ø.r. = 4600.

C_D	i	ψ'	$i-\psi'$	ψ''	$i-\psi''$
.75	60	1	59	175	-115
.775	51	2.5	48.5	140	-89
.80	44	6	38	103	-59
.825	38	20	18	70	-32

TABLE 14.4.

w.ø.r. = 2400.

.75	60	0	60	-	-
.76	56	5	51	156	-100
.78	50	14	36	98	-48
.79	47	18	29	80	-33
.80	44	50	-6	64	-24

TABLE 14.5.

w.ø.r. = 1200.

.728	69	0	69	180	-111
.73	67	1	66	168	-101
.74	63	7	56	143	-80
.75	60	13	47	120	-60
.76	56	20	36	100	-44
.77	53	60	-7	-	-

When plotted as in fig. 14.6. these curves reveal that the difference between the flow lines and the orifice bevel angle gradually diminishes as the orifice bevel is increased, and even becomes negative for most values of ψ greater than 40°. When $i - \psi$ becomes negative the flow cannot leave the leading edge of the orifice as in fig. 14.6 (a) (insert) but must instead, leave by the "trailing" edge. It is obvious therefore that at a value of ψ = 40° approx. the discharge through an orifice is approaching a maximum and at higher values the flow at the edges is disturbed, a conclusion substantiated in fig. 14.2 and table 14.2.

CHAPTER 4.

Characteristics of the Flow - Submerged.

15. Upstream pressure distribution.

When static pressure tappings are taken from the side of a pipe through which liquid is flowing it has been found that the flow some considerable distance upstream is unaffected by the obstruction caused by an orifice. The pressure along the pipe therefore falls uniformly along the pipe down to about one pipe diameter from the orifice plate.

Measurements by Johansen (26) of the pressure difference between two sections 4 and 16 diameters upstream of an orifice in a brass pipe established the fact that the disturbances at the orifice did not extend to this region as the results which he obtained were in good agreement with those predicted from the works of Stanton and Pannell (70).

Johansen also determined the position of the minimum upstream pressure for various Reynolds numbers and orifice-ratios. The results of these tests have been replotted in fig. 15.1. from which it will be seen that in the turbulent range from an Re of about 4000 the position of the minimum upstream pressure increases as Re is increased, up to a constant value which varies according to the orifice ratio. When the values given in fig. 15.1. are used to plot this distance against 'm' as in fig. 15.2. it will be seen that the distance increases with increase in 'm'. Although these values were obtained fairly satisfactorily for turbulent flow, Johansen was unable to determine accurately the position of the minimum during viscous flow as the pressures involved were so very small. It appears however from the few readings which Johansen did manage to obtain that the impact pressure follows entirely different rules under viscous flow than during turbulent flow, for after decreasing to a minimum at approximately Re = 3,500 the impact pressure (and also the distance of minimum pressure) increases very rapidly as Re is further reduced.

The graph given by Johansen to relate the pressure-rise at the orifice plate to the Reynolds number is shewn in fig. 15.3. to be very similar to fig. 15.1. relating distance and Re in that, for the turbulent range the impact pressure increases asymptotically as Re is increased, while for laminar flow a similar condition appears to exist as the Reynolds number is decreased.

When this pressure rise occurs upstream of an orifice the "corner" between the orifice plate and the pipe must be filled with disturbed fluid. The existence of this disturbance has been investigated by Betz (71) whose statements lead to the conclusion that a vortex similar to a trapped "smoke-ring" is formed in this space. This, Betz attributes to the collection of fluid particles rolling along the wall and returning backwards so as to form a vortex which is maintained by the constant regeneration of fluid particles from the retarded body of the fluid. The author does not consider this a completely satisfactory explanation of the vortex-formation, but agrees with Betz (although some others appear to doubt) that a vortex will be formed. The photograph, fig. 15.5 which Betz used, shows quite clearly that at high values of Re a strong vortex will exist at this point.

An attempt to calculate the impact pressure was made by Engel & Davies (53) who considered the pressure to be caused by the change in momentum of the axial velocity of the fluid. Under this assumption the uniform excess pressure p_1 over the surface of the orifice plate is given by

$$p_1 . \pi . (r_1^2 - r_2^2) = \int_{r_2}^{r_1} (\rho u_1)\, u_1 .\, 2\pi r .\, dr. \quad \ldots\ldots\ldots\ldots\ 15.1.$$

thus, the impact pressure P is given by,

$$P \propto \frac{2}{r_1^2 - r_2^2} . \int_{r_2}^{r_1} (\rho u_1)\ u_1 .\ 2\pi\, r .\, dr. \quad \ldots\ldots\ldots\ 15.2.$$

so that if the parameters $\frac{u}{U}$, $\frac{r}{r_1}$, and the area ratio m are introduced,

$$P \propto \rho . U^2\ \frac{2}{1 - m} \int_{\sqrt{m}}^{1} \left[f\left(\frac{r}{r_o}\right)\right]^2 \frac{r}{r_o} .\ d\left(\frac{r}{r_o}\right) \quad \ldots\ldots\ 15.3.$$

$$\propto \beta \left[\rho . U^2\right] \quad \ldots\ldots\ 15.4.$$

where $\beta = \frac{2}{1 - m} \int_{\sqrt{m}}^{1} \left[f\left(\frac{r}{r_o}\right)\right]^2 . \frac{r}{r_o} . d\left(\frac{r}{r_o}\right)$ and $f\left(\frac{r}{r_o}\right)$ is contained in

equation 9.10. Applying the general expression for the differential pressure across an orifice, i.e.

$$p_1 - p_2 = \tfrac{1}{2}\ U^2 .\ \frac{1 - m^2}{m^2} \quad \ldots\ldots\ldots\ldots\ldots\ 15.5.$$

and dividing into equation 15.4., the impact pressure will then be expressed as a ratio of the pressure across the orifice by,

$$\frac{P}{p_1 - p_2} \propto \beta \frac{m^2}{1 - m^2} \quad \ldots\ldots\ldots\ldots\ldots\ 15.6.$$

To compensate equation 15.5 for the effects of discharge, the coefficient C_D must be included in equation 15.5 so that the pressure rise may be given by the expression

$$\frac{p}{p_1 - p_2} \propto C_D^2 . \beta . \frac{m^2}{1 - m^2} \qquad \text{.......................... 15.7.}$$

The results of Witte (2) and Engel (72), when plotted by these investigators (53) showed a very good agreement with the values of $\frac{p}{p_1 - p_2}$ given by the equation

$$\frac{p}{p_1 - p_2} = C_D^2 . \beta . \frac{m^2}{1 - m^2} \qquad \text{........................ 15.8.}$$

(in which the constant of proportionality in equation 15.7 is unity), for both long nozzles ($C_D = 0.98$) and thin plate orifices ($C_D = 0.61$) and for rough and smooth approach pipes.

16. The Vena-contracta.

After leaving the orifice the jet of fluid continues to contract down to a minimum at the vena contracta, which lies some distance downstream from the orifice. At this point the ratio of the area of the jet to the area of cross section of the orifice is defined as the coefficient of contraction, fuller details regarding which have been given in Chapter 1. 2(a).

When the assumptions of parallel-flow are used the position of the vena-contracta is generally regarded as being identical with the position of the minimum downstream pressure. Such an assumption is generally sufficiently accurate as to give satisfactory results. The author considers, however, and it must be remembered, that when transverse readings are made from a stream which is either contracting or diverging the reading which is observed will be given by

$$p = p_o \pm \frac{w.V_y^2}{2g} \quad \text{.......... 16.1.}$$

where Vy is the mean transverse velocity component which must be added to Po when the flow is diverging but subtracted from it when the flow is contracting.

If then we assume Bernoullis' equation to be sufficiently accurate for a determination of p_o,

$$p_o = w\left(h - \frac{V_x^2}{2g}\right) \quad \text{.......... 16.2.}$$

where h is the total head at the point under consideration,

Vx is the mean axial velocity of flow, and d_x is the effective jet diameter,

$$\text{But } V_x = \frac{Q}{\pi/4\ d_x^2} = \frac{4\,Q}{\pi}\left(\frac{1}{d_x}\right)^2 \quad \text{.......... 16.3.}$$

so that substituting from equations 16.2 and 3 in 16.1. we have

$$p = w\left(h - \frac{1}{2g}\left[\frac{4\,Q}{\pi}\left(\frac{1}{d_x}\right)^2\right]^2\right) \pm w\frac{V_y^2}{2g}$$

$$= w\left[h - \left(\frac{k}{d_x}\right)^4\right] \pm \frac{V_y^2}{2g} \quad \text{.......... 16.4.}$$

where $K = \left(\frac{4\,Q}{\pi}\right)^{\frac{1}{2}} \left(\frac{1}{2g}\right)^{\frac{1}{4}}$

When the stream is contracting to the vena-contracta it can be shown that there is very little loss of head if any at all, there is instead an exchange of energy between the pressure and velocity heads. Hence, for the region of contracting fluid measured transverse pressure $p = w\left[h - \left(\frac{K}{d_x}\right)^4 - \frac{Vy^2}{2g}\right]$ .... 16.5.

although the theoretical pressure should be

$$p^1 = w\left[h - \left(\frac{K}{d_x}\right)^4\right] \quad .... \quad 16.6.$$

During the contracting period therefore, the measured head will be less than that corresponding to the shape of the contracting jet.

At the vena-contracta it is assumed that $Vy = 0$ and so the measured pressure should be equal to the theoretical pressure if all the particles of fluid are moving in a parallel path.

Downstream of the vena-contracta the head h will be reduced by the formation of eddies in the diverging stream, the loss of head being considered equal to

$$h - \frac{(Vx - Vx_{+dx})^2}{2\,g} \quad .... \quad 16.7.$$

which indicates that the measured head will be reduced if only the effect of total head is considered. The effects of impact will be to increase the measured head. It is therefore obvious that the loss of total head is offset by the impact pressure due to the transverse velocity Vy and so the pressure which is actually measured at a "static" tapping point will be,

$$p = pc - w\left[\left(\frac{Vx - Vx + dx}{2g}\right)^2 - \frac{Vy}{2g}^2\right. \quad .... \quad 16.8.$$

The recovery of theflow (as discussed in greater detail at section 17) is initially very slow as shewn in fig. 2.5. until the pressure-recovery curve becomes steep and linear. During this initial period the value of Vy must be very small, and it is quite possible that during this phase the pressure-loss will exceed the impact pressure and so the measured pressure may be slightly less than at the vena-contracta.

From these elementary considerations it is thought that the position of the minimum "static" pressure as measured by the transverse tappings will not necessarily coincide with the position of the vena-contracta but will be located farther downstream, i.e. the true position of the vena-contracta will be nearer to the orifice than is the position of the minimum transverse pressure reading. No experimental or theoretical evidence is available on this subject, but from the reasoning which has been given it would appear that the error would be greater at larger rates of flow than when the velocity and energy of the system is small.

The author considers however, that despite the foregoing conclusions the position of the minimum transverse pressure reading is not likely to be far from the true vena-contracta so that the error introduced by using this point is likely to lie within the range of experimental discrepancies. For this reason the author proposes to accept without further comment, the position of the least transverse pressure as determined by many investigators, as the true position of the vena-contracta.

Only in the case of Johansen, however, have the investigations been sufficiently detailed for observations to be made of the characteristics of the vena-contracta. It was found that the position of the vena-contracta depended upon (1) the Reynolds number and (2) curvature of the flow. In the study of the effects of viscosity on the discharge coefficient (Chapter 2 section 5) it was explained that at low values of Re, i.e. very viscous flow, the fluid conformed very closely to the orifice and so the position of the vena-contracta almost coincided with the transverse central plane of the orifice. Fig. 16.1. relates Johansen's observations of the minimum downstream pressure to the Reynolds number. It will be seen that this position varies considerably at low rates of flow but becomes constant as the turbulence is increased. The position for laminar flow with $\frac{d}{D} = 0.401$ decreases from constancy at Re = 10,000 and although a similar tendency is indicated from his plotted points Johansen extrapolated the curve of $\frac{d}{D} = 0.595$ to show an increase in downstream minimum pressure for any further reduction of Re. This construction certainly appears to conform with the point plotted for $\frac{d}{D} = 0.794$. at about Re = 2000, but in view of the initial slope and the absence of further confirmation of the accuracy of this plot the author considers this result to be erroneous and that as the value of Re is reduced so the position of the minimum pressure recedes back to the orifice centre-plane. If the last point on the $\frac{d}{D} = 0.794$ curve is omitted then it is possible that the correct orientation of the curves should be as indicated in fig. 16.1.

The effect of diameter ratio is shown in fig. 16.2 which was obtained from fig. 16.1. and upon which the results given by Judd(73) have been produced. The values attributed to Johansen have been taken from his readings at Re = 20,000 as it is assumed that variations with Re have become sufficiently small at this flow for the position of the minimum pressure to be regarded as being independent of the value of Re. The values given by Judd were however, not stated for any particular rate of flow although as his experiments were mainly confined to the turbulent zone it is assumed that his curves also apply to the region of stability where the position of the vena contracta depends only upon the diameter ratio $\frac{d}{D}$.

There is not a very good agreement between the results of these two investigators. When $\frac{d}{D}$ is small the results given by Johansen give no indication of decreasing although with Judd a slight decrease is observed. It would seem however from purely abstract reasoning that when $\frac{d}{D} = 0$, i.e. orifice diameter d = o so that the pipe is in effect "blanked-off," that the vena-contracta will coincide with the orifice plate. The falling tendency of Judd's curve would therefore be quite logical. At the other end however where $\frac{d}{D} = 1.0$ the vena contracta would be non-existant and its position again at the orifice plate. This agrees with the values given by Johansen when extrapolated to $\frac{d}{D} = 1.0$.

Considerable divergencies exist between the values in the central region given by Johansen and by Judd. A careful study of the records published by both experimenters reveals that these deviations may be due to the considerable differences in the sizes of pipe and orifice used, thus while Judd used pipes of 5, 4 and 3 inches bore, Johansen experimented with a 3.194 cm. (1.25 ins.) diameter brass pipe. It is probable that accidental champfering of Johansen's orifices would be more critical than with Judd, so that the slope of the pressure curve was not so great. This would be in agreement with the results of section 14 that when the orifice is champfered C_D is large because, for the same mean velocity the head across the orifice would be less with Johansen than with Judd owing to the smaller slope of the pressure-head curve in the installation used by the former.

17. Recovery of the Flow.

When the submerged jet from the orifice has passed beyond the vena-contracta it commences to grow larger so as to fill the pipe, i.e. the flow commences to recover its characteristic orientation with respect to the pipe. Reference to fig. 2.5. shows that in recovering from the vena contracta the pressure increases linearly to a maximum, at which point the full recovery is assumed to occur. After the maximum-pressure point has been passed the pressure begins to decrease, slowly at first and then more steadily at the rate characteristic of the pressure drop for the conditions which prevail. Three stages in the recovery of the flow downstream of the vena-contracta remain to be studied, (1) the slope of the pressure-recovery curve, (2) position of the maximum pressure recovery, (3) the head lost between the upstream and downstream sections of the jet due to the obstructing influence of the orifice.

When the jet attempts to recover it commences to spread in the same manner as a jet spreading into an unrestricted space (see section 18.) This free-spread of the jet only lasts for a very short distance as impact with the pipe walls causes it to be deflected back to the normal flow distribution. The results obtained by several investigators indicate that during the "free-jet" period the pressure rises in approximately a linear manner. The slope of the straight part of the pressure curve varies inversely as the Re (although over the turbulent range this variation is small) but directly as $\frac{d}{D}$ (which is considerable) thus under viscous flow the stream diverges rapidly, but when the jet issues at high velocity the stream issues almost parallel.

Since the slope of this curve varies as the ratio $\frac{d}{D}$ it would appear that the transverse velocity of the jet is very small when the orifice is small and large when the orifice is large, which indicates that the annulus of fluid surrounding the jet may be the criterion of the divergence. The slope of the "free-jet" may therefore be taken as proportional to the ratio of the area of the jet to that of the annulus of liquid,

$$\text{i.e.} \quad \frac{dp}{dx} \propto f\left(\frac{\pi/4\, d_c^2}{\pi/4\,(D^2 - d_c^2)}\right)$$

$$\propto f\left(\frac{(dc/D)^2}{1 - (\frac{dc}{D})^2}\right)$$

$$\propto f\,(\tfrac{dc}{D})^2\,(1 + (\tfrac{dc}{D})^2\,) \quad \text{approx.}$$

But the area at the vena-contracta is $\pi/4\, d_c^2 = \pi/4\, d^2.\, C_c.$

$$\text{i.e.} \quad d_c^2 = Cc.\, d^2.$$

Hence, $\frac{dp}{dx} \quad \mathcal{L} f \left(\frac{d}{D}\right)^2 \quad . \quad C_c \left[1 + C_c \left(\frac{d}{D}\right)^2\right]\Big\}$.......... 17.1.

Tabulating the values of $\frac{dp}{dx}$ plotted by Johansen in his fig. 14 in table 17.1. we have, assuming $C_c = 0.60$

TABLE 17.1.

$\frac{d}{D}$	0.1	0.2	0.3	0.4	0.5	0.6	0.7	0.8
$dp/_{dx}$	.01	.04	.06	.10	.14	.22	.36	.64
$\left(\frac{d}{D}\right)^2$	.01	.04	.09	.16	.25	.36	.49	.64
$0.60 \left(\frac{d}{D}\right)^2$	.006	.024	.054	.096	.15	.216	.294	.384
$1 + 0.60 \left(\frac{d}{D}\right)^2$	1.00	1.02	1.05	1.10	1.15	1.22	1.29	1.38
$\left(\frac{d}{D}\right)^2 \left[1 + 0.60 \left(\frac{d}{D}\right)^2\right]$	.01	.04	.095	.176	.288	.439	.635	.883

When equation 17.1. is plotted as in fig. 17.1. it will be seen that the pressure-recovery is not quite linear, although it is probable that if the variation of C_c with $\frac{d}{D}$ is allowed for it will be found that a linear relationship may exist indicating that the "impeding" theory advanced in the foregoing may be substantiated by experiment.

The transverse velocity is reduced to zero when the pipe wall restricts the free-jet spread, so that the filaments of fluid will be compelled to move along the pipe in the normal manner. It is possible that during the flow-recovery period in which the transverse velocity is eliminated, that a "rebound" effect may occur at the pipe wall for the interval during which full recovery of the flow takes place. The effects of violent turbulence and vorticity in the downstream flow are however sufficiently large as to completely mask this phenomenon.

After the flow has recovered its normal distribution the transverse pressure (which may then be taken as a fairly accurate measurement of the static pressure since there is no transverse velocity component) reaches a maximum. Further downstream the transverse pressure commences to decrease at a rate proportional to the flow and characteristic of the roughness of the pipe. From the results given by Johansen (replotted in fig. 17.2) the position of the maximum downstream pressure is seen to be very sensitive to variations of Re in the laminar region but to remain almost independent of Re in the turbulent region.

The values given by Johansen for the positions of the maximum pressure recovery do not however agree well with those given by other authorities. In all the tests, however, the position from the orifice was shown to have the same characteristic of decreasing as $\frac{d}{D}$ was increased. The values of Judd are not available for comparison and Johansen advanced no explanation for the discrepancies. The author considers however that as the downstream position of the maximum pressure when measured from the orifice is the sum of

(1) distance of the vena-contracta downstream,
(2) distance of the maximum pressure from the vena-contracta,

and that as (1) is considerably influenced by the orifice shape whereas (2) is not believed to be so sensitive to the orifice design, then the variations between the results due to Johansen and those of other investigators are due to slight amounts of champfering of the orifice.

The magnitude of the pressure-recovery, or more accurately, the amount of the pressure-loss has interested many investigators since it is a measure of the restriction caused by an orifice. In all the papers which have been studied, the pressure loss is given as the difference between the upstream minimum pressure and the downstream maximum. Although for practical purposes this gives values of the pressure loss which lie within the range of experimental error, the author wishes to record that the restriction-loss as measured in this manner should be modified to allow for the normal pressure-drop in a pipe. Thus it is considered that the true loss of head due to an orifice must be measured between the difference in ordinate at a point when one of the two curves is extrapolated as at point A. fig. 17.3. To be even more precise, the author would even stipulate measurement at the vena-contracta - assuming that all the loss occurred during the re-expansion of the jet - if the slopes of the pressure-drop (pipe) curves are different, due to either differences in roughness, shape or bore of the upstream and downstream sections.

It has been stated by Gibson and verified by other authorities that the overall loss due to a thin-plate orifice in a pipe-line is entirely due to the downstream enlargement of the jet from the vena-contracta. This indicates that only negligible friction occurs during the contraction of the jet to the vena-contracta. With long orifices, the jet returns to the walls of the nozzle before emerging and then diverging to the pipe walls. Three losses must therefore arise, (1) internal nozzle loss on divergence to the nozzle walls (2) friction loss inside the nozzle walls (3) divergence loss during the discharge from the nozzle. So far as the author is aware, no attempts have been made to measure each of these losses separately.

Johansen stated that if the velocity distributions across the pipe and across the jet at the positions of minimum pressure (both upstream and downstream) were the same, then if the mean velocity v_c at the vena contracta were calculated and the mean velocity V_R downstream were deduced, then the loss of head could be estimated from the ordinary momentum equation

$$h_f = \left(\frac{V_c - V_R}{2.g}\right)^2 \quad \text{.. 17.2.}$$

These values were then compared with those obtained by experiment, table 17.2.

TABLE 17.2.

$\frac{d}{D}$	Ratio $\frac{\text{Overall Loss of Head}}{\text{Pressure Drop (Orifice)}}$ Calculated	Measured	Diff.
.2	0.950	0.947	.003
.3	0.897	0.894	.003
.4	0.821	0.812	.009
.5	0.727	0.724	.003
.6	0.608	0.617	-.009
.7	0.483	0.490	-.007

From the column of differences between the calculated and measured ratios it is evident that the discrepancies follow no definite law. The conclusion is therefore reached, that for a thin-plate orifice, the values given by equation 17.2 correspond very closely with those given in practice.

Assuming $C_V = 1.00$, then for elementary calculations we may assume that

$$v_c = \sqrt{2.g.h.} \quad \text{.............................. 17.3.}$$

where h = head across the orifice,

and that $V_R = \frac{a_c}{A} v_c$

$$= C_c \frac{a}{A}. \quad 2gh \quad \text{.................................... 17.4.}$$

where a_c = area of jet at vena-contracta

a = area of orifice

A = area of pipe.

Hence, substituting in equation 17.2.

$$hf = (1 - C_c \cdot \frac{a}{A})\, h$$

$$= \left[1 - C_c\left(\frac{d}{D}\right)^2\right] h \quad \text{.. 17.5.}$$

When the values of C_o derived from the application of 17.5 to the measured values of Table 17.2. are plotted against $\left(\frac{d}{D}\right)^2$ and superimposed on fig. 2.2. the values are found to be greater than those of Witte. This variation is considered to be due to the use of $C_v = 1.00$ and that a correction for velocity would secure greater accuracy of co-relation.

18. Characteristics of the Jet.

When a jet leaves the back edge of the orifice or nozzle plate the boundary layer is compelled to "break-away" from the orifice walls. This phenomena is similar to the break-away of the boundary layer from the surface of a flat plate or aerofoil but is influenced very considerably by the convergence of the flow and its effect upon the distribution of pressure at the orifice walls. In fact, to distinguish briefly between the two kinds of breakaway, when a fluid passes over a flat plate 2 dimensional forces predominate whereas when a fluid flows through an orifice or nozzle all 3 dimensional forces influence the motion.

This breakaway of the stream from an edge-wise plate has been discussed by Goldstein (74). It was considered that this breakaway occurs when the fluid in the boundary-layer was made to move against a pressure-gradient. Such a condition arises when the flow diverges on the downstream side of a submerged orifice and the mean velocity of flow is reduced by the considerable increase in cross-sectional area. The pressure on the downstream side of the jet therefore attempts to increase so that the conditions for breakaway are introduced. Examples of this breakaway in a diverging nozzle have been published by Prandtl while Goldstein refers to demonstrations made by Farren at Cambridge University to illustrate the flow breakaway in a diverging channel.

Prandtl (75) showed mathematically that a vortex sheet would be set up by an inviscid fluid when the jet broke away and demonstrated this conclusion experimentally (76) with air.* Townend (77) found with his tests on the free-air jet in a small 3 inch open wind tunnel that the downstream shape of the orifice or nozzle had a very considerable effect on the form of the downstream vortex. This implies that the back face of the orifice or nozzle has a critical effect on the downstream flow pattern. Thus, with a sharp-edged back face the well-known Kármán vortex sheet was observed in which the eddies were shed alternatively from the top and bottom of the jet whereas with an orifice suitably rounded to give a radial jet the vortices appeared to be shed simultaneously from the top and bottom in the manner of an unstable Karman vortex sheet. The author believes it possible that the vortex spacing varies with the rate of divergence of the jet. An interesting observation made by Townend was that the vortex formation influenced the interior of the jet so that with the "alternate" vortex formation the jet was "wriggled" or "snaked," whereas with the "simultaneous" vortex formation the jet was squeezed by each vortex so that a pumping action takes place within the jet. It is possible however, that these pressure fluctuations are only restricted to the mixing region of the transverse section of the jet and do not influence the core.

---

*The formation of vortices behind a sharp edge is used considerably in the design of whistles and syrens where the aeolian tones of the vortex sound waves possess a frequency corresponding to a certain pitch. Similarly the effect on a sensitive flame is also the result of these vortices. A greater explanation of these phenomena is given by E. G. Richardson in "Sound" publ. Arnold, London (1935.)

It was suggested by Kretschmer (78) that a depression of pressure existed in the vortex given off at the jet, which caused the flow to be sucked back to the walls of a long nozzle. Although no experiments have been published it would appear that by creating an artificial turbulence at this point the return of the jet would take place in a much shorter orifice length.

When a jet discharges into an atmosphere and is dispersed by the diffusion of its molecules into the surrounding media it has been shewn both experimentally and analytically by Andrade (79), and confirmed by Binnie & Squire (80) that

(1) the mean axial velocity of the jet decreases as the distance from the orifice increases,

(2) the velocity across any cross-section of the jet decreases outwards to zero at the jet boundary,

(3) the jet diverges outwards from the central core of undisturbed fluid which is absorbed into the surrounding media at a rate which is proportional to the distance from the orifice.

It was found by Andrade that the jet from a slit-orifice was very sensitive to even slight disturbances and that steadiness could only be ensured (without taking very special precautions) at values of Re less than 10 to 20 while at Re greater than 30 definite turbulence could be observed.

When a submerged orifice is fitted into a pipe the theories of free jets cannot be readily applied since the wall effects modify the general flow characteristics. The author does not claim any advanced knowledge of the mathematical theory of fluid dynamics but would suggest that the analysis by Schlichtung (81) which was simplified by Bickley (82) and gave the axial and transverse velocity distributions for a jet, may be applied to this problem.

Very little attention has been paid to the velocity distribution downstream of the orifice so that only hazy conjectures can be made of the true behaviour of the jet. Nusselt (83) showed that for a nozzle with the flow retarded at the boundary layer, the axial velocity was negative at this region. On purely conjectural grounds the author has therefore considered that the velocity distribution through an orifice is similar to that depicted in fig. 18.1. In this the maximum velocity increases up to the vena-contracta and then steadily decreases so that after passing the turbulence-diffusion region of vortex formation it regains its original distribution. Throughout the orifice flow the velocity is negative at the pipe walls except at the inlet where it is almost constant, - a conclusion also reached by Prof. Andrade. The champfering of an orifice definitely effects this distribution and reduces the "negative-velocity" region. A further series of conjectures for long orifices or nozzles could be based on the flow-distribution at the entry to pipes.

19. Downstream Vortex Formation.

At low Reynolds Numbers the downstream flow pattern consists of visible vortices the rate of generation of which varies with Re so that with very viscous flow their creation is scarcely perceptible while out of the laminar range and with turbulent flow the whole downstream is confused by the very rapid creation of vortices and their dissipation into the downstream mass.

Visual experiments were carried out by Johansen on the vortex pattern at low Reynolds Numbers, from the published results of which the photographs of fig. 19.1. have been taken. The flow at 'a' with Re = 30 is symmetrical around the orifice plate with the fluid close to the plate being deflected at right angles yet adhering to the sides of the diaphragm. This effect corresponds very closely to the quantitative evidence for viscous flow that at low Re the coefficient of contraction is almost unity. At slightly higher rates of flow the fluid passing around the sharp edge of the orifice is thrown clear, i.e. separates, for a small distance, but soon diverges again rapidly to the pipe walls. In accordance with the conclusions of section 18 it will be seen that at higher Reynolds numbers the jet diverges less rapidly, while when Re = 100 a slight vena-contracta may be observed which forms close to the orifice edge.

These characteristics of the jet continue to develop as the rate of flow is increased until a more or less cylindrical jet 2 pipe diameters long issues from the orifice. These limitations usually exist at Re = 250 to 350. A return flow between the jet and the pipe becomes increasingly noticeable at these Reynolds numbers, which has a mean velocity about 0.2 of that of the central filament of the jet. At Re = 250 some ripples appear along the boundaries of the jet, the starting point for which comes closer to the orifice face as the flow is increased, then, at Re = 350 the ripples travel about one-half a pipe diameter downstream and then appear to coalesce into imperfect vortex rings, fig. 19.1.d. Further increase of Re enables sufficient fluid to be carried along with the jet to form a train of more or less complete vortex rings spaced about 1 orifice diameter apart; the mean diameter of these rings is initially less than the orifice diameter but as the rings travel downstream they are "stretched" by the expanding jet so that they increase in diameter. These rings - which appear to be connected to each other by a thin film of fluid - maintain almost constant size and spacing for about 2 pipe diameters downstream after which they increase in bulk, decrease in velocity and spacing until the whole train becomes unstable and merges into the general turbulence about 5 diameters downstream. Under very favourable conditions Johansen observed small individual rings which formed at the orifice and passed downstream at high velocities so that they passed through two or three of the larger rings comprising the train. It is of interest to note that all these vortices were contained in the plane normal to the pipe, i.e. the plane of the orifice, there was no tendency for them to be shed from the edge of the orifice in the form of a spiral.

Attempts were made by Johansen to time the frequency of the vortices by means of a stop watch. The results are given in table 19.1. for the rate of vortex formation at various Reynolds numbers

TABLE 19.1.

ORIFICE 1.346 c.m. diameter. PIPE 2.685 c.m. diameter, $(\frac{d}{D}) = 0.502$.

Re	Rings/Second	$\frac{fd}{v}$
222	0.78	0.576
234	0.87	0.610
344	1.25	0.594
600	2.40	0.655
768	2.71	0.578
1020	3.42	0.548

In spite of the large variations from the mean in those figures deduced for column 3 above, these variations are not systematic. For this reason it has been suggested that the function $\frac{f.d.}{v}$ is almost a constant. The author believes however that with more accurate means of measuring f and v that it will be found that $\frac{f.d.}{v}$ varies with Re, m, and the other variants.

At Re of about 1500 the vortices continue to form about 1 orifice diameter downstream but are rapidly dissipated. Under these conditions a violent turbulence extends for about one to five pipe diameter downstream from the orifice.

The foregoing results were obtained by Johansen for three sizes of orifice ($\frac{d}{D} = 0.095, 0.246$ and 0.502) who found that although those sequences which have just been described were followed, the Reynolds number for a given event varied with $\frac{d}{D}$, increasing progressively with this ratio.

A noteworthy feature of the downstream flow is the distance which the jet issuing from the orifice penetrates into the downstream fluid. This length increases steadily from zero at Re = 10 to a maximum upon the first appearance of vorticity. The jet length then decreases at all further increases of Re. When the jet length is maximum the resistance to flow is a minimum, which corresponds with the conditions of maximum CD given in section II. The author also considers (and this is a point overlooked by Johansen) that the point of vortex formation must correspond with that of the jet re-expansion, since vortices always form when the fluid diverges; the point of vortex formation [redacted] is the vena-contracta and being shed from this source the vortices will inherit the characteristics associated with it.

The available literature on this section of orifice characteristics is very meagre, in fact Johansen appears to have made the only serious attempt to study this aspect. In view of its relationship with CD, pressure recovery, Cv and pressure loss it will be necessary for this subject to be developed more thoroughly in the very near future.

CHAPTER 5.

Characteristics of the Flow - Free Discharge.

In order to cover that aspect of orifice flow not dealt with in Chapter 4 an attempt is made to survey briefly the more outstanding characteristics of a fluid when discharged into an atmosphere of much lower density and with which it cannot readily diffuse.

20. Pendant Drops.

Under the influence of very low hydrostatic heads with large surface-tension properties and fine bores an orifice may pass only just sufficient fluid to enable a drop to form, for which the capillary or surface-tension forces balance the other loads, i.e. for which static equilibrium is attained.

The shape of this drop may be determined from an analysis of the stresses which maintain the drop in static equilibrium; such calculations being based on the fundamental equations derived by Young (84) and also by Laplace (85) that the pressure caused by the curvature of the surface is equal to the product of the boundary (surface) tension and the mean curvature and that also for conditions of equilibrium the vertical forces across any horizontal plane shall balance. Working on these principles, Freud and Harkins (86) substituted the cartesian coordinates for the radii of curvature R_1 and R_2 in the familiar Laplace equation

$$p = 6\left(\frac{1}{R_1} + \frac{1}{R_2}\right) \quad \ldots\ldots\ldots\ldots\ldots\ldots\ldots\ldots\ldots\ldots\ldots\ldots \quad 20.1.$$

these coordinates being measured from the bottom of the drop as X - axis and through the vertical axis of symmetry as the Y - axis, then

$$p = 6\left[\frac{y^{11}}{\{1 + (y^1)^2\}^{3/2}} + \frac{y^1}{x\{1 + (y^1)^2\}^{\frac{1}{2}}}\right] \quad \ldots\ldots\ldots\ldots\ldots \quad 20.2.$$

where y^1 and y^{11} are the first and second derivatives of y with respect to x.

Now the pressure p at any point on the surface will be equal to w (h-y) where h is the capillary head over the bottom of the drop, so that if we put $a^2 = \frac{2w}{6}$, i.e. double the ratio of the density to the surface tension, then for equation 20.2 we may write

$$\frac{y^{11}}{[1 + (y^1)^2]^{3/2}} + \frac{y^1}{x[1 + (y^1)^2]^{\frac{1}{2}}} = \frac{2}{a^2}(h - y) \quad \ldots\ldots\ldots \quad 20.3.$$

This represents the basic equation for the contour of a pendant drop and may be solved by integration in series.

This task was carried out by Freud and Harkins who gave their results in the form of a graph, reproduced as fig. 20.1. which gives the drop profiles for values of h ranging from o to 4 cms. and which uses as ordinates $\overline{x}$ and $\overline{y}$ to avoid the application of the character 'a' so that the physical coefficients are not involved.

If the head over an orifice remains constant, then a stable drop will form for which any variations due to increasing the head will cause it to grow so that when the head is reduced the drop will be too large, it will be unstable with respect to the diminished head and will therefore fall off. On the other hand a reduction of pressure from the normal will cause the drop to "shrink" and so any increase in pressure will find it in a stable condition, capable of increasing in size without becoming severed. It will be seen from fig. 20.1. that at each particular head a drop has an optimum stable volume which led Lohnstein (87) to conclude that if through any cause this volume was exceeded, the drop must ultimately be severed.

When failure occurs a "neck" is formed in the suspension of the drop which continues to increase until finally the drop becomes severed. Theory gives the simple expression (see Edser, "General Physics for Students," MacMillan, (1933) p.319)

$$W = 2\pi r.\,\sigma \quad \text{.......................................} \quad 20.4.$$

for the weight of a single drop severed from an orifice of radius r after fully developing. This value is, however, too large as it includes that small volume contained between the orifice and the "neck." For practical purposes this is allowed for by introducing a factor F, so that the true drop-weight is given by the expression

$$W_1 = F.\,2\pi\,r.\,\sigma \quad \text{.......................................} \quad 20.5.$$

Experiments show that at $\frac{r}{a} = 1.0$, $F = 0.6$ but when $\frac{r}{a}$ is lowered the value of F is considerably increased since the proportionate size of this "neck" is then much smaller; a value of 0.93 having been referred to by Freud & Harkins.

It is interesting to note that after the drop falls a long neck is distended after it, which may also become detached at one or more places so that a secondary drop or drops will follow behind the larger drop. This has been called Plateau's spherule and can easily be observed in many instances when the rate of formation is slow.

21. Low Velocity Jets.

When fluid issues from an orifice at velocities outside the range for which capillary (or surface tension) forces are effective or comparable with the viscous or momentum forces, a column of fluid will be maintained at the end of which drops may form. This column appears to be a development of the "retained fluid" between the neck and the orifice referred to in section 20 as being left behind when a drop is formed.

The length of jet which can be maintained before drops are formed, was studied experimentally by Smith and Moss (88) who showed that in the first stage the effects of surface tension predominate while in the second stage the effects of viscosity were more important. From a dimensional analysis of the conditions Tyler and Richardson (89) showed that for the zone of surface-tension domination the jet length L defined as the "continuous length of cylindrical portion" may be evaluated from the expression

$$\frac{L}{d} = \text{Constant} \times V. \sqrt{\frac{w.d.}{6}} \quad \ldots\ldots\ldots\ldots\ldots\ldots\ldots\ldots \quad 21.1.$$

for which the experimental results would appear to offer a value in the region of 16.0 for the constant of all fluids with a density about unity (water, methylated spirits, etc.) In plotting $\frac{L}{d}$ against $V.\sqrt{\frac{w.d.}{6}}$ it was found that two straight lines of different slope were obtained from which it was concluded that two critical velocities v_1 and v_2 could exist, one of these velocities being very small while the other was fairly large. The slope of the $\frac{L}{d}$ curve is much greater at low velocities, i.e. for the V_1 region, than for the other region. After the upper critical velocity V_2 has been exceeded the straight-line law fails, the slope decreases to zero and then becomes zero so that the jet length decreases as the velocity increases. It is possible that the lower critical velocity is only influenced by surface tension and represents the change-over from slow to fast drop formation, while the upper limit involves both surface tension and viscosity; when the length of the jet shortens the viscous forces commence to predominate. It was shown by Tyler & Richardson that the upper critical velocity was controlled by an equation of the form

$$V2 = A_1 . \sqrt{\frac{6}{w.d.}} + B_1 . \frac{\mu}{w.d.} \quad \ldots\ldots\ldots\ldots\ldots\ldots\ldots \quad 21.2.$$

where the first term covers the surface tension effect and the second covers the viscosity effect.

While falling this jet will exchange some of its potential energy for kinetic energy and in order to maintain continuity the cross sectional area will decrease as the velocity is made to increase. The jet does not however, maintain a regular circular cross-section but divides up into very regular swellings as shown in fig. 21.1. which was obtained by the author in pouring coloured water from a jug. These swellings are caused by extremely slight disturbances to the jet where it leaves the orifice, and will be set up by the discharge of fluid through an aperture of any shape.

Of the various theories put forward to explain this behaviour of a jet, the suggestion made by Plateau and developed by Lord Rayleigh (90) that such swellings are the result of oscillations in the fluid which travel with it and appear ultimately as stationary waves or swellings, has met with the greatest success. Thus, by means of a mathematical analysis of the stability of the stationary oscillations of the fluid column about a central figure of equilibrium and superimposed upon the general motion of the jet, Rayleigh found the frequency (t) of these oscillations to be given by

$$t = \frac{2\pi}{p} \qquad \ldots\ldots\ldots\ldots\ldots\ldots\ldots\ldots \quad 21.3.$$

where $p = \pi^{\frac{3}{4}} .\ \sigma^{\frac{1}{2}} .\ \rho^{-\frac{1}{2}}\ A^{-\frac{3}{4}}\ \sqrt{N^3 - N}.$

A = cross-sectional area of orifice.

N = number depending on shape of orifice = 1 for a circular orifice
= 2 for a elliptical orifice
= 3 for a triangular orifice
= 4 for a square orifice.

It was shown that the wavelength (λ) of these oscillations was constant down the jet despite the reduction of area which occurs, and was given by

$$\lambda = V.t = \sqrt{2gH}\left(2\pi \Big/ \pi^{\frac{3}{4}} .\ \sigma^{\frac{1}{2}} .\ \rho^{-\frac{1}{2}}\ A^{-\frac{3}{4}}\ \sqrt{N^3 - N}\right)$$

$$= 2\pi^{\frac{1}{4}} \sqrt{\frac{A^{3/2}\rho .\ 2g.H}{\sigma.(N^3 - N)}} \qquad \ldots\ldots\ldots\ldots\ldots\ldots \quad 21.4.$$

The accuracy of these deductions was checked by Rayleigh against experiments with distilled water and the results in Table 21.1. obtained.

TABLE 21.1.

Orifice	n	λ Measured	λ Calculated, CMS.
Elliptical	2	3.95	3.93
Triangular	3	2.30	2.10
Square	4	1.85	1.78

The agreement between the measured and calculated wave-length is sufficiently accurate to allow equation 21.4. to be accepted. It is obvious that the wavelength increases with increase of area, density or head or if the surface tension is reduced; while with the smaller value of N for circular orifices the wavelength is greater for this than for any other shape. (It appears as though N varies with the number of sides of the orifice. But as a circle may be regarded as a multi-sided orifice it would seem that N for a large sided polygon will tend towards the value for an orifice of circular shape. For this reason it is suggested that a graph relating N to the "number of sides" may not be linear as suggested from the foregoing notes. This requires to be determined.)

The amplitude of these oscillations or "swellings" is a critical factor in the stability of these jets. It was shown both analytically and theoretically by Plateau, that a column of liquid would remain stable if the wave-length were less than the circumference of the orifice. If λ is greater than 2π r the necks between the swellings will become deeper and deeper until they are finally severed and the drop is free. More recent work by Litteye (91) confirms that 2π r represents limit to stability.

22. Formation of Drops.

When jets are unstable, the protuberations grow at the expense of fluid in the neck. The capillary forces are reduced and the fluid at the end of the jet separates or ruptures away from the main column with the result that a drop is formed.

It was shown by Rayleigh that with a non-viscous flow the time of disintegration of a liquid droplet depended upon the initial disturbance at the orifice (a_o) and its rate of growth, according to the expression

$$t = \frac{1}{y} \cdot \log_e \left(\frac{a}{a_o}\right) \times \sqrt{\frac{p.d.^3}{6}} \qquad \text{22.1.}$$

where a = final amplitude of disturbance before rupture, this is measured in the transverse plane of the jet.

y = function of $\frac{\pi d}{\lambda}$ controlling the degree of instability of the jet.

This equation should be modified by a multiple of $f\left(\frac{\sqrt{6\rho.d.}}{\mu}\right)$ to allow for viscosity. The experiments carried out by Tyler and Watkin (92) suggest that this function should be $\left[1 + \frac{1}{4095}\left(\frac{\sqrt{6\rho d}}{\mu}\right)^{3/2}\right]$

Tyler showed (93) that the frequency of drop formation ($N = \frac{1}{t}$) was related to the velocity of the jet at the disruption and to the drop spacing (λ_o) by the expression

$$V = N. \lambda_o \qquad \text{22.2.}$$

and that assuming continuity, with d = jet diameter at break-up,

D = effective diameter of a spherical drop,

by neglecting Plateau's spherule,

$$\frac{\pi}{6} D^3 N = \frac{\pi}{4} d^2 V$$

i.e.

$$\frac{V}{N} = \frac{3}{2} \cdot \frac{D^3}{d^2} \qquad \text{22.3.}$$

Thus from equations 22.2 and 3,

$$\frac{\lambda_o}{d} = \frac{V}{N.d} = \frac{3}{2}\left(\frac{D}{d}\right)^3 \qquad \text{22.4.}$$

In order to determine the drop size it is necessary to modify equations 20.4. and 5. for these conditions where the rate of formation is high, inertia forces weaken the neck between protuberations and therefore the drop weight is less then the theoretical. In general, drop weight increases to a maximum at a rate of drop formation for which the droplets are most completely formed. By using distilled water, Adler (94) obtained the following results to relate the drop weight to the rate of drop formation:-

TABLE 22.1.

= .00	t	0.57	0.62	0.65	0.70	0.80*	0.88	1.02	1.38	2.05	3.14	3.85	5.25
1.	w	78.87	79.67	80.05	80.65	81.30	81.25	80.65	80.15	79.05	78.00	77.60	77.00
= .40	t	0.74	0.77	0.91	1.15*	1.55	2.05	2.95	4.00	4.47	5.06	6.50	
1.	w	137.6	138.5	140.15	140.8	140.3	139.1	137.7	136.6	136.1	135.9	135.1	
= 5.90	t	1.18*	1.51	1.66	1.75	2.04	2.47	2.96	3.54	4.05	5.43	6.41	8.33
1.	w	249.0	247.9	246.0	245.8	244.7	242.5	241.7	239.0	237.7	235.3	234.4	232.4

t = rate of drop formation, secs. w = drop weight, mg.

Thus it will be seen that for d = 5.00 m.m. the maximum weight is obtained when t = 0.80 sec., for d = 9.40 m.m. when t = 1.15 sec. and when d = 15.90 m.m. when t = 1.18 sec. (probably less, even)

23. Formation of Sprays.

When a fluid is sprayed from an orifice under high pressure the number of factors affecting the spray formation are very considerable. Under the conditions for spray formation the foregoing theory by Rayleigh for the formation of (single) drops by a non-viscous fluid under potential flow does not hold; while the effects of inertia forces only extend over the range of comparatively low velocities. It was in fact, shewn by Hainlein (95) and also by Lee & Spencer (96) that the disintegration of a jet into a spray, passes through several stages as the injection velocity (or pressure) is increased, the stages proceeding through the surface tension, viscosity, inertia-forces range to the formation of an unstable jet which "snakes" and then disintegrates. Under these conditions it must be remembered that the single drop formation by the detachment of whole portions of the jet, is replaced by the disruption of many parts of the jet and in turn, the tearing-off of portions of these disrupted parts as well. The whole process is cumulative.

A survey has been made by Schweitzer (97) of the many theories which have been advanced to explain the disruptions of a jet and the formation of sprays. The process of "atomisation" when a jet is caught up in an airstream, as for example, in a carburettor, was described by Castleman (98) as the result of a portion of fluid being detached from the main jet at a point where the surface was ruffled. One end of this detached portion of fluid remains attached to the main jet, while the other, free, end is drawn off so that the ligament of fluid so produced is compelled to draw out finer and finer while a "dent" grows at the neck securing it to the main jet. Finally, this fluid becomes detached and is drawn into the air stream, while rapidly drawing itself up into a spherical droplet. It was suggested by Castleman that as the air speeds increased so the ligaments became finer, their time of disintegration shorter and drop size smaller. Still further, it was proposed that the disintegration of a jet depended very largely upon the air friction.

That air friction does influence the disintegration of a jet has been proved by several investigators when injecting fine sprays of various liquids into atmospheres of various pressures and densities. The physical properties of the fluid, the nozzle proportions and the injection pressures are important factors which also control the atomisation of the jet. By using many modifying assumptions in order to simplify his deductions and by studying the disruption of a fluid mass with a cylindrical body and hemispherical ends, Triebnigg (99) managed to produce a formula for the globule diameter, a generalised version of which is

$$d = \frac{62.2}{(p_1 - p_2)w} \quad \text{m.m.} \qquad \ldots\ldots\ldots\ldots\ldots\ldots\ldots\ldots\ldots\ 23.1.$$

where $p_1 - p_2$ = pressure difference, Kg./sq.mm. causing injection,

w = density, Kg./cub.mm. of the air into which the fluid is injected.

In reviewing the suitability of this equation and comparing the values which it gives against those obtained by experiment, Sass (100) showed that it was unsuitable for sprays injected into low-pressure chambers, but that some measure of agreement could be obtained when used with jets injected into high pressure air. These comparisons are given in Table 23.1.

TABLE 23.1.

Back Pressure, atmospheres.		1		30
Injection Pressure, atmospheres.	100	150	200	300
Calculated Drop Diameter, mm.	0.516	0.344	0.258	0.0174
Measured (Mean) Drop Diameter, mm.	0.035 to 0.005	0.030 to 0.004	0.020 to 0.003	0.020 to 0.010

Other attempts to calculate the drop size have been made by Kuehn (101) who unsuccessfully attempted to apply the laws of flow similarity, while Scheubel (102) endeavoured to analyse the phenomena somewhat empirically from his experimental records. None of these attempts have yet evolved a satisfactory explanation of the phenomena of spray formation.

24. Atomisation and Penetration of Sprays.

The irregular drop formation which is created within a spray, not only complicates the calculations for mean drop size, but involves practical difficulties with regards to the uniformity of atomisation. This subject is of particular importance with regards to the solid-injection of fuels in compression-ignition engines and from the investigations into this aspect of 'free' discharge of fluids through apertures, the following notes have been drawn.

In the design of sprays for fuel injection engines it is desirable to inject small droplets into the cylinder, all of these droplets having the same diameter. To test these sprays, a sample is obtained - by various means, of which one is the insertion of a lamp-blacked plate into the spray - of the droplets in the spray over one area. For this sample, the number of droplets of a certain size-group are counted and their number plotted against the mean diameter of the group. By this means it is possible to draw curves such as fig. 24.1.(a) and (b) which are described by Sass as "frequency-curves," probably in view of their similarity to the amplitude-frequency curves plotted in the study of vibration (and where the maximum or peak amplitude occurs at the resonant frequency, i.e. the natural frequency of the elastic system.) With these curves, the fineness is represented by the drop size of the maximum ordinate, i.e. the absicca of the maximum ordinate, for, the smaller this value becomes, the smaller do most of the droplets become and therefore the finer is the atomisation. In fig. 24.1. curve (a) represents a spray which is much finer than curve (b). Uniformity is represented by the mean slope of the first part of the frequency curve, the smaller this slope the greater is the uniformity of the spray; curve (b) is therefore a more uniform spray than curve (a).*

The distribution of a spray inside the cylinder depends when (i) energy of the droplets and (ii) width or angle of the spray. Miller & Beardsley (103) showed from a series of cine-pictures that the penetration of a fluid spray into a high pressure gas increased as the spray developed until it reached a constant value for which further prolongation failed to increase the penetration. The limiting penetration, i.e. the asymptote of the penetration-time curve, depends upon the injection and chamber pressures. The actual duration of a spray (as compared with its time of development) has no effect upon the penetration, so that from the point of

---

*It is interesting at this stage to note the photographs, fig. 24.2. of the sprays through an orifice (i) under blast injection (ii) solid injection. The atomisation for blast injection at low pressures is equal to that of solid injection which is attained only by using high injection pressures, thus the 75/30 blast is approximately equal to the 300/30 solid while the 65/30 blast is equal to the 250/30 solid. While not pretending to be in any way conclusive of the efficacy of blast injection these photographs offer striking evidence of the superior injection to be obtained from blast injection.

view of injection characteristics a short intermittent spray penetrates and atomises exactly the same as a "stationary" spray. It should also be recorded that the work of Gellales and Marsh (104) indicates that an intermittent injection does not itself alter the performance of a compression-ignition but that the accompanying valve action is detrimental to atomisation. Schweitzer (105) showed from tests in which the penetration was measured by impinging the spray on a sensitive electric contact, that the most important variables in spray penetration could be expressed in the formulae

$$S = f(t.\sqrt{p}.) \quad \ldots\ldots \quad 24.1.$$

$$\frac{S}{d} = f\left(\frac{t}{d}\right) \quad \ldots\ldots \quad 24.2.$$

$$S(1 + p_a) = \quad (t.\ p_a) \quad \ldots\ldots \quad 24.3.$$

in which t = time, (millisecs.)

p = injection pressure

d = orifice diameter

p_a = chamber pressure.

The actual phenomena associated with the penetration of a spray have not yet been studied from the physical aspect in spite of the many quantitative experiments which have been performed. Schweitzer (106) has stated that although the initial velocity of the jet depends upon the injection pressure this influence only extends for a short distance along the jet. A precise interpretation of these remarks is difficult to make, but from the previous notes on drop formation it would appear that the influence of air/droplet friction render the flow unstable. Some allowance will also be required to account for the inflow of mixing air. It is also interesting to record the observations made by Bird (107) who stated that the flow of oil in the conditions under review fell between stream-lined (laminar or viscous) and turbulent flow, thus the flow of the oil is changed in a manner which has not previously been subjected to a close physical review. It was also noticed by Bird that the injection pressure and velocity varied according to the expression

$$p = \text{Constant} \times V^N$$

where the index N was about 1.2 at 1000 lb./sq. in. and increased to 2.0 at 5000 lb./sq. ins.

Spray angle does not appear to vary to any great extent but forms an angle of 60° under nearly all conditions of flow. Experiments by Joachim and Beardsley (108) showed that the spray angle would first decrease and then increase with the length/diameter ratio of an orifice. By collecting measured samples of the spray De Juhasz (109) found (1) that the cone angle increased with injection pressure and air density (2) decreased with the viscosity of the fuel.

It would appear, that related to the penetration and cone angle is the variation in size of the drops at distances from the orifice. This subject has been examined by several authors in connection with fuel injection but is complicated by the evaporation of the particles at the boundary of the spray. From the evidence at present available it would seem that (1) the droplets have an average smaller size at the boundaries than at the core (2) the average drop size decreases as the distance from the orifice is increased. Other than these bald statements of fact there is insufficient information available to develop this subject further.

REFERENCES.

1. E. Ower. "Measurement of Air Flow." Chapman & Hall. 1933, p.78.
2. R. W. Witte. Forschung auf dem Gebiete des Ingenieurwesens (T.M.T.) Vol. II. 1931, p.291.
3. L. Prandtl. "The Physics of Solids and Fluids," Part II. Blackie & Sons, 1936, p.191.
4. R. De Villamil. "Motion of Liquids." E. F. Spon, 1914.
5. W. E. Howland & J. D. Richetts. J. Franklin Institute, Vol. 233, 1937, p.83-94.
6. Prof. Hooper. Journal of the Society for the Promotion of Engineering Education, Vol. XVI, № 7, March, 1926.
7. F. Wittenbauer. "Aufgaben aus der Technischen Mechanik," 1921, III Band.
8. Lord Rayleigh. Phil. Mag. II, 1876, pp.441-447.
9. H. Lamb. "Hydrodynamics," Cambridge University Press, 1932, p.98.

*10. Kirchoff. "Zur Theorie freier Flussigkeitsstrahlen," Crelle LXX, (1869.)

11. M. C. Jacob. Comptes Rendus, 205, Dec. 1937, p.1365-67.
12. H. W. Swift. Phil. Mag. Vol. II, Dec. 1926, p.852.
13. D. Smith & W. J. Walker. Proc. Inst. Mech. Eng. Jan. 1923, p.23.
14. W. E. Howland. Journal of Applied Mechanics, June 1937, Vol. 4.
15. A. L. Mellanby & W. Kerr. N.E. Coast Institution of Engineers & Shipbuilders, 18th Feb. 1921.
16. G. L. Tuve & R. E. Sprenkle. Instruments, November 1933, p.201.
17. H. Mawson. Proc. Inst. Mech. Eng. 1927.
18. R. J. Cornish. Phil. Mag. 1936, 22, p.181.
19. Riabouchinsky. L'Aerophile, 1907, p.407.
20. De Borda. Mem. de l'Acad. des Sciences (1766.)
21. G. Bidone. Experiences sur la forme des Veines, Turin (1829.)

22. L. J. Weisbach. — Versuche uber die unvollkommene Contraction des Wassers, Leipzig (1883.)

23. W. C. Unwin. — A Treatise on Hydraulics (1907.) Black.

24. A. M. Binnie. — Proc. Royal Soc. A. Vol. 168, p.219 (1938.)

25. F. C. Johansen. — Proc. Royal Soc. A. Vol. CXXVI, p.231.

26. F. C. Johansen. — R. & M. 1252, June 1929.

27. W. N. Bond. — Proc. Phys. Soc. 33, 1920-21, p.225.

28. G. L. Davidson. — Proc. Royal Soc. Vol. LXXXIX, 1913-14, p.94.

29. J. R. Pannell. — Brit. Aero. Research Comm. Report & Memoranda 243, June (1916.)

30. W. H. McAdam. — "Heat Transmission," McGraw-Hill Book Co. (1933.)

31. Albert & Constance H. Griffiths. — Proc. Phys. Soc. 33 (1920-21) p.203.

32. Howard Emmons. — Mechanical Engineering, April (1933.) p.23.

33. Smith & Steele. — Mechanical Engineering, December (1935) p.260.

34. E. S. Smith. — Trans. A. S. M. E., Vol. 52, 1930.

35. S. G. Davies & C. M. White. — Proc. Royal Soc. A. Vol. 119 (1928) p.92-107.

36. F. V. A. Engel & J. W. E. French. — "Engineering," Oct. 16 & Nov. 6., 1936.

37. R. J. Cornish. — Phil. Mag. 1936 (22) p.181-186.

38. S. Venant. — Comptes Rendus, 1839.

39. J. L. Hodgson. — Inst. Civil Engineers. Selected Paper Nº 31 (1925.)

40. C. Monteil. — Ann. d. Phys. et. Chim. XXVII (3) Nº 35 p.139 (1907.)

41. Hamilton Smith & Bovey. — Proc. I. Mech. E. 1886.

42. Hamilton Smith & Bilton. — Hydraulics (London) 1886.

43. J. G. Mair. — Proc. Inst. Civil Engineers, Vol. LXXXIV, p.427.

44. H. Bazin. — Experiments on the Contraction of the Liquid Vein (trans. pub. Chapman & Hall) (1896.)

45. K. Pohlhausen. — Zeitschrift f. ang. Math. u. Mech. 1. (1921) p.261-3.

46. L. Schiller. — Zeitschrift f. ang. Math. u. Mech. 2. (1922) p.96-106.

47. L. Schiller. — Proc. 3rd International Congress for Applied Mechanics, Stockholm (1930.)

48. A. Naumann. — Forschung auf dem Gebiete des Ingenieurwesens (2) 1931, p.85-98.

49. H. Latzo. — Zeitschrift f. ang. Math. u. Mech. 1. (1921) p.277-280.

50. L. Schiller. — Handbuch der Experimentalphysik (4), Part 4, (Leipzig 1932) 191, 192.

51. "Modern Developments in Fluid Dynamics," Oxford Press, 1938, Part I, p.311.

52. Boris A. Bakmetoff. — "The Mechanics of Turbulent Flow," Princeton University Press, 1936.

53. F.V.A.E. Engel & A. J. Davies. — Engineer, Dec. 30, 1938.

54. H. W. Swift. — Phil. Mag. (8) 1929 pp.409-435.

55. L. H. Mitchell. — Phil. Trans. Royal Society (1890) p.405.

56. H. W. Swift. — Phil. Mag. (5) 1928, p.1.

57. F.V.A.E. Engel. — "Civil Engineering," December, 1931.

58. S. R. Beitler. — Ohio State University, Engineering Experimental Station Bulletin Nº 89 (1935.)

59. A. A. Barnes. — Transactions Inst. Water Engineers, Vol. 38. Bristol (1933) p.133-157.

60. A. G. Gelalles & E. T. Marsh. — N.A.C.A. Technical Note, Nº 369, March (1931).

61. D. R. Pye. — Oxford University Press, p.231.

62. E. Buckingham. — J. Research U.S. Bureau of Standards, Vol. 2 (1929) p.561.

63. G. Ruppel. — Zeitschrift der Verein Deutsche Ingenieur, November (1936) p.138.

64. H. J. Buckrow. Trans. A.S.M.E. (1929) APM-51-19.

65. C. H. Fisher. "Carburation and Carburettors," Chapman & Hall (1939.)

66. J. F. Downie Smith. Transactions A.S.M.E. October (1934.)

67. W. Watson & H. Schofield. Proc. I. Mech. E. (1912.)

68. M. J. Zuckrow. Transactions A.S.M.E. (1929) APM-51-19.

69. H. S. Bean, E. Buckingham & P. S. Murphy. Bureau of Standards Journal of Research, Vol. 2 (1929) p.561-658.

70. T. E. Stanton & J. R. Pannell. Phil. Trans. Roy. Soc. A. Vol. 214 (1914.)

71. A. Betz. Engineering, April 5 (1929) p.434.

72. F. V. A. E. Engel. Die Waerme, Vol. 60 (1937) p.415.

73. H. Judd. Transactions A.S.M.E. (1916) p.331.

74. S. Goldstein. "Modern Developments in Fluid Dynamics," Part I, Oxford (1938.)

75. L. Prandtl. "Vortrage aus dem Gebiete der Hydro - und Aerodynamik," Leipzig (1922) p.18.

76. L. Prandtl. "Handbuch der Experimentalphysik" (4) Part I (Leipzig 1931) p.20.

77. H. C. H. Townend. The Flow Induced by a Jet. R. & M. 1634.

78. F. Kretschmer. Forschungsheft 381, Vol. 7, Nov.-Dec. (1936) p.28.

79. E. N. da C. Andrade. Proc. Phys. Soc. 51 (1939) p.784.

80. A. M. Binnie & H. B. Squire. Engineer, Vol. 171, April 11 (1941) p.236.

81. H. Schlichtling. Zeitschschrift fur angew. Mathematik und Mechanik, 13 (1933.)

82. R. Bickley. Philosophical Magazine, 7, (1937) p.727.

83. W. Nusselt. Zeitschrift fur Flugtechnik und Motorluftschiffart, 6 (1915) p.179.

84. Thomas Young. Phil. Trans. 5 (1805) p.65.

85. P. S. Laplace. Mechanique Celeste (1806.)

86. B. B. Freud & W. D. Harkins. Journal of Physical Chemistry 33 (1929) p.1217.

87.	Th. Lohnstein.	Ann. Physik. (4) 20, p.237, 606 (1906).
88.	S. W. J. Smith & H. Moss.	Proc. Royal Soc. (A). 93 (1917) p.373.
89.	E. Tyler & E. G. Richardson.	Proc. Physical Soc. Vol. 47 (1924) p.297.
90.	Lord Rayleigh.	"Theory of Sound," Vol. II, p.357.
91.	G. Littaye.	Comptes Rendus, April 29 (1940) p.600.
92.	E. Tyler & F. Watkin.	Phil. Mag. XIV. Supplement Nov. 1932.
93.	E. Tyler.	Phil. Mag. (16) 1933 p.504.
94.	Ad. Adler.	Physikalische Zeitschrift, № 35 (1934.)
95.	A. Haenlein.	Forschung (V.D.I) (2) p.139 (1931.)
96.	Dana W. Lee & Robert C. Spencer.	N.A.C.A. Report № 454 (1933.)
97.	P. H. Schweitzer.	Journal of Applied Mechanics, Vol. 8. Aug. 1937, p.513.
98.	R. A. Castleman.	National Bureau of Standards, Journal of Research (7), p.269 (1931.)
99.	H. Triebnigg.	"Der Einblase und Einspritzvorgang bei Dieselmaschinen," Wien, Julius Springer (1925.)
100.	F. Sass.	"Kompressorlose Dieselmaschinen," Berlin, Julius Springer (1929.)
101.	R. Kuehm.	Der Motorwagen (Berlin) 1924 & 1925 (a series.)
102.	F. H. Schmiebel.	"Jahrbuch der Wissenschaft Gesellschift f. Luftfuhrt" (1927.)
103.	H. E. Miller & E. G. Beardsley.	N.A.C.A. Report № 222.
104.	A. G. Gelalles & E. T. Marsh.	N.A.C.A. Report № 433.
105.	P. H. Schweitzer.	Automobile Engineer, Feb. 1938, p.61.

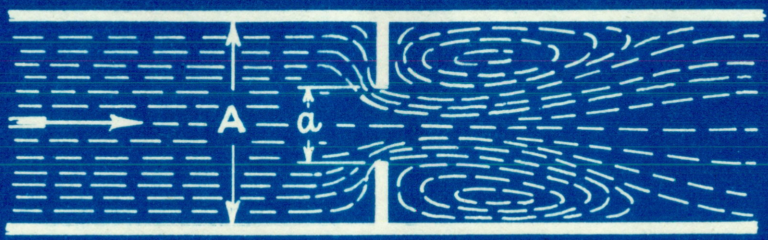

Fig. 2.1 Section through a parallel pipe shewing the acceleration of the fluid stream through an orifice.

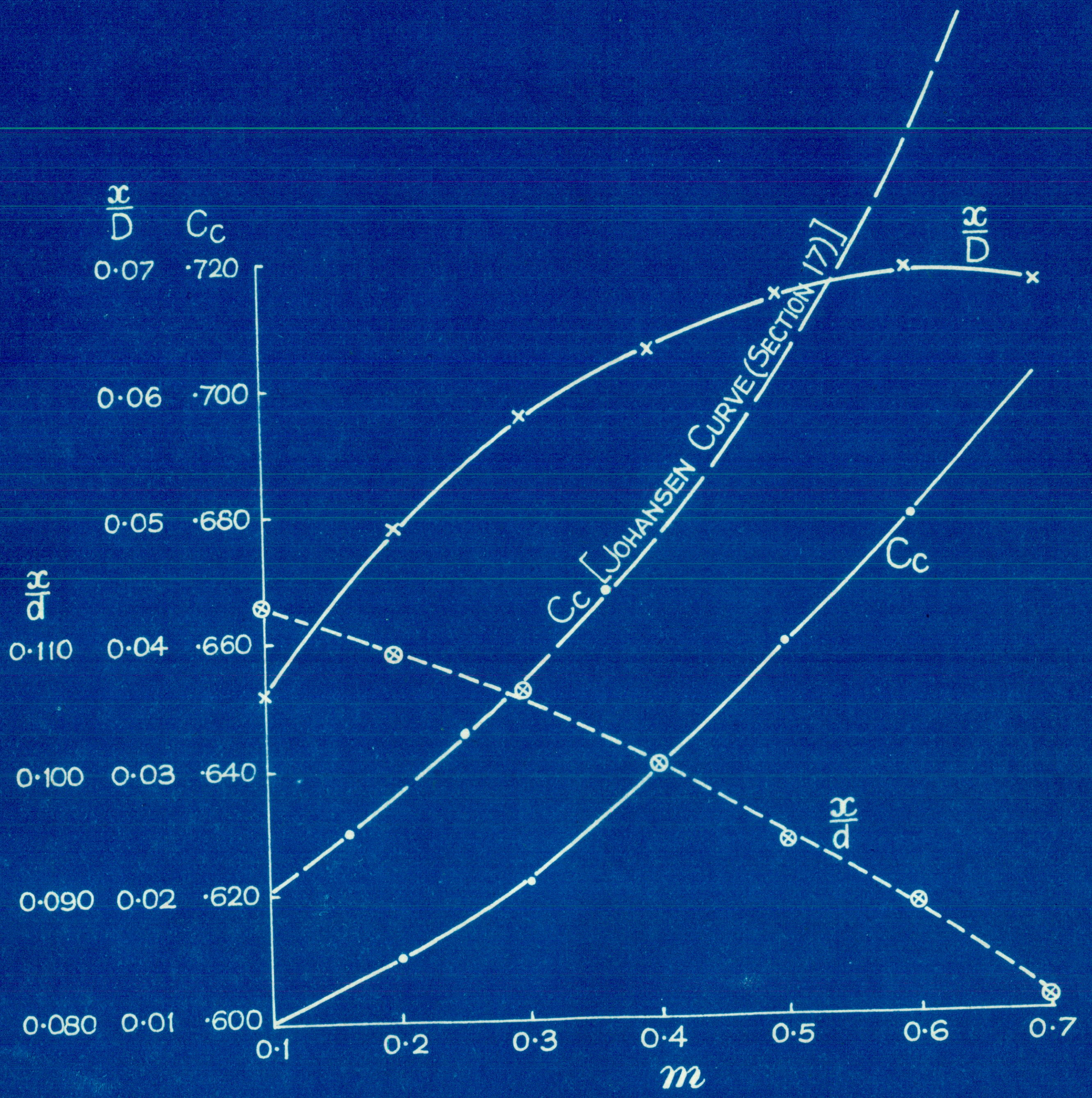

Fig. 2.2 The effect of the orifice-pipe diameter ratio on the coefficient of contraction. Values given by WITTE (2)

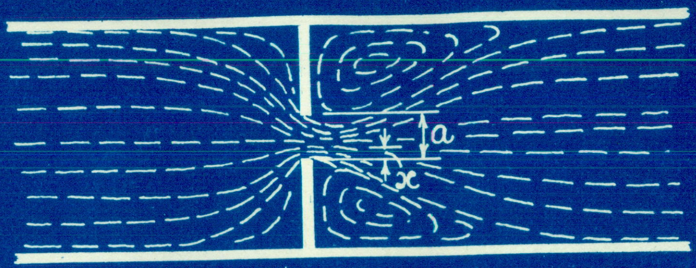

(a)

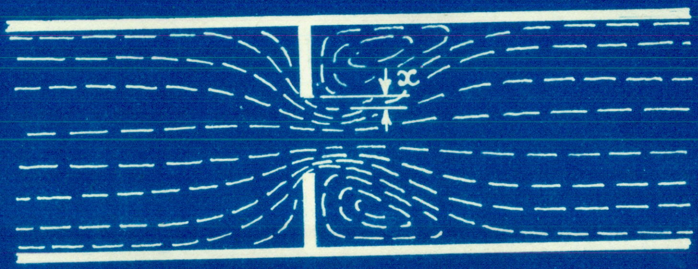

(b)

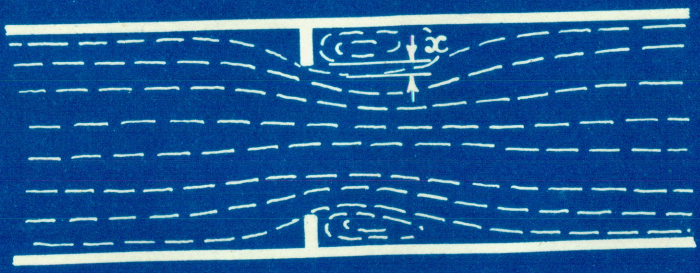

(c)

Fig. 2.3 Pictorial representation of the effect of the orifice-diameter ratio on the coefficient of contraction.

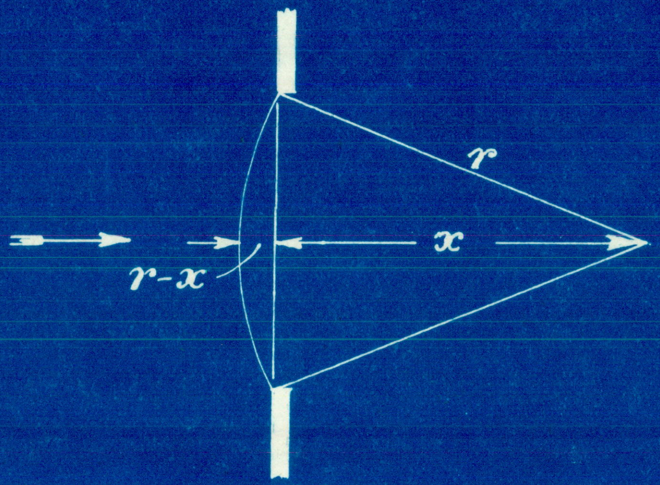

Fig. 2.4 Diagrammatic representation of an equi-velocity spherical-cap surface.

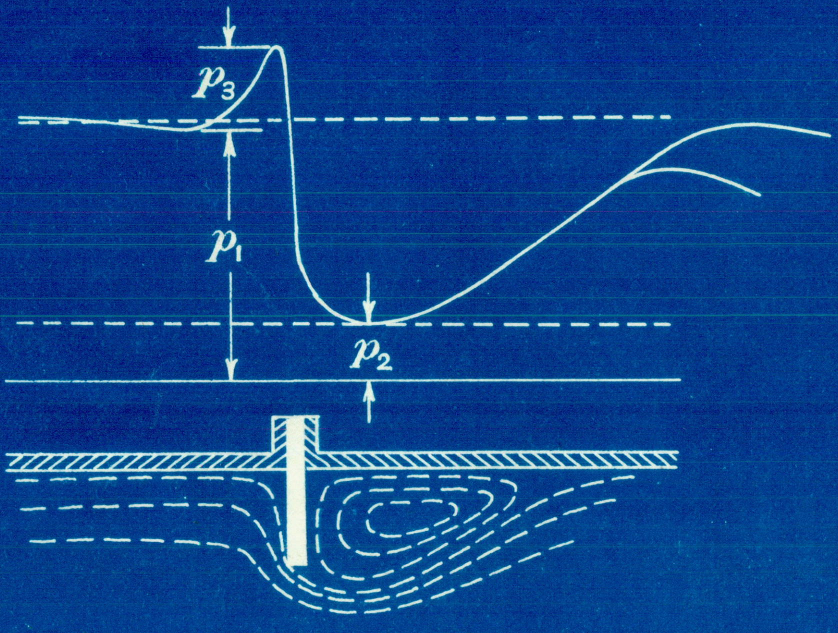

Fig. 2.5 The pressure distribution across a thin orifice plate.

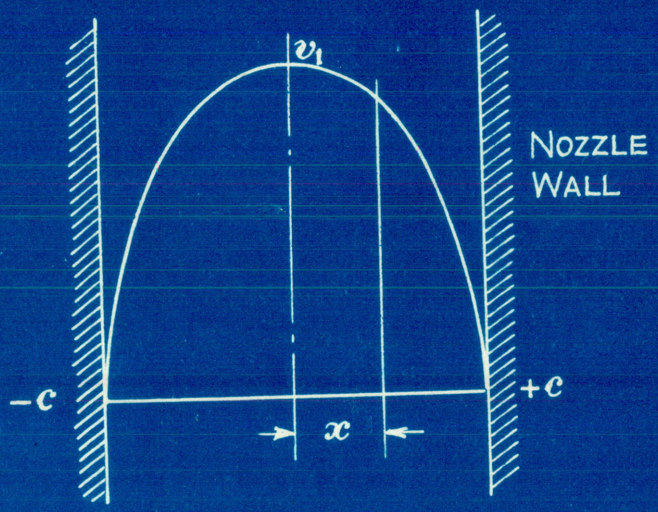

Fig. 2.6 Velocity distribution across the wall of a nozzle.

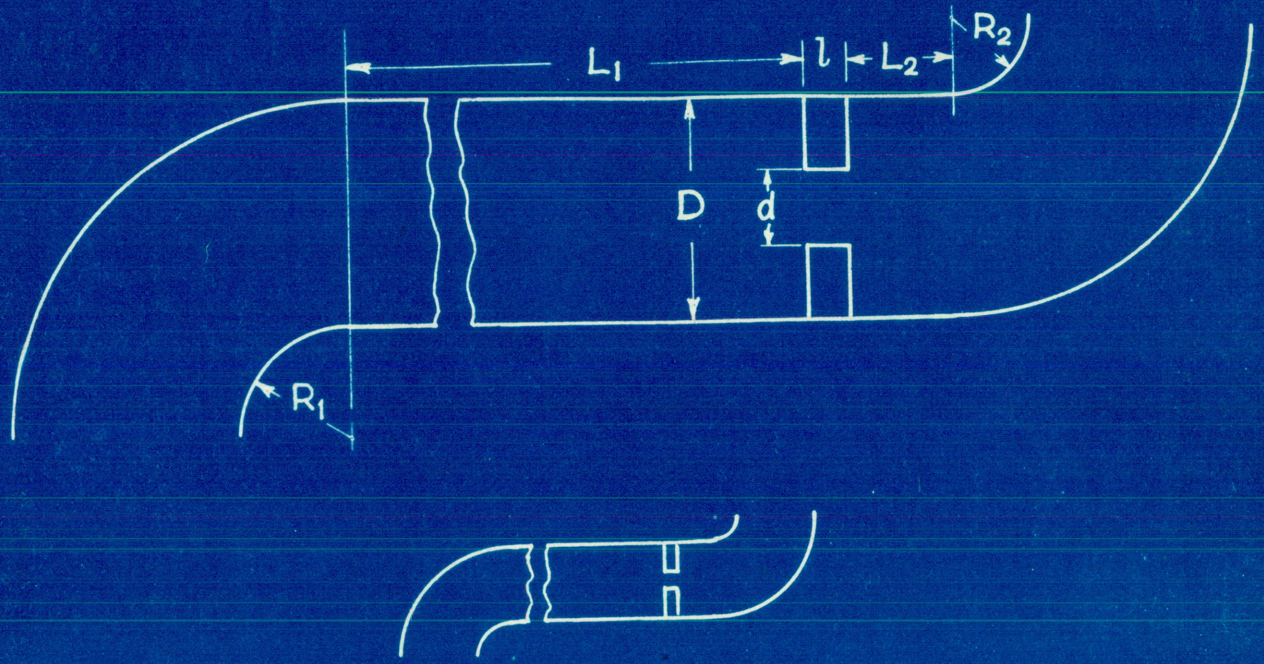

Fig. 3.1 (a) Geometrical similarity of two systems.

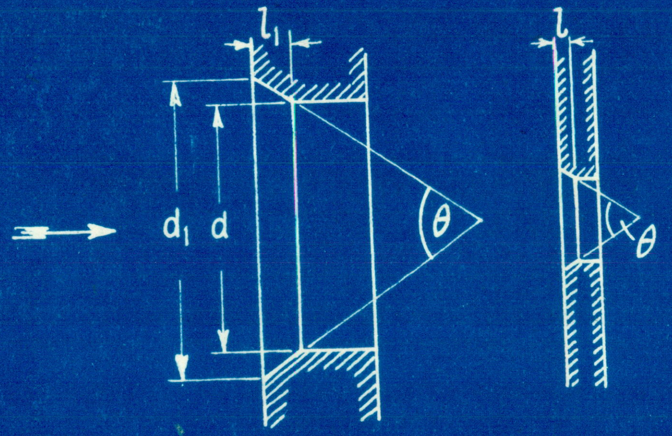

Fig. 3.1 (b) Geometrical similarity of a champfered orifice.

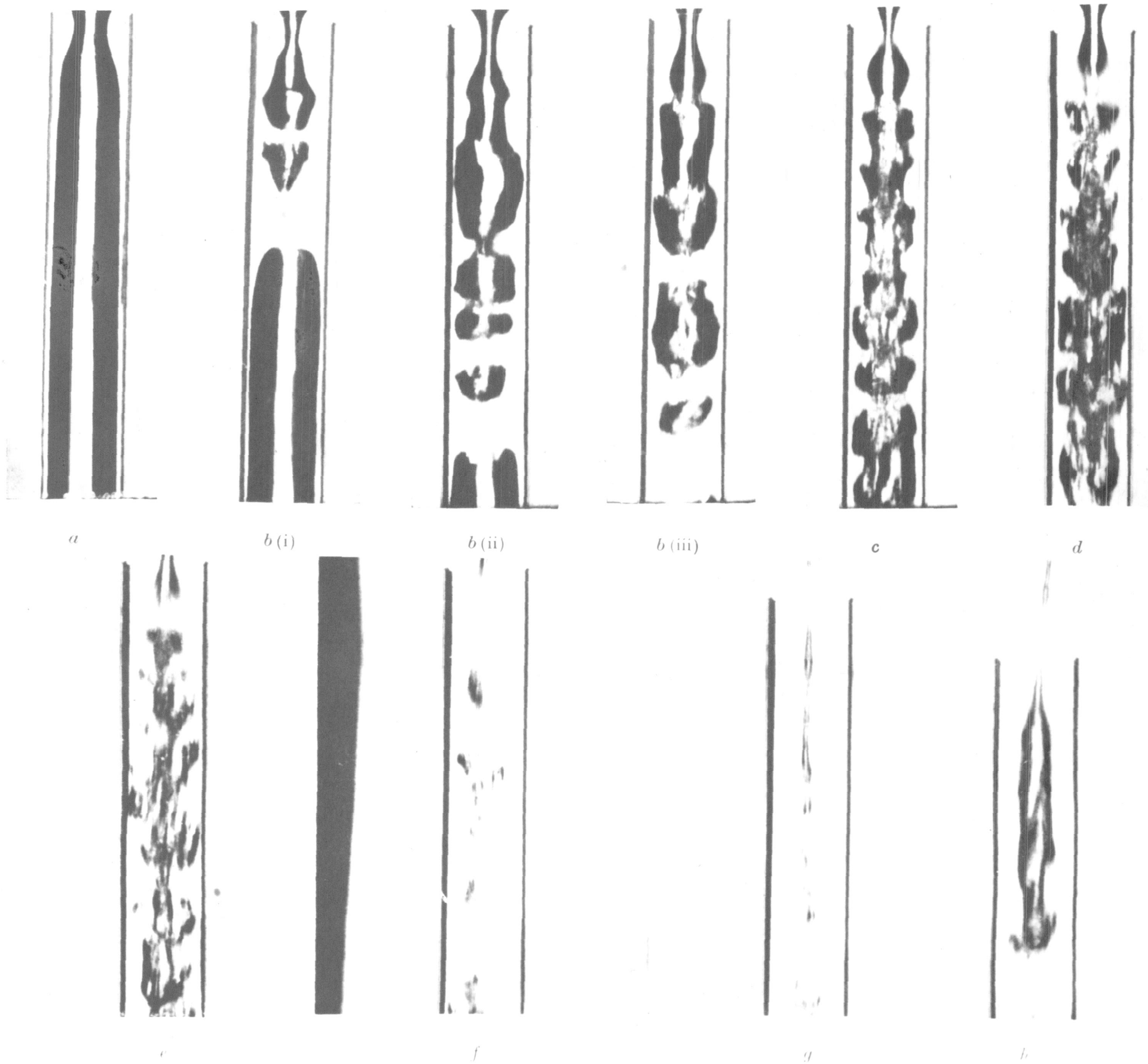

FIG. 4.1. Development of the flow in a re-entrant noppe.

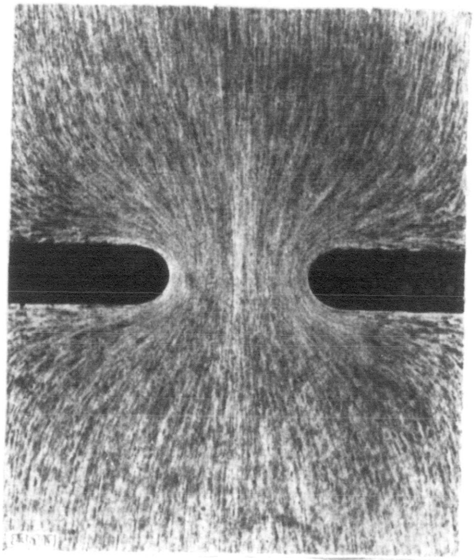

Fig.5.1. Flow through a rounded orifice.

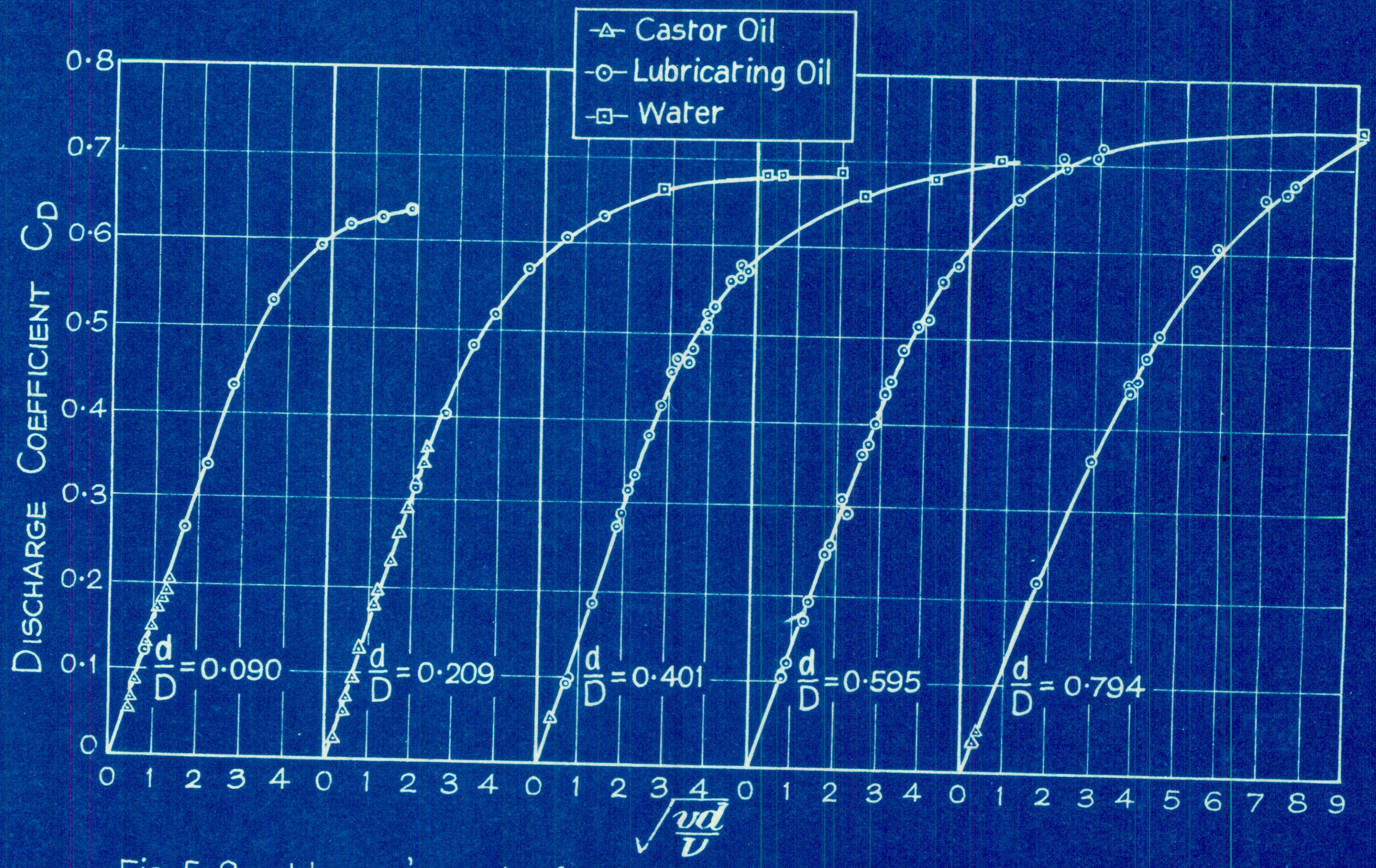

Fig. 5.2 Johansen's results for the viscous flow of fluids through orifices.

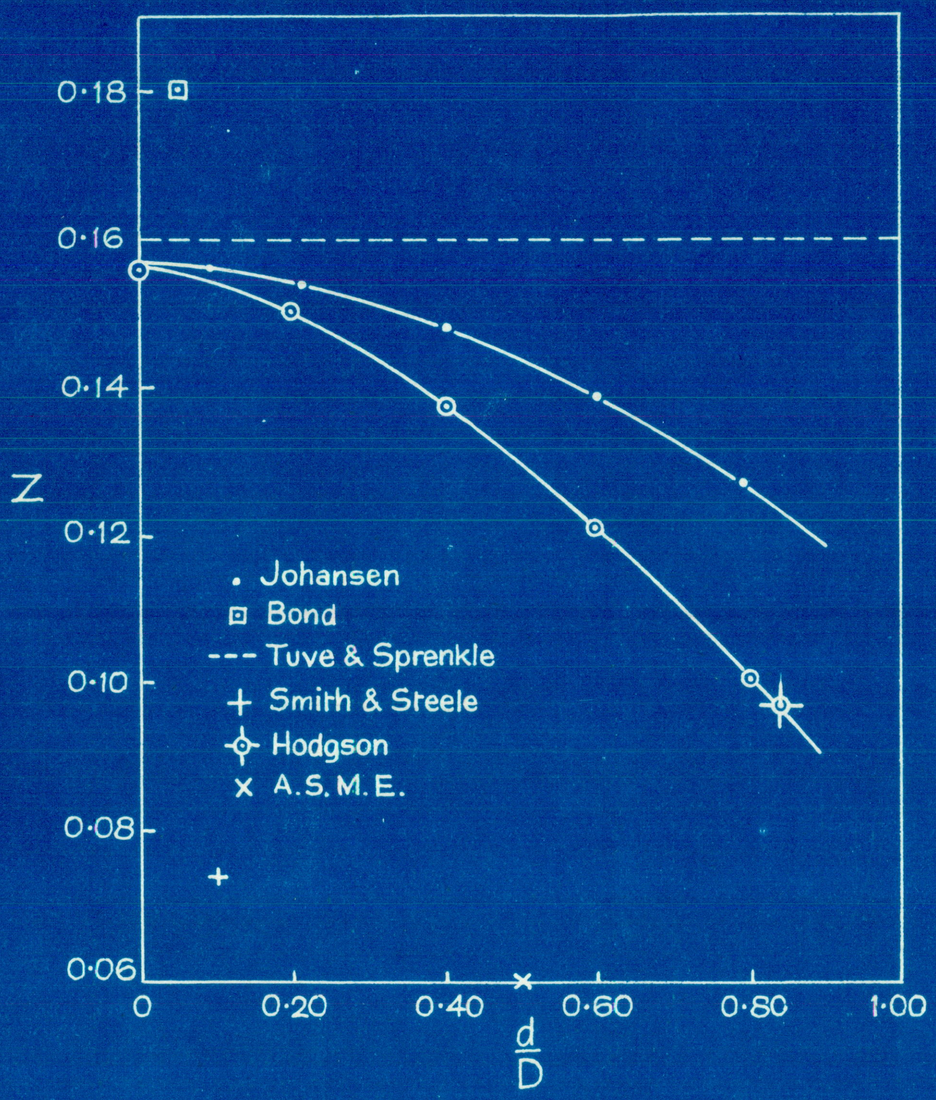

Fig. 5.3 The effect of orifice size on the viscous discharge.

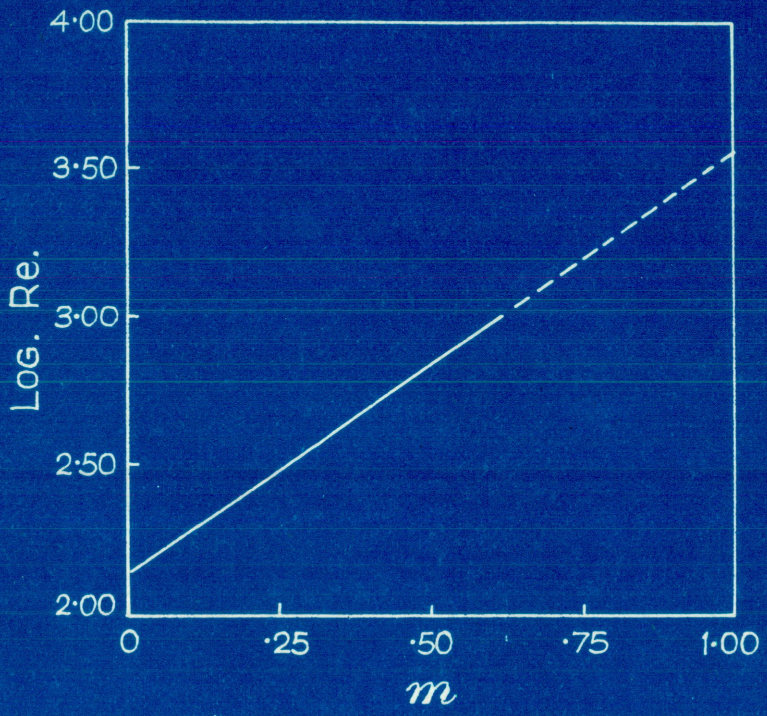

Fig. 5.4 The variation of Reynolds Number for maximum discharge coefficient with the orifice ratio.

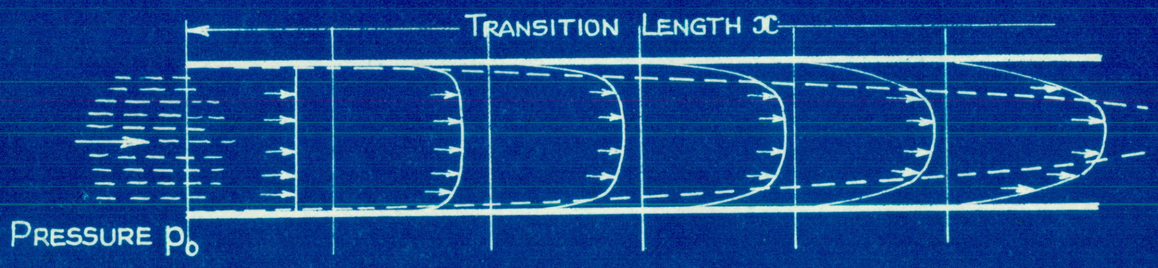

Fig. 9.1 The development of the velocity profile in the "inlet length" of a pipe.

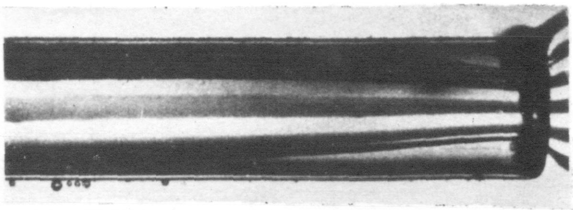

(a) Undisturbed Flow Re = 86

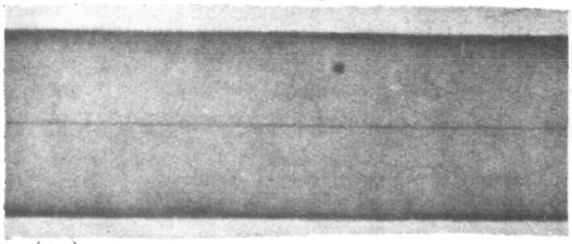

(b) Laminar Re = 90

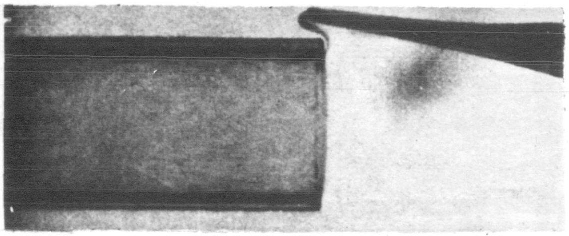

(c) Slight Contraction Re = 100

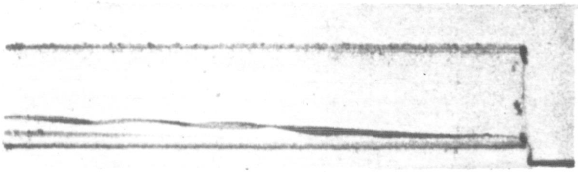

(d) Waves forming Re = 525

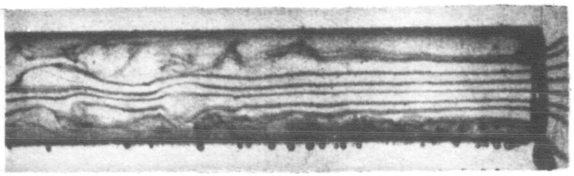

(e) Periodic Vortices Re = 700

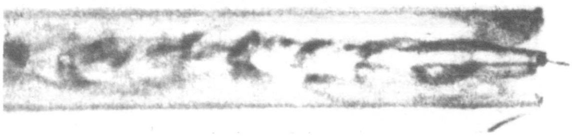

(f) Numerous Vortices Re = 1200

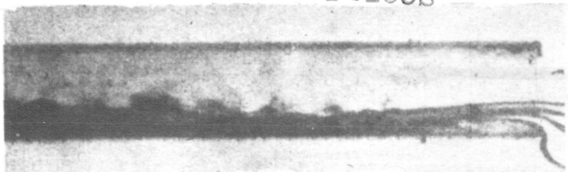

(g) Turbulence Re = 1600

Fig. 9.2. Inlet characteristics under various flow characteristics.

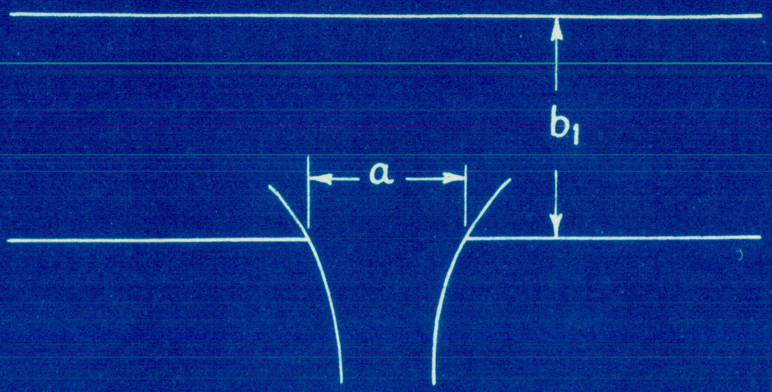

Fig. 9.3 Dimensions of an orifice in the wall of a pipe.

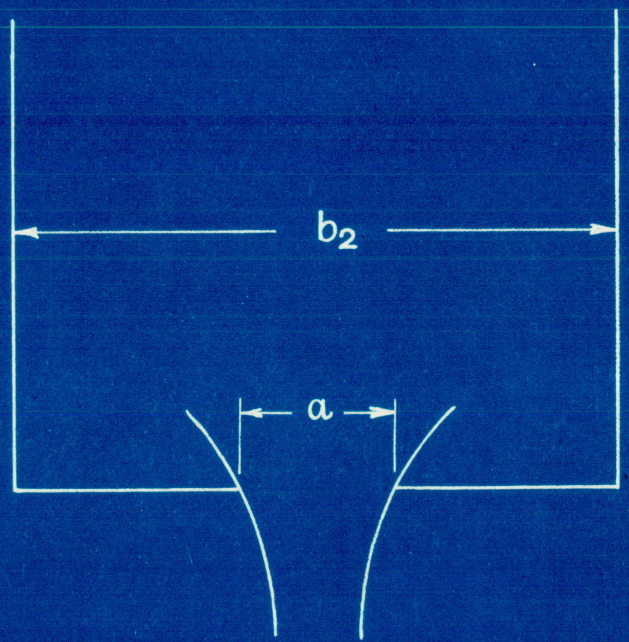

Fig. 9.4 Dimensions of an orifice in the end of a pipe.

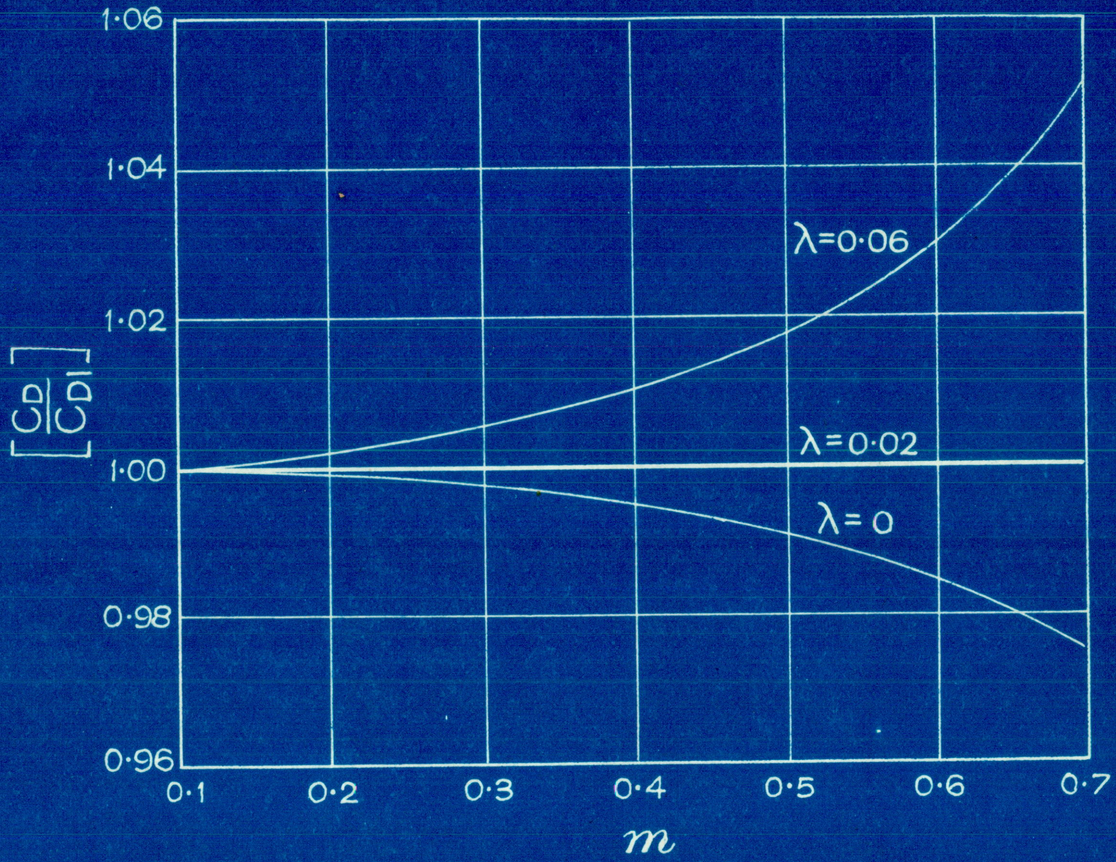

Fig. 9.5 The effect of a pipe roughness on orifice discharge

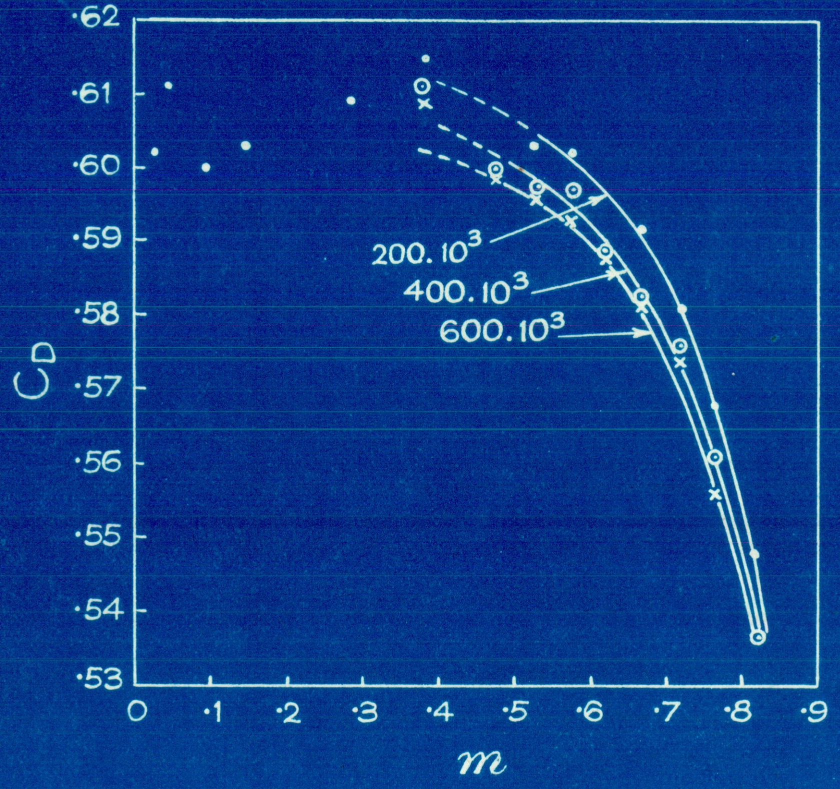

Fig. 11.1 The variation of C_D with "m" for various Reynolds Numbers (TURBULENT ZONE)

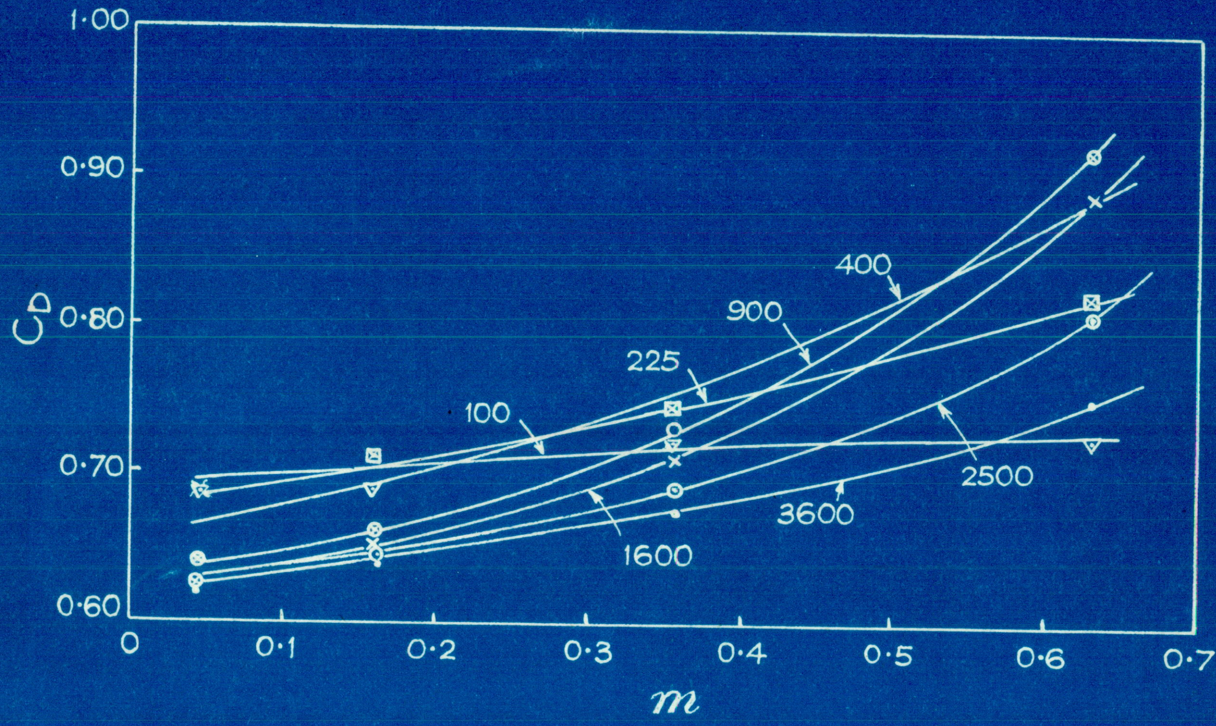

Fig. 11.2 The variation of C_D with "m" for various Reynolds Numbers (TRANSITION ZONE)

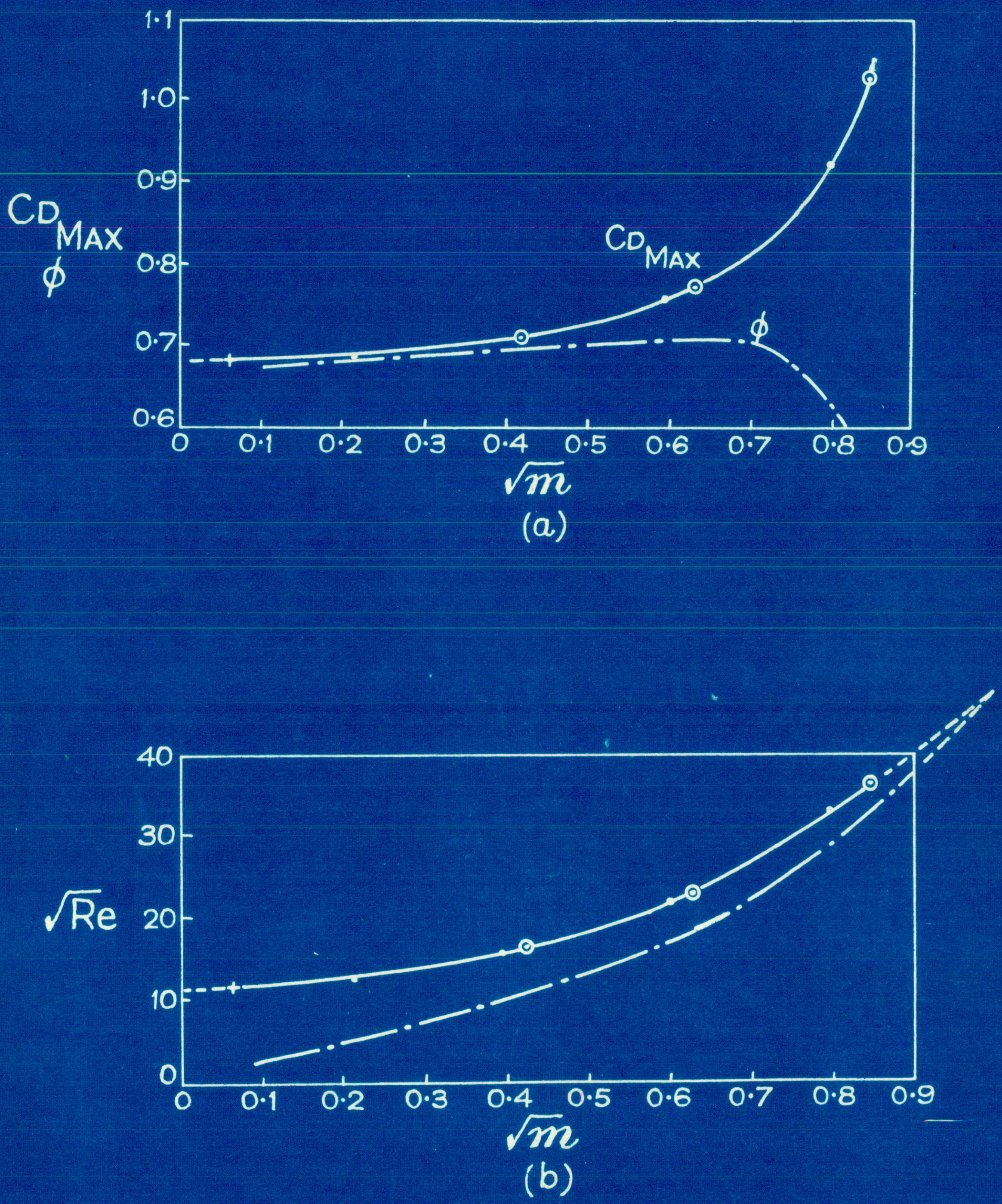

Fig. 11.3. The Maximum Discharge Coefficient and Limiting Reynolds Number.

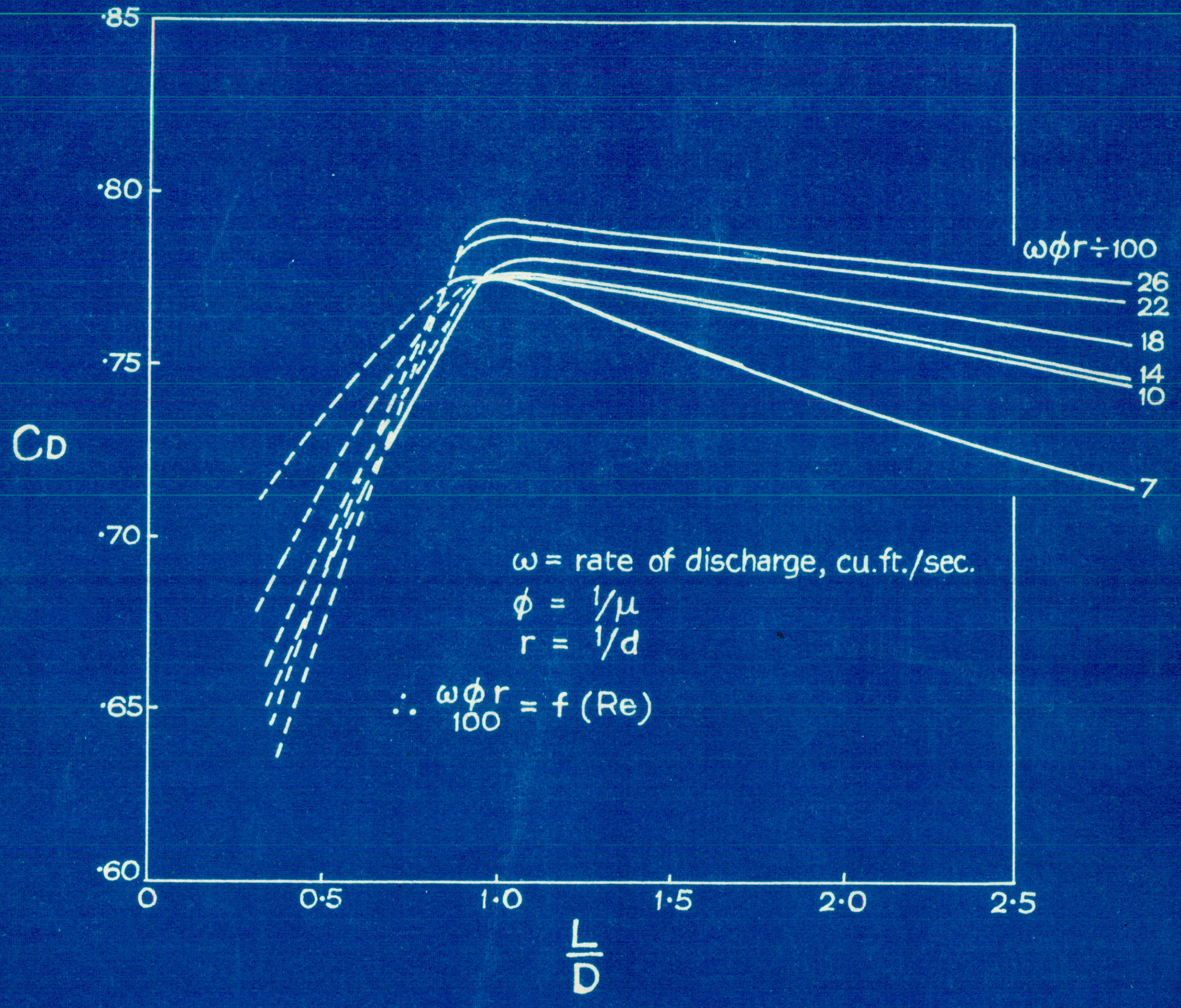

Fig. 13.1 The variation of CD and $\frac{L}{D}$ at various values of Re. (Zuckrow)

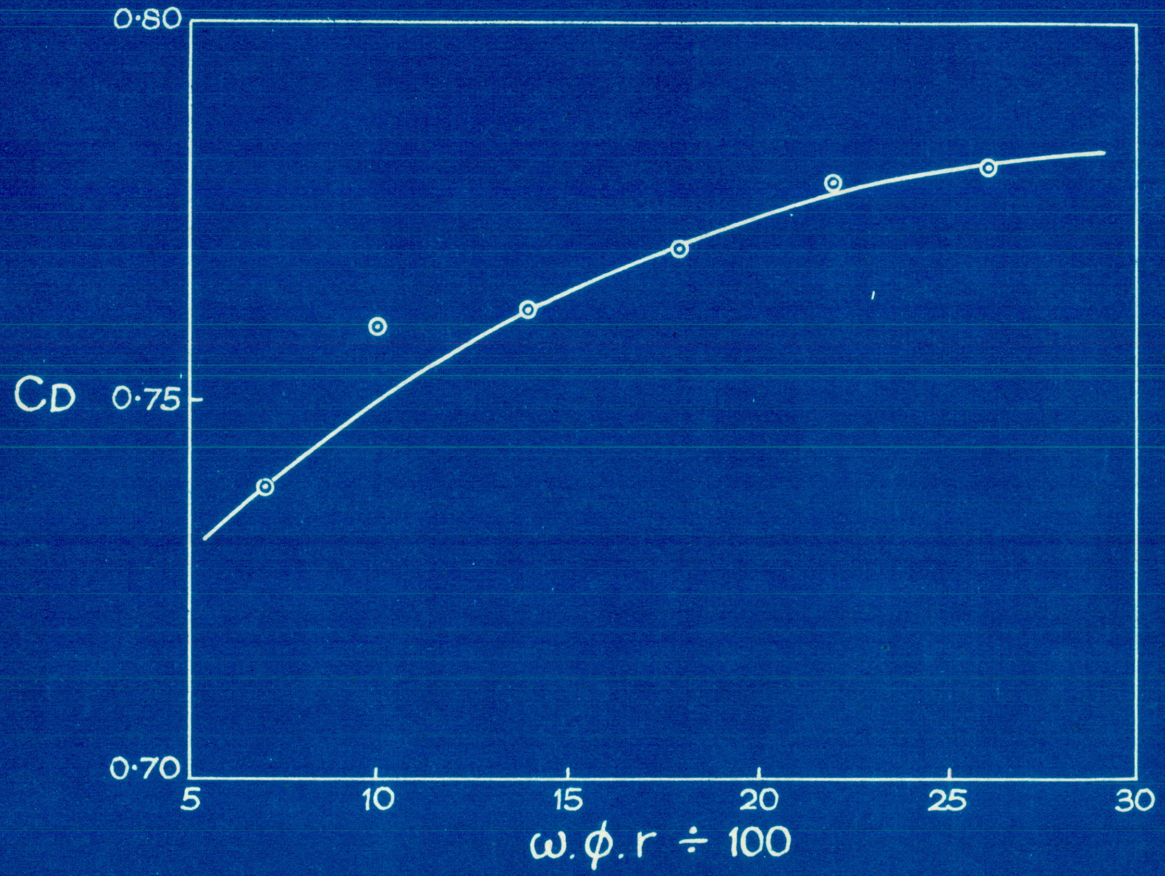

Fig. 13.2 The effect of Re on the C_D of a mouthpiece $\frac{l}{a} = 2{\cdot}0$.

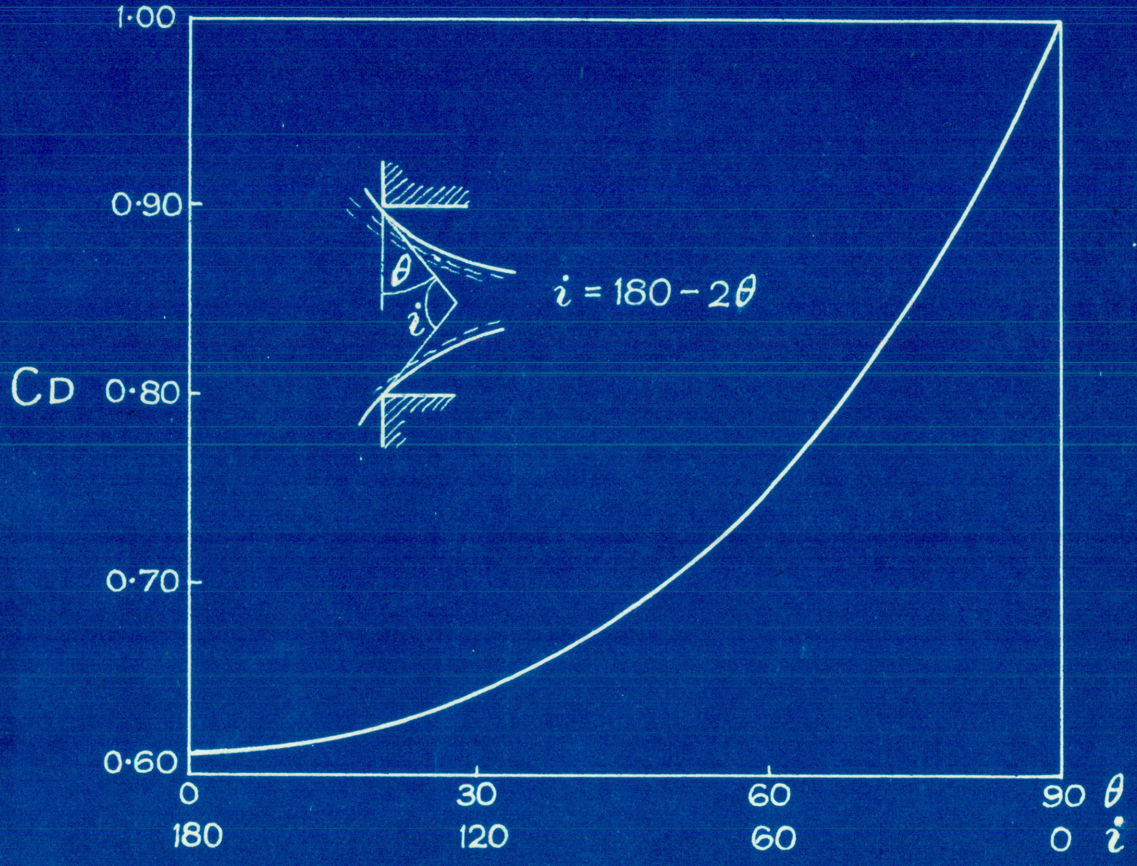

Fig. 14.1 The theoretical relationship between CD and θ (Swift)

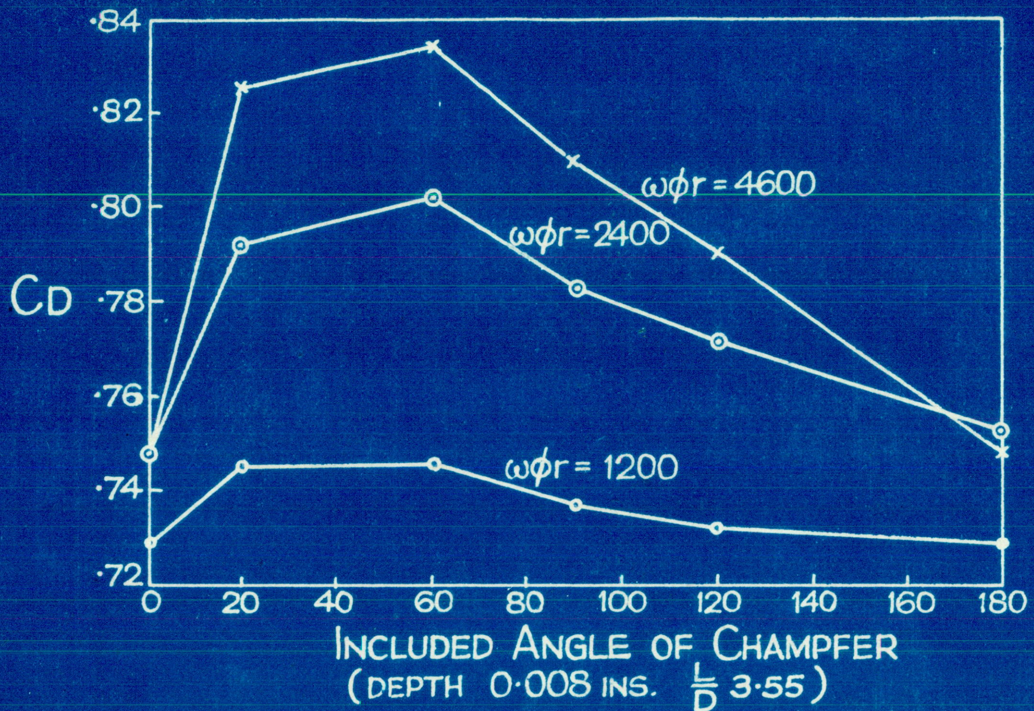

Fig. 14.2

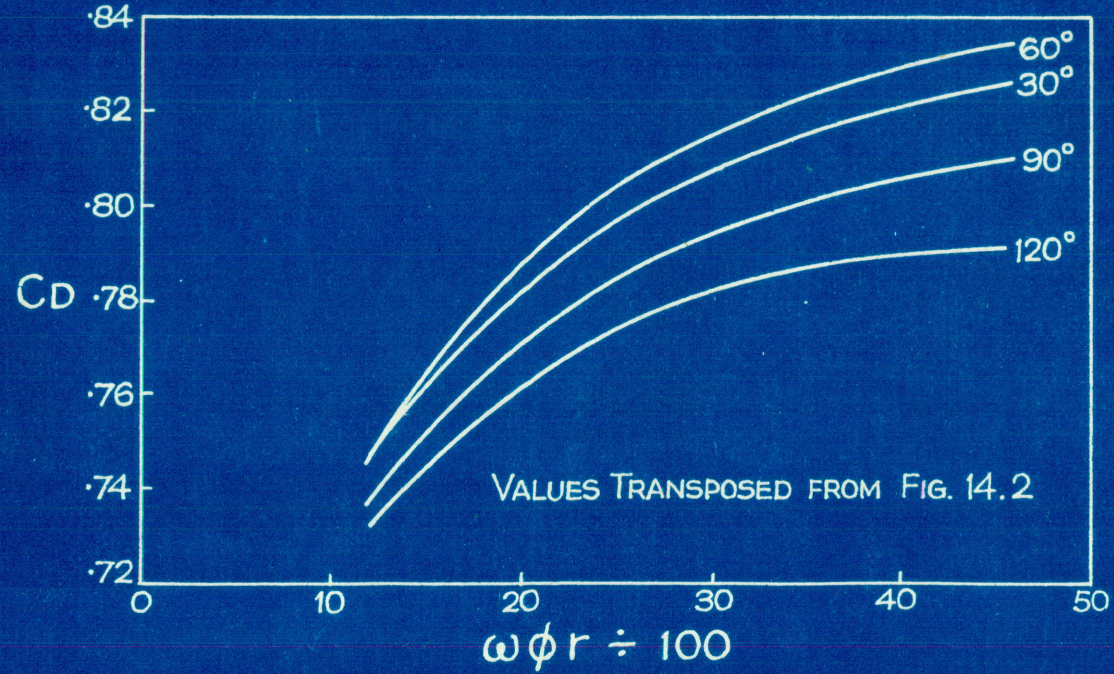

Fig. 14.3

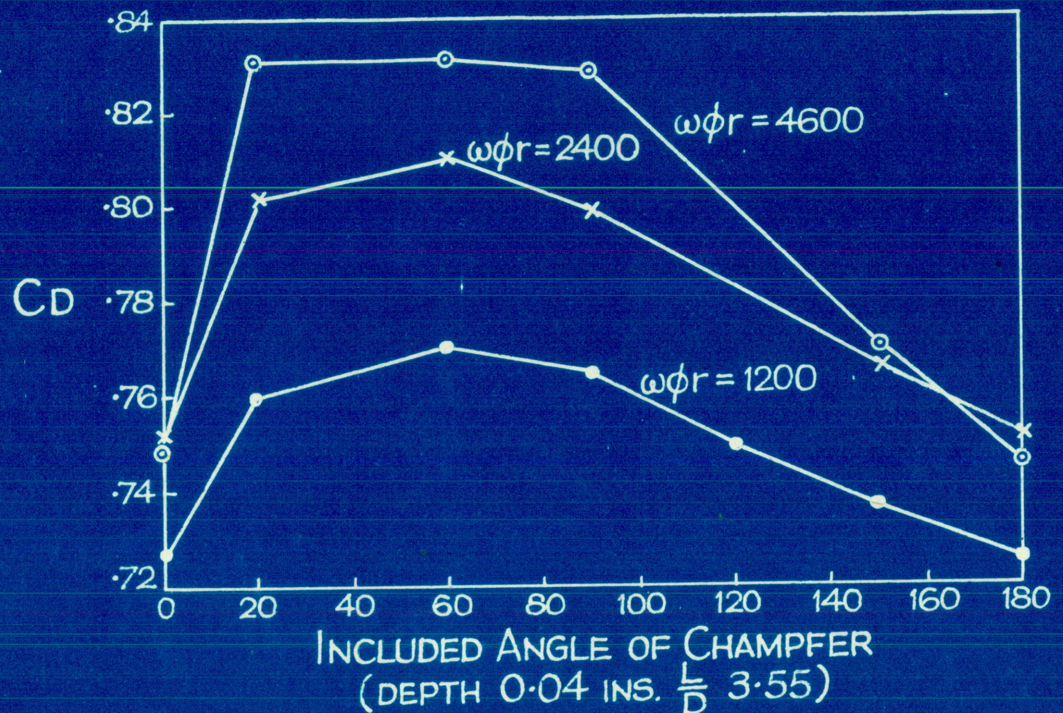

Fig. 14.4

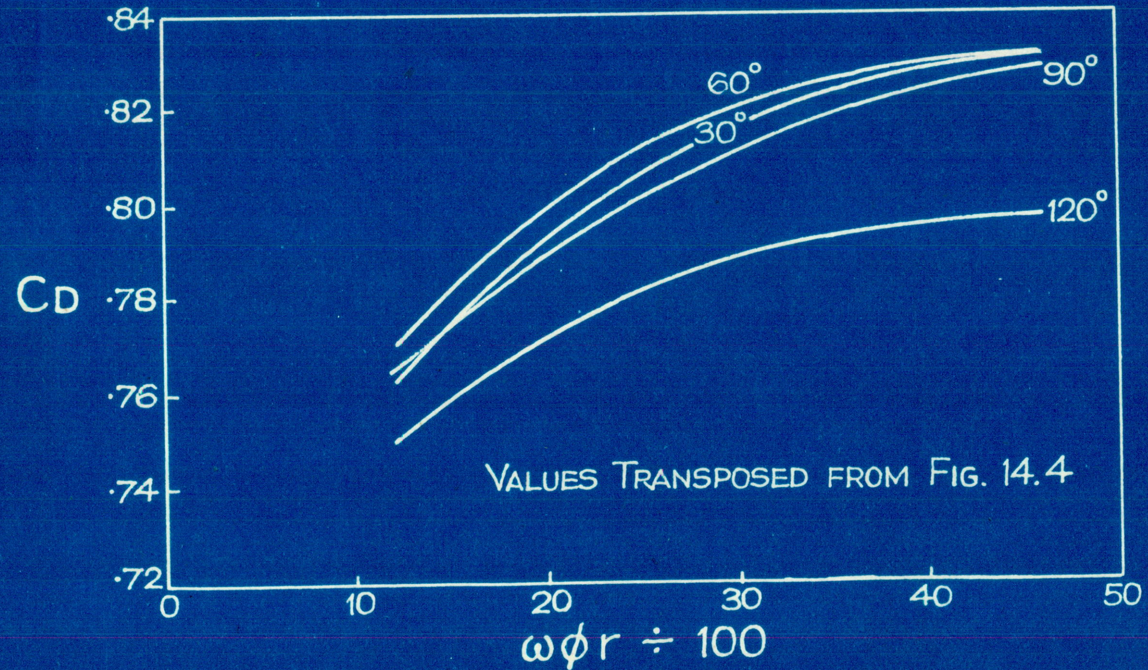

Fig. 14.5

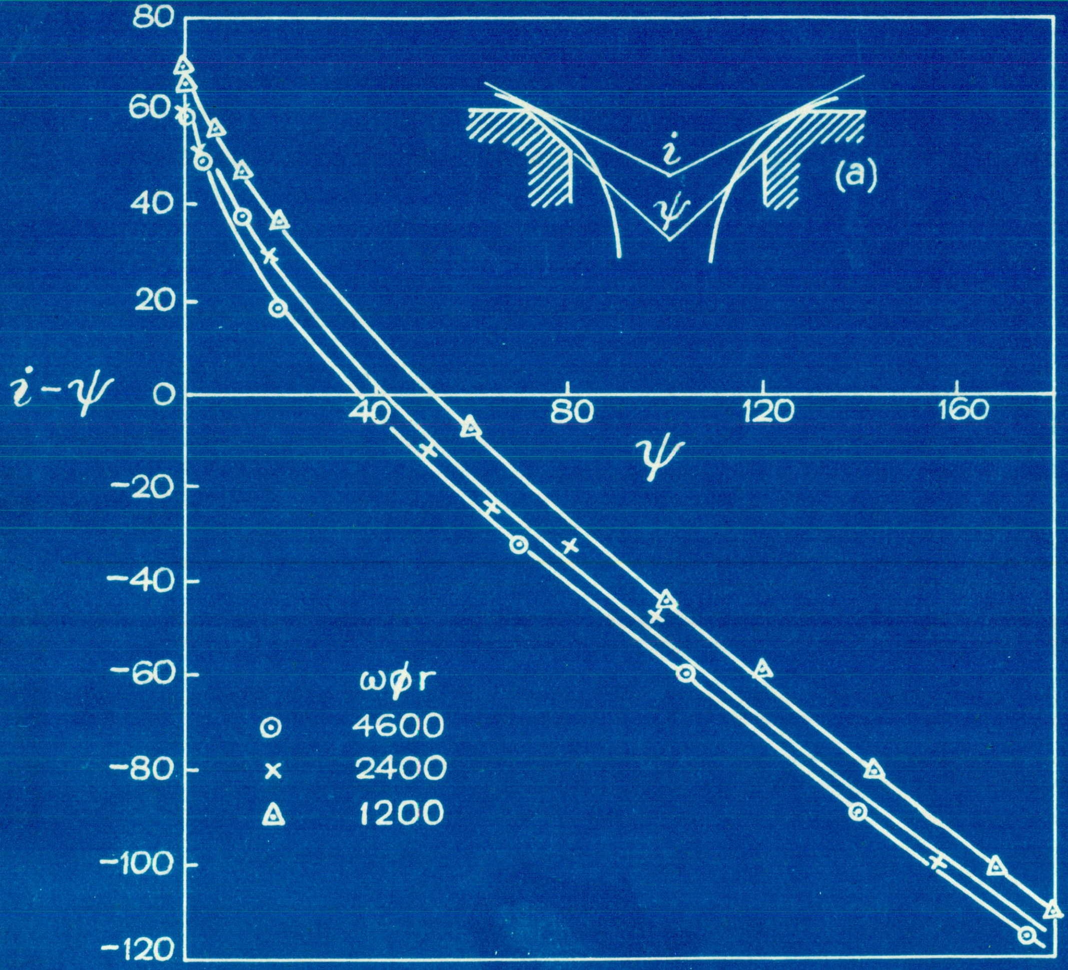

Fig. 14.6 The relationship between the curvature of the flow lines and the orifice champfer.

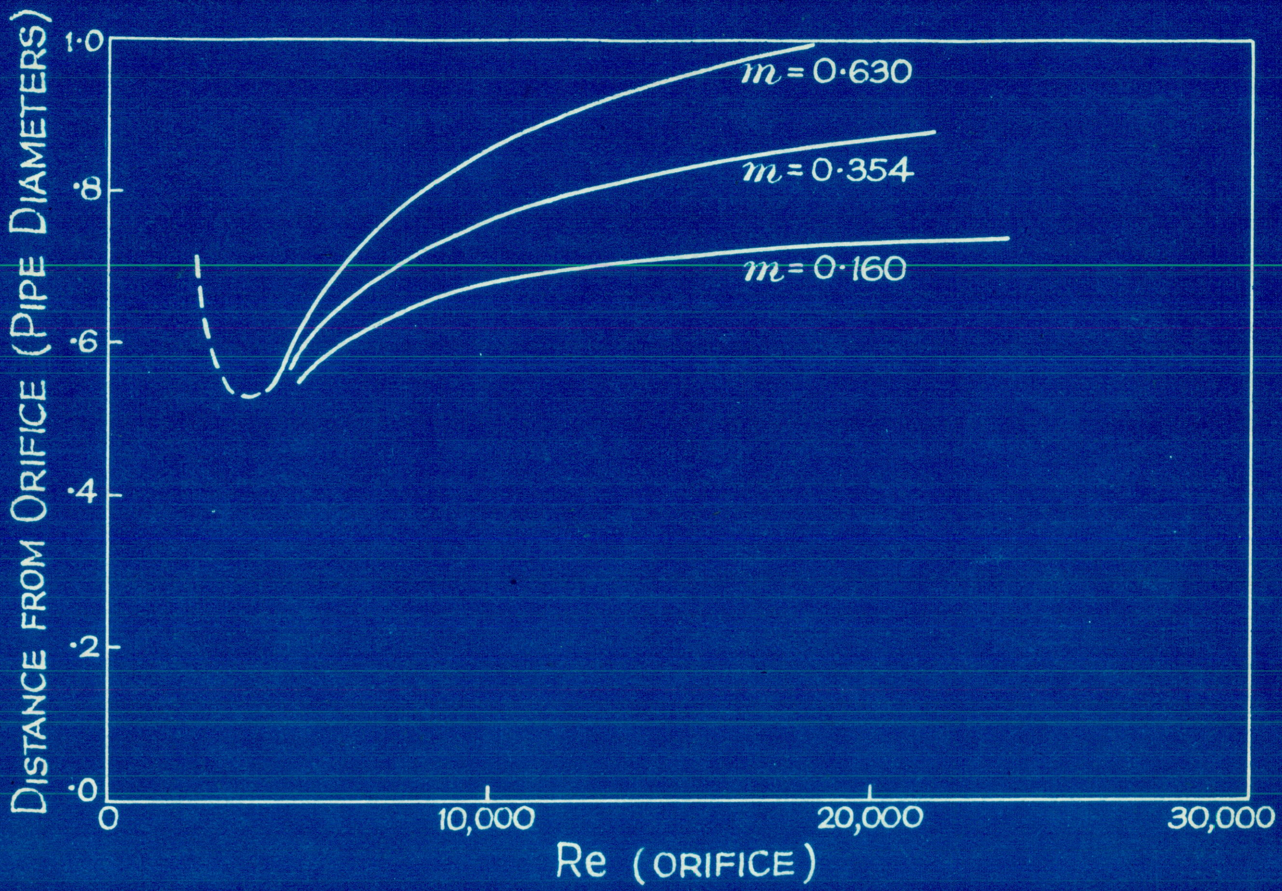

Fig. 15.1

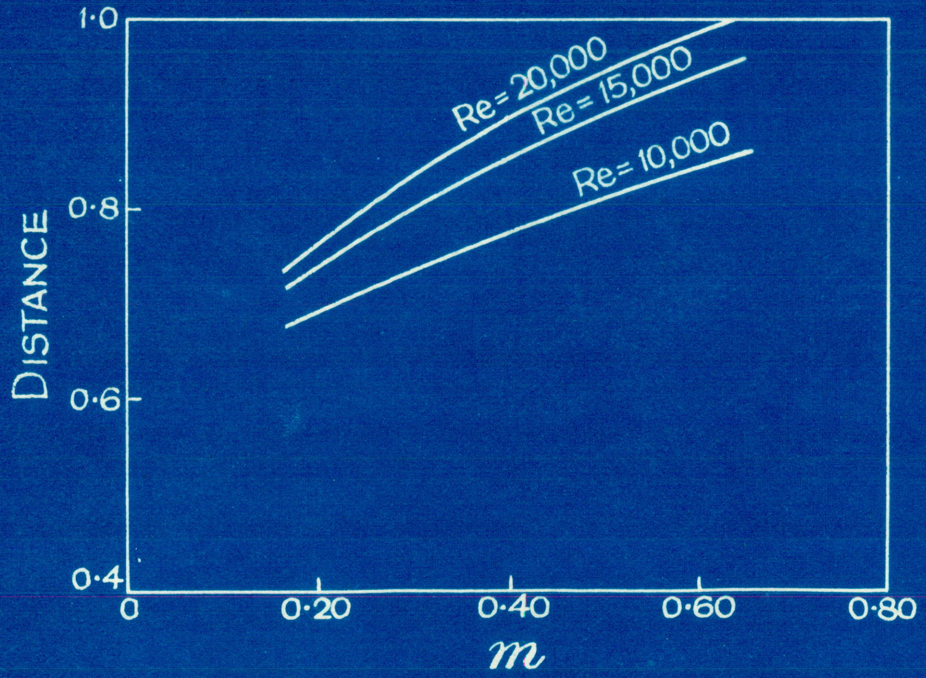

Fig. 15.2

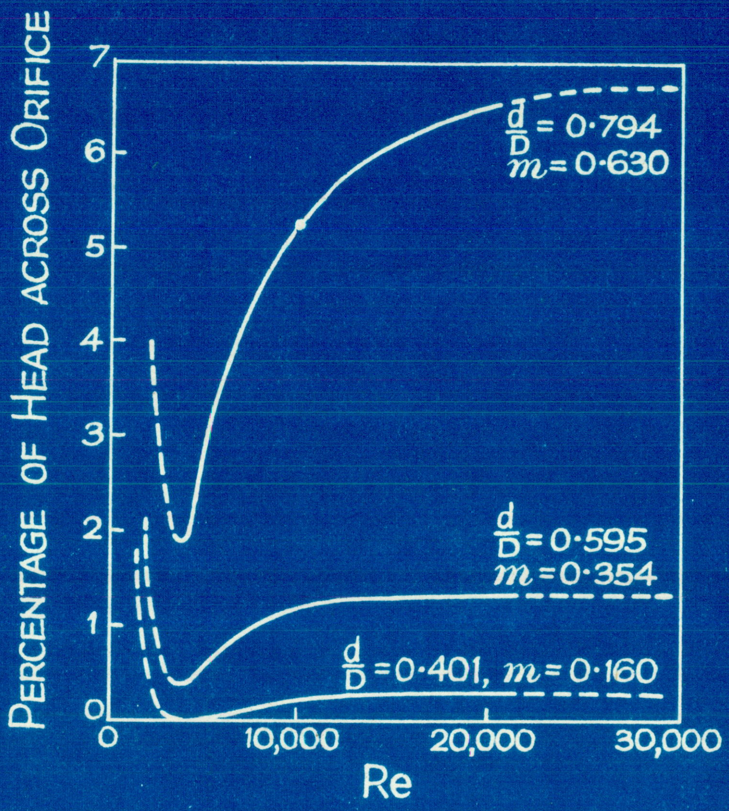

Fig. 15.3 The variation of orifice pressure-rise with Re and m

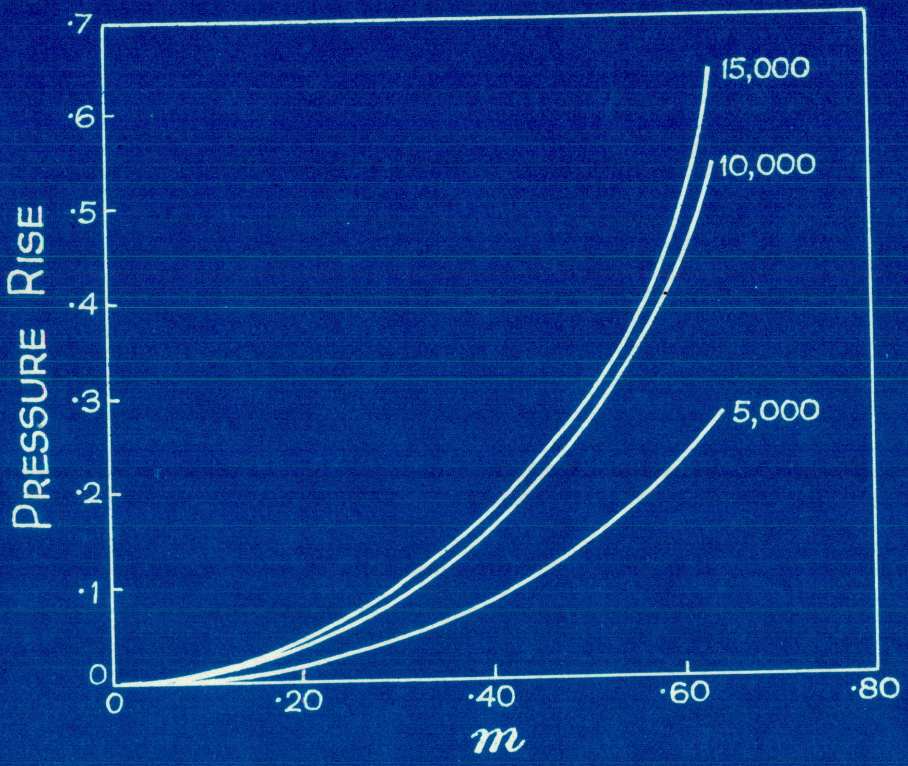

Fig. 15.4 Pressure rise across the orifice

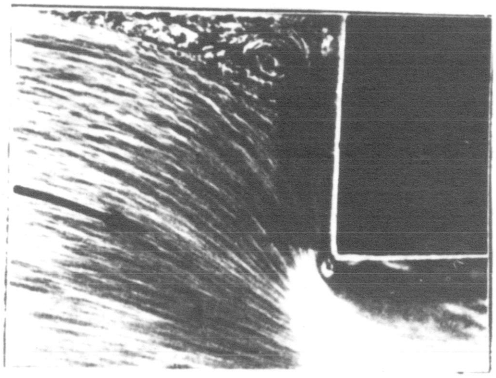

Fig.15.5. Corner Vortex Upstream of the Orifice.

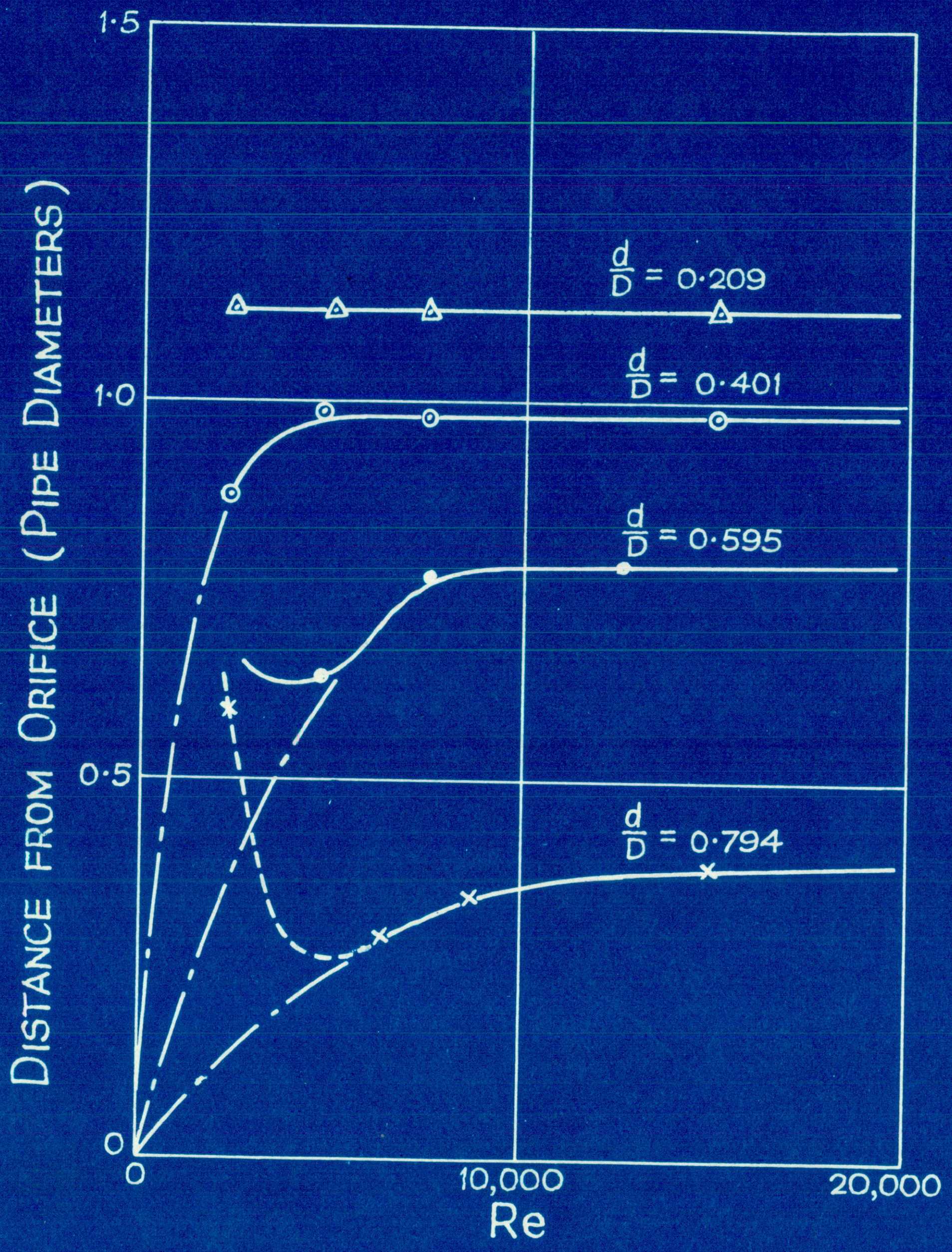

Fig. 16.1 Position of the downstream minimum pressure.

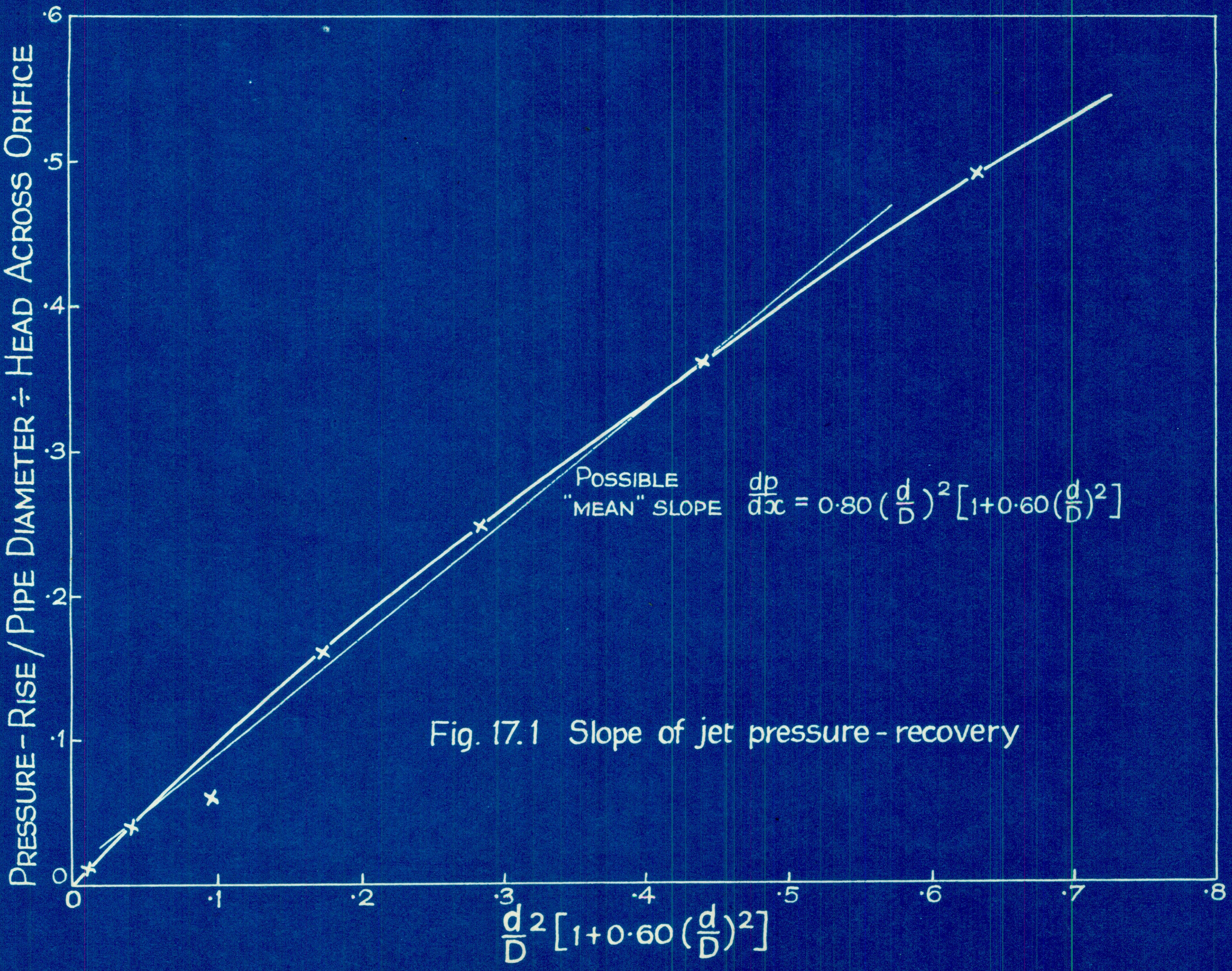

Fig. 17.1 Slope of jet pressure-recovery

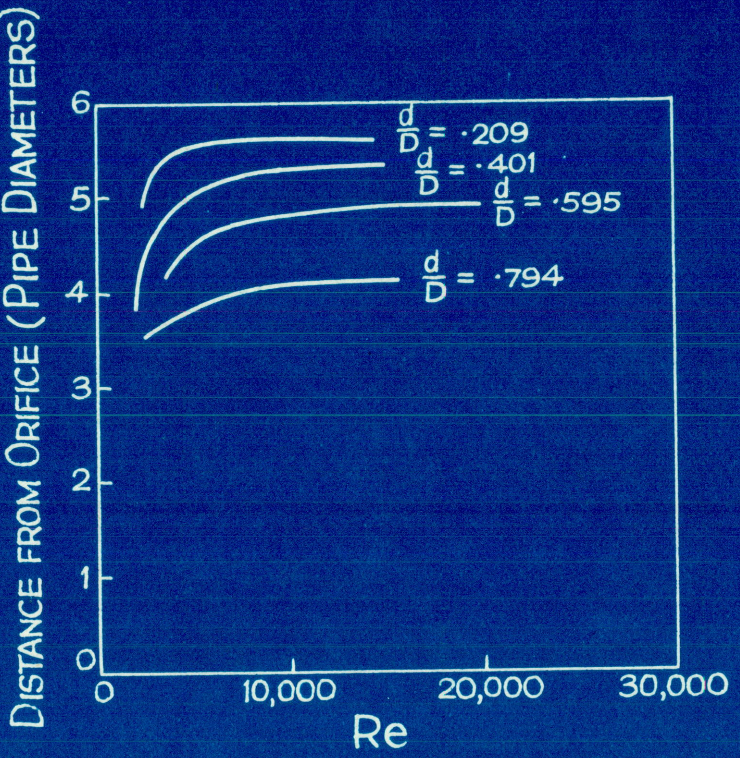

Fig. 17.2 The position of the maximum pressure recovery.

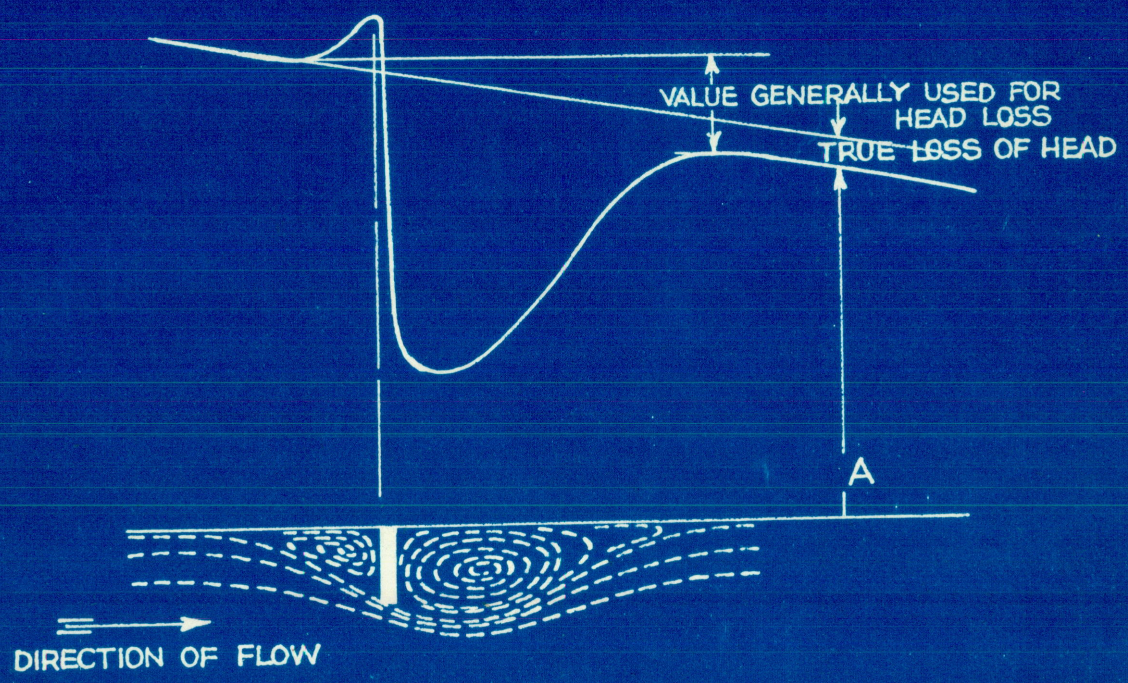

Fig. 17.3 Illustration of the correct measurement of head-loss due to an orifice.

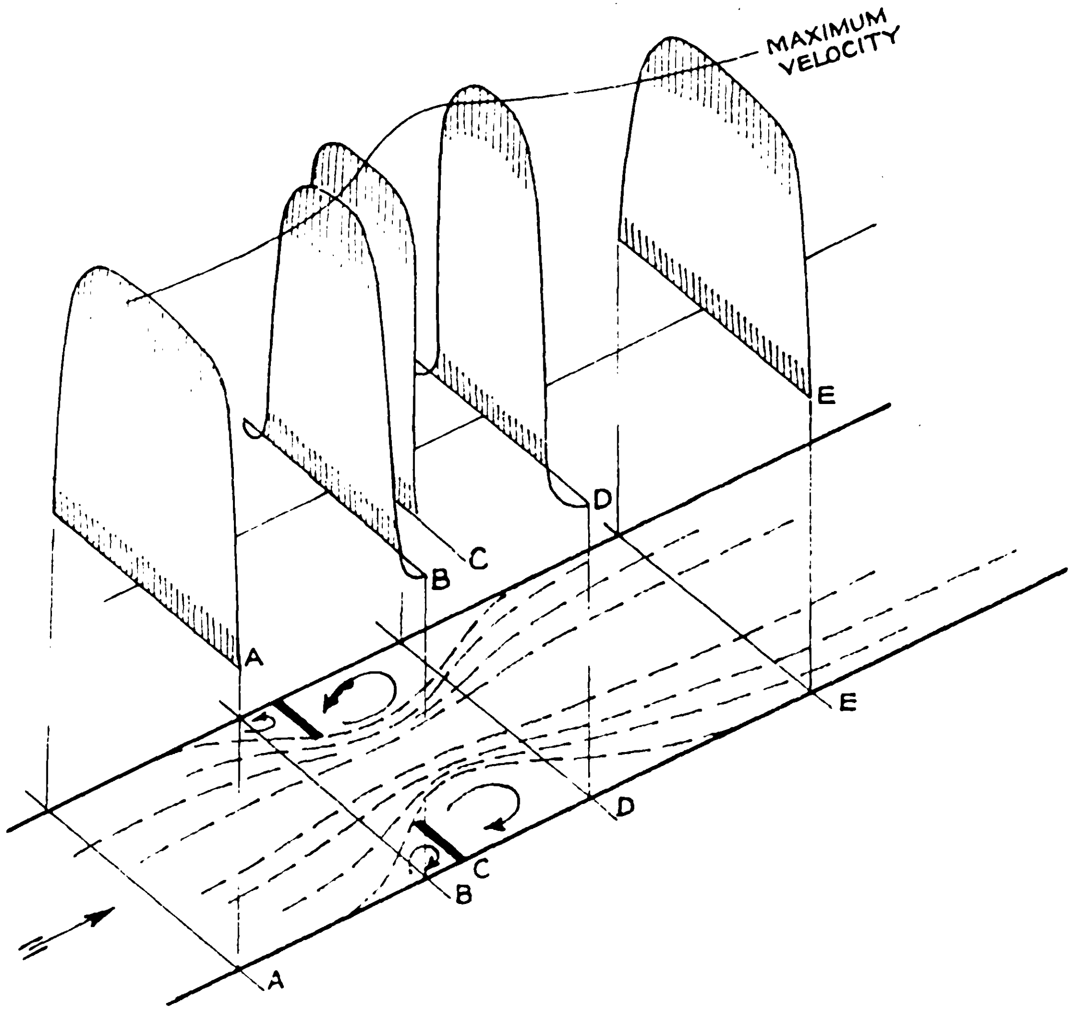

Fig. 18.1 Deduced distribution of velocity (axial) in the vicinity of an orifice.

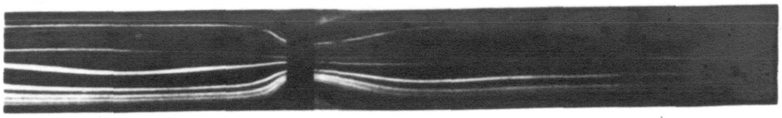

a

$vd/\nu \doteqdot 30.$

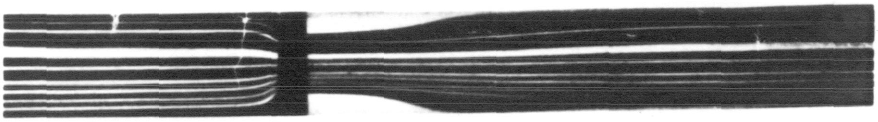

b

$vd/\nu \doteqdot 100.$

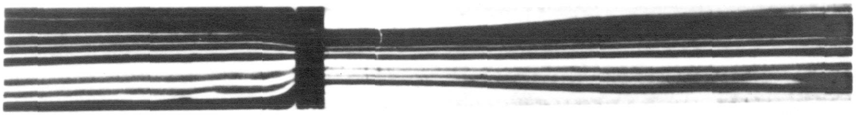

c

$vd/\nu \doteqdot 150.$

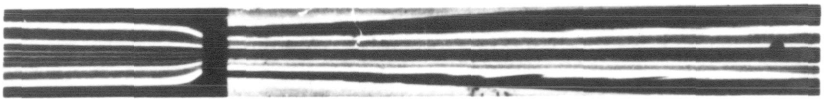

d

$vd/\nu \doteqdot 250.$

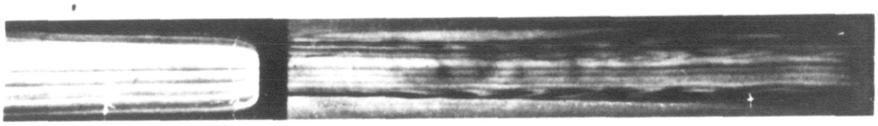

e

$vd/\nu \doteqdot 600.$

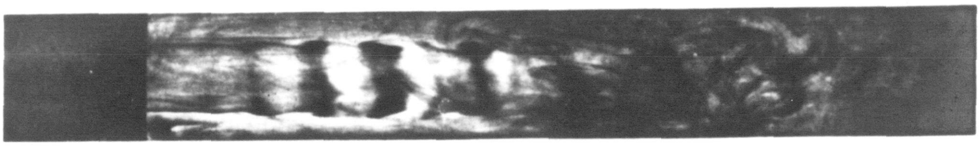

f.

$vd/\nu \doteqdot 1000.$

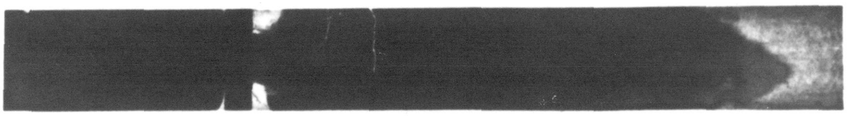

g.

$vd/\nu \doteqdot 2000.$

Fig.19.1. Flow through orifices at various values of Reynolds Number.

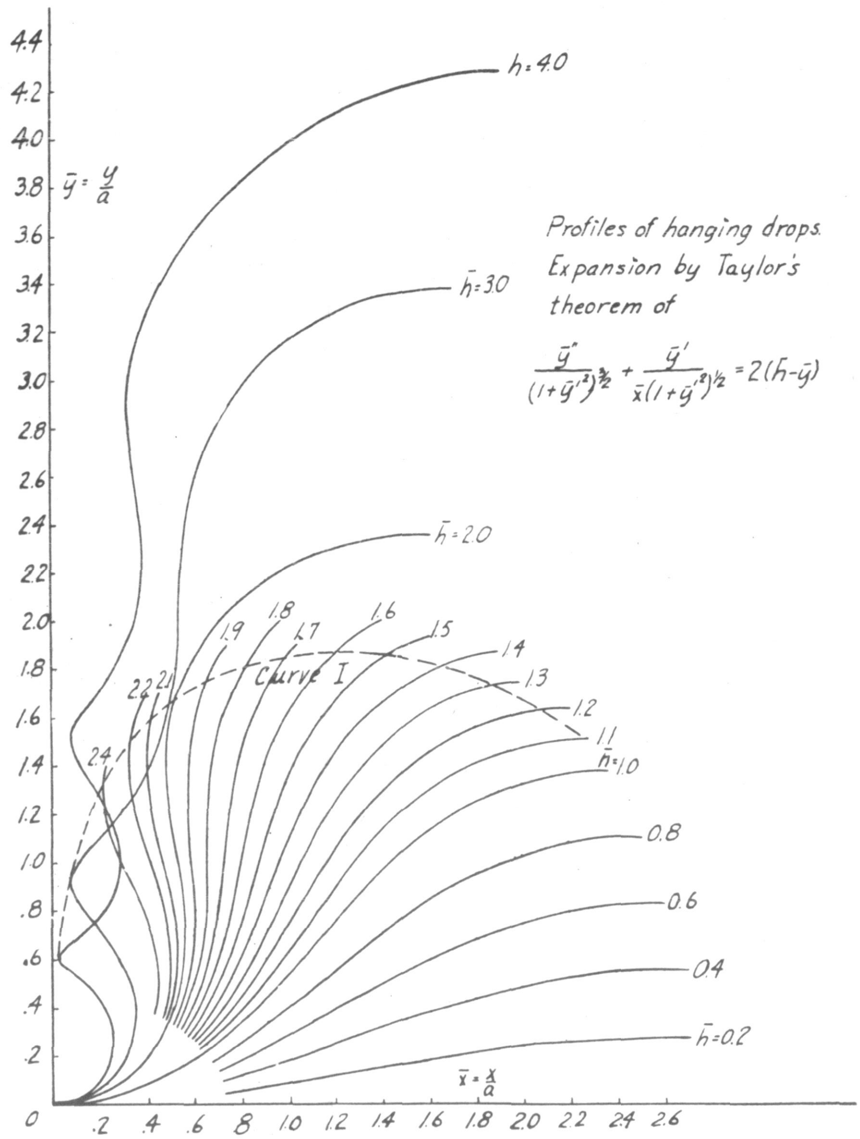

Fig.20.1. Profile of Hanging Drops(calculated by Freud and Harkins)

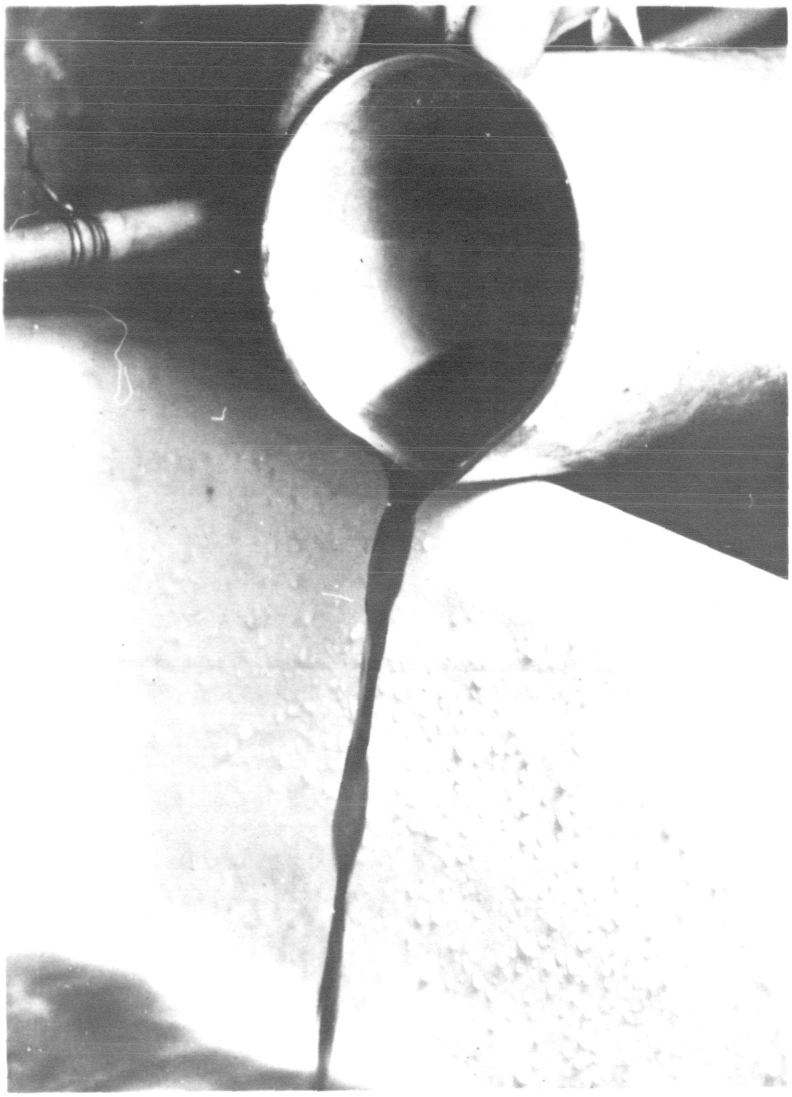

Fig.21.1. Stationary Waves of a jet.(Obtained by Author).

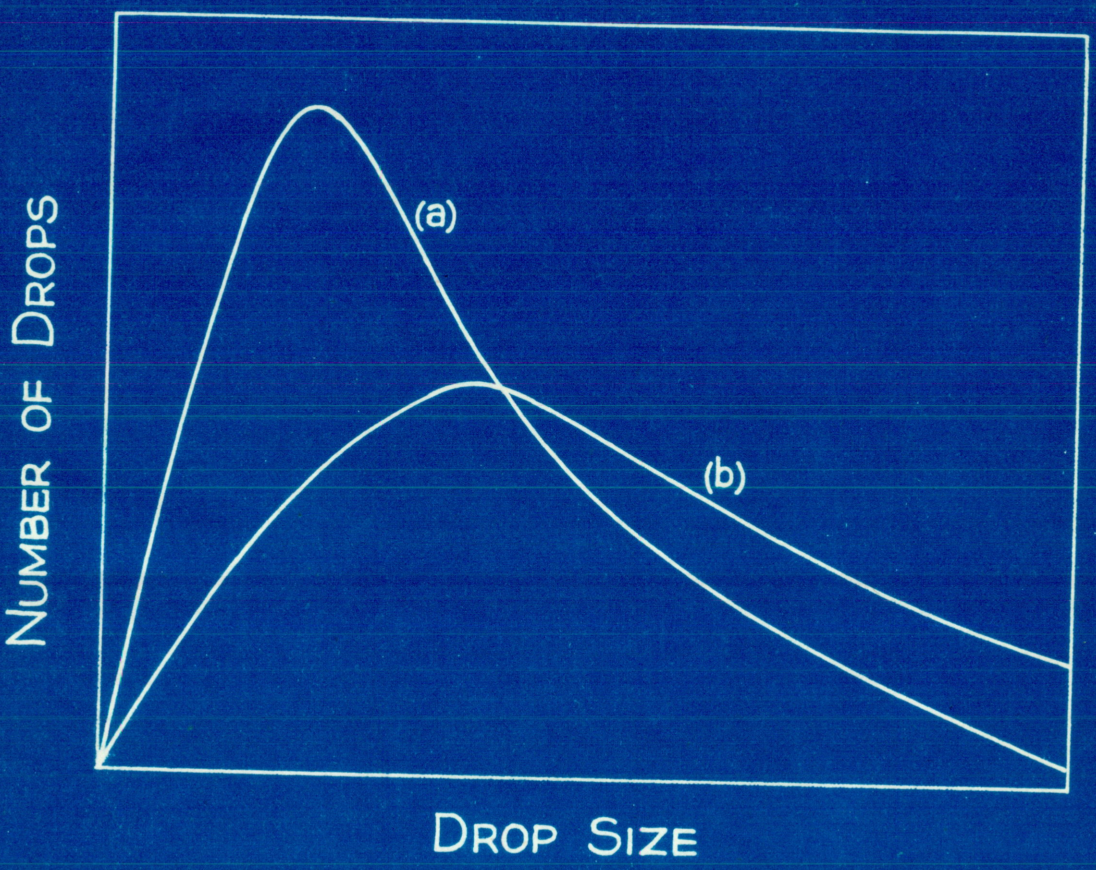

Fig. 24.1 Frequency curves measuring the atomisation of a spray.

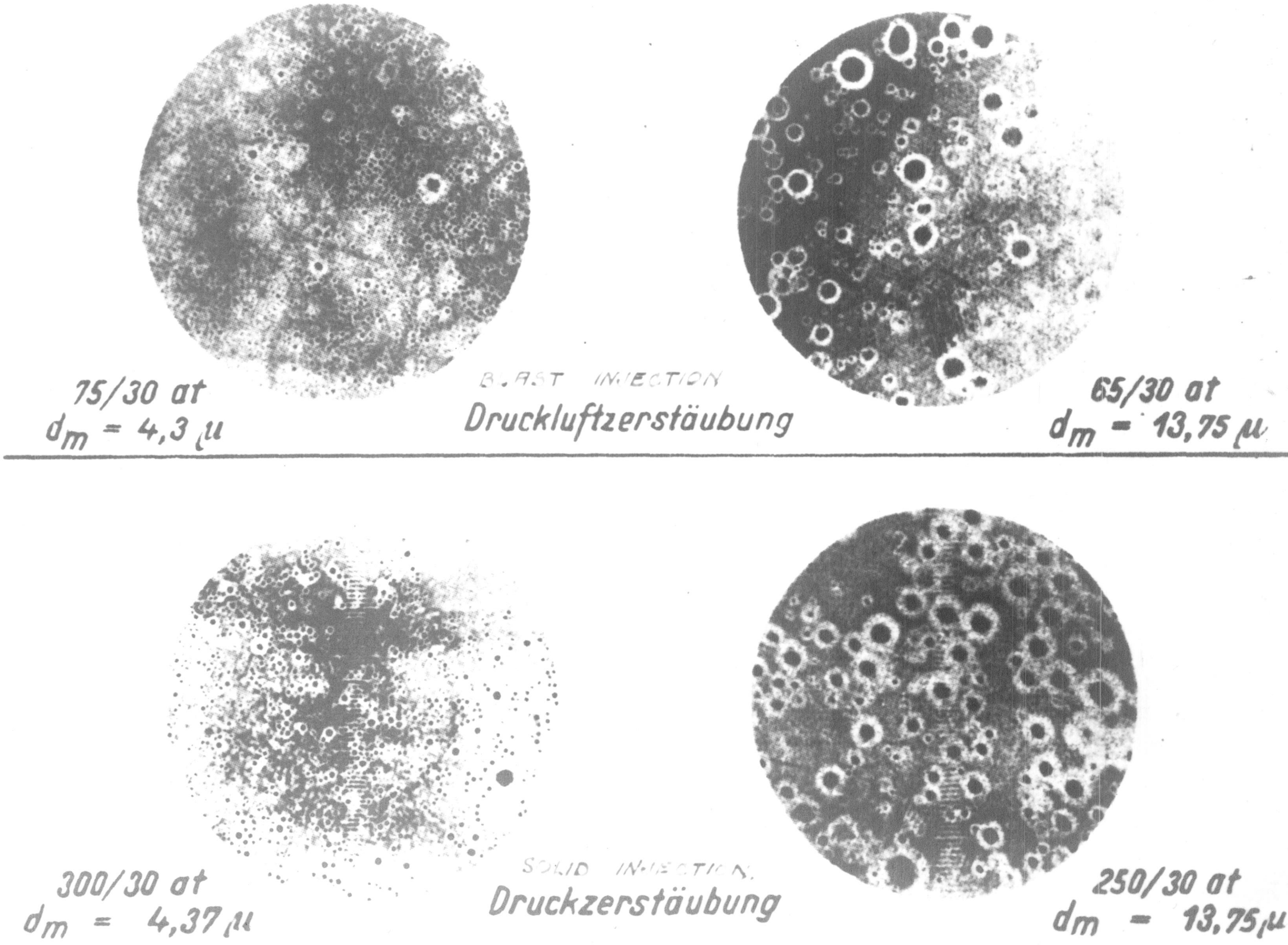

Fig.24.2. Spray photographs for blast and solid injection.